

FUNCTIONAL CROSSLINKED POLYMER MICROSPHERES

By

KAI LI, M.Sc.

A Thesis
Submitted to the School of Graduate Studies
in Partial Fulfilment of the Requirements
for the Degree
Doctor of Philosophy

McMaster University

© Copyright by Kai Li, March 1994

To my wife, Lijuan
my parents,
and Christopher

- ii -

DOCTOR OF PHILOSOPHY (1994)
(Chemistry)

McMASTER UNIVERSITY
Hamilton, Ontario

TITLE: Functional Crosslinked Polymer Microspheres

AUTHOR: Kai Li, M.Sc. (Filin University, P.R. China)

SUPERVISOR: Professor Harald D. H. Stöver

NUMBER OF PAGES: 263

FUNCTIONAL CROSSLINKED POLYMER MICROSPHERES

- iv -

ABSTRACT

Novel procedures for the preparation of highly crosslinked polymer microspheres by single step process have been developed. Poly(divinylbenzene) microspheres with narrow size dispersity have been prepared using dispersion polymerization techniques. Moreover, monodisperse poly(divinylbenzene) microspheres have been produced by precipitation polymerization with acetonitrile as solvent. The process does not require stabilizers of any type, and produces monodisperse microspheres with diameters between 2 and 8.5 micron depending on the conditions. The stability of microspheres during polymerization is attributed to their rigid, crosslinked surfaces. The mechanisms of particle formation and growth are discussed. This new process has been used to prepare a series of mono-disperse functional and crosslinked microspheres.

In addition, polymer resins containing chiral crown-ether binding sites have been prepared by template (or imprinting) polymerization using chiral ammonium salts. The ability of these resins to separate enantiomers of the original template molecules have been evaluated.

- v -

ACKNOWLEDGEMENTS

I wish to express my sincere gratitude to my supervisor, Dr. H.D.H. Stöver, for the valuable guidance and continuous help he generously provided throughout the course of this thesis. You have always been a great source of encouragement and support. Your patience, enthusiasm and high standards are greatly appreciated. I am proud of being your first graduate student. You shall continue to be a source of motivation for my future work.

I wish to thank Drs. A.E. Hamielec, M.A. Brook and B.E. McCarty for being my supervisory committee members. Your excellent advice and your chemistry/polymer expertise are greatly appreciated.

Thanks go to Brian Sayer, Dr. Don Hughes and George Timmins for the assistance in using NMR and IR facilities; Klaus Scholtes from the Electron Microscopy (EM) facility at the Department of Life Sciences for the help in using scanning electron microscopy (SEM). SEM has revealed a fantastic world which is presented throughout this thesis.

Thanks are also due to the staff in the Department office for their help provided through many years. In particular, I am grateful to Carol Dada for her valuable help and advice.

I would like to thank the following people who have worked in Dr. Stöver's lab during my stay:

Dr. Mei Lin Yang for his friendship and collaboration on living cationic polymerization. I had one more area of fun beyond this thesis.

- vi -

Lorenzo Ferrari, Frank Lenzmann, Casey Elliott, and Chris Brown for the fruitful cooperation and friendship.

Wen Hui Li for her collaboration on the synthesis of a new crosslinker and supplying suspension particles.

Robert Shaver for many things, especially our lunchtime talks and coffee breaks.

Su Li, Dr. George Vlaovic, Rhonda Whittaker, Nadia Batelic, Steve Sundquist, Quan Sheng and Pei Li for their friendship and help.

The financial support of the Natural Sciences and Engineering Research Council of Canada, Ontario Center for Material Research, McMaster Institute for Materials Research, Department of Chemistry and McMaster University are gratefully acknowledged.

Finally, my everlasting love goes to my wife, Lijuan Li; my parents, Fuhong Li and Jinyun Xie; my son, Christopher Li for their patience, understanding and moral support during the course of this work. A special debt of gratitude is due to my wife, Lijuan, and son, Christopher, my aim could not have been realized without their sacrifices.

- vii -

PUBLICATIONS BASED ON THIS RESEARCH

In Refereed Journals:

1. K. Li and H.D.H. Stöver, "Highly Crosslinked Micron-Range Polymer Microspheres by Dispersion Polymerization of Divinylbenzene", *J. Polym. Sci. Polym. Chem.*, **31**, 2473 (1993).
2. K. Li and H.D.H. Stöver, "Synthesis of Poly(divinylbenzene) Monodisperse Microspheres", *J. Polym. Sci. Polym. Chem.*, **31**, 3257 (1993).
3. K. Li, L.P. Ferrari, C. Brown, and H.D.H. Stöver, "High Affinity Crown Ether Resins Prepared by Cationic Template Polymerization", *Macromol. Chem. Phys.*, **195**, 391 (1994).
4. F. Lenzmann, K. Li, A.H. Kitai, and H.D.H. Stöver, "Thin Film Micropatterning using Polymer Microspheres", *Chem. Mater.*, **6**, 156 (1994).
5. W.H. Li, K. Li, H.D.H. Stöver, and A.E. Hamielec, "An Improved Synthesis of 1,2-Bis(vinylphenyl) Ethane", *J. Polym. Sci. Polym. Chem.*, **32**, 2023 (1994).

In Conference Proceedings:

6. K. Li and H.D.H. Stöver, "Highly Crosslinked Polymer Microspheres from Commercial Divinylbenzene", *Proceedings of the 42nd Canadian Chemical Engineering Conference*, p177, 1992.

In Conferences:

7. K. Li and H.D.H. Stöver, "Formation and Growth of Polydivinylbenzene Microspheres in Precipitation Polymerization", *77th Canadian Chemical Conference*, Winnipeg, Manitoba, May 29-June 2, 1994.
8. K. Li and H.D.H. Stöver, "Functional Polymer Microspheres having Highly Crosslinking Structure", *27th Canadian High Polymer Forum*, Gananoque, August 18-20, 1993.

- viii -

9.	<u>K. Li</u> , C. Elliot and H.D.H. Stöver, Precipitation Polymerization of Commercial Divinylbenzene: The Effect of Initiator Type on the Particle Formation, <i>76th Canadian Chemical Conference</i> , Sherbrooke, Québec, May 30 - June 3, 1993.
10.	<u>W.H. Li</u> , K. Li and H.D.H. Stöver, An Improved Synthesis of 1,2-Bis(3[or 4]-Vinylphenyl) Ethane, <i>76th Canadian Chemical Conference</i> , Sherbrooke, Québec, May 30-June 3, 1993.
11.	<u>K. Li</u> and H.D.H. Stöver, Highly Crosslinked Polymer Microspheres from Commercial Divinylbenzene, <i>42nd Canadian Chemical Engineering Conference, Toronto, Ontario</i> , October 18-21, 1992.
12.	<u>K. Li</u> and H.D.H. Stöver, A New Way to Synthesize Monodisperse Crosslinked Polymer Microspheres, <i>1992 Ontario Centre for Materials Research (OCMR) Retreat</i> , Alliston, Sept. 25-27, 1992.
13.	<u>H.D.H. Stöver</u> , L.P. Ferrari, R.T. Shaver, D. Vlaovic, K. Li, Functional Polymers Derived from Poly(4-methylstyrene), <i>34th IUPAC International Symposium on Macromolecules</i> , Prague, 13-18 July 1992.
14.	<u>K. Li</u> , R.T. Shaver and H.D.H. Stöver, Functional Polymer Microspheres, <i>75th Canadian Chemical Conference</i> , Edmonton, Alberta, May 31-June 4, 1992.
15.	<u>K. Li</u> and H.D.H. Stöver, Narrow-disperse Highly Crosslinked Polymer Microspheres from Commercial Divinylbenzene, <i>75th Canadian Chemical Conference</i> , Edmonton, Alberta, May 31-June 4, 1992.
16.	<u>K. Li</u> and H.D.H. Stöver, (L)-Phenylalanine-Selective Polymers Synthesized by Template Polymerization, <i>74th Canadian Chemical Conference</i> , Hamilton, Ontario, June 2-6, 1991.

TABLE OF CONTENTS

	Page
Abstract	v
Acknowledgements	vi
List of Figures	xvi
List of Schemes	xxiv
List of Tables	xxv
CHAPTER 1: TEMPLATE POLYMERS BEARING CROWN ETHER AS CHIRAL SEPARATION MEDIA	1
1.1 Introduction	1
1.1.1 Molecular Recognition of Template Polymers	2
1.1.2 Using Crown Ether Binding Sites in the Resolution of Enantiomers	8
1.2 Aim of the Research	12
1.3 Results and Discussion	13
1.3.1 Syntheses of Dibenzo-18-Crown-6 Derivatives	13
1.3.2 Novel Crosslinking Agent	22
1.3.3 Synthesis of <i>l</i> -Phenylalanine Methyl Ester (PAME) Selective Template Polymers	28
1.3.3.1 Choice of crosslinking reagent and porogen	28
1.3.3.2 Solubility of the template molecule	31
1.3.3.3 Polymerization	33
1.3.4 <i>l</i> -Lysine Methyl Ester Dihydrochloride Selective Template Polymer	37
1.3.5 Characterizations of PAME Selective Template Polymers	44
1.4 Experimental	49
References	56

- ix -

- x -

Table of Contents (continued)

	Page
CHAPTER 2: AN INTRODUCTION TO THE METHODS OF SYNTHESIS AND CHARACTERIZATION OF POLYMER MICROSPHERES	60
2.1 General Features of Heterogeneous Polymerization Processes	60
2.2 Synthesis of Polymer Microspheres	63
2.3 A Critical Review on Dispersion Polymerization	64
2.3.1 Process Description	64
2.3.2 Steric Stabilization and Stabilizers	67
2.3.3 Initiation and Polymerization	68
2.3.4 Comparison of Dispersion and Precipitation Polymerization	70
2.4 Solubility and Solubility Parameters of Polymer	72
2.5 Characterizations of Polymer Microspheres	75
2.5.1 Scanning Electron Microscopy (SEM)	75
2.5.2 Coulter Multisizer	78
References	80
CHAPTER 3: NARROW DISPERSE POLYDIVINYLBENZENE PARTICLES BY DISPERSION POLYMERIZATION	83
3.1 Recent Research on the Synthesis of Narrow Disperse Crosslinked Polymer Particles	83
3.2 Aim of the Research	87
3.3 Experimental	88
3.3.1 Materials and Their Purification	88
3.3.2 Dispersion Polymerization of DVB55 (DPDVB55, General Procedure)	88
3.3.3 Conversion of Monomer	89

- xi -

Table of Contents (continued)

	Page
CHAPTER 3 (continued)	
3.3.4 Size and Size Distribution of the Microspheres	90
3.3.5 Morphology of DPDVB55 Particles	91
3.3.6 Determination of Porosity of DPDVB55 Particles	92
3.4 Results and Discussion	93
3.4.1 Choice of Agitation Method	93
3.4.2 Parameters Influencing the Formation of DPDVB55 Particles	95
3.4.2.1 Effect of initial monomer concentration	96
3.4.2.2 Solvent effects	99
3.4.2.3 Effective crosslinker concentration	103
3.4.2.4 Effect of stabilizer concentration	106
3.4.3 Scale-up of DPDVB55 Microspheres Production	107
3.4.4 Porosity of DPDVB55 Particles	109
3.4.5 Morphology of DPDVB55 Particles	111
3.4.6 Proposed Mechanism of DPDVB55 Particle Formation	113
References	116
CHAPTER 4: MONODISPERSE POLYDIVINYLBENZENE MICROSPHERES BY PRECIPITATION POLYMERIZATION	118
4.1 Polymer Particles by Precipitation Polymerization	118
4.2 Aim of the Research	120
4.3 Experimental	121
4.3.1 Materials	121
4.3.2 Description of the Reactor	121
4.3.3 Typical Precipitation Polymerization of DVB55 (PPDVB55)	123
4.3.4 Determination of Size, Size Distribution and Yield of PPDVB Microspheres	124

- xii -

Table of Contents (continued)		Page
CHAPTER 4 (continued)		
4.3.5	Porosity of PPDVB55 Microspheres	125
4.3.6	Calculation of Distance Between Microspheres and of Solubility Parameter of the Solvent Mixture	126
4.5	Results and Discussion	127
4.5.1	Basic Parameters Influencing the Formation of PPDVB55 Microspheres	127
4.5.1.1	Reactor setup and operation conditions	127
4.5.1.2	Effect of initial monomer concentration	131
4.5.1.3	Effect of crosslinker concentration	137
4.5.1.4	Initiator concentration	139
4.5.1.5	Polymerization Temperature	144
4.5.2	Effect of Initiator Type on PPDVB55 Microspheres	147
4.5.2.1	Oil soluble initiator	147
4.5.2.2	Solvent soluble initiator	149
4.5.3	Effect of Solvent	158
4.5.3.1	Single solvent system	158
4.5.3.2	Binary solvent system-(acetonitrile/propionitrile)	161
4.5.3.3	Binary solvent system-(acetonitrile/n-butanol)	163
4.5.3.4	Binary solvent systems-(acetonitrile/water)	166
4.5.4	Cause of Low Conversion in PPDVB	171
4.5.5	Kinetic Considerations	174
4.5.5.1	Overall rate of polymerization at different temperatures	174
4.5.5.2	Apparent rate constants of individual monomers	174
4.5.6	Composition of PPDVB55 Microspheres	182
4.5.7	Growth of PPDVB55 Microspheres	183
4.5.8	Porosity of PPDVB55 Microspheres	183
4.5.9	Morphology of PPDVB55 Microspheres	191
4.5.10	Proposed Mechanism of Microsphere Formation and Growth in PPDVB55	194
References		197

- xiii -

Table of Contents (continued)		Page
CHAPTER 5: INTRODUCING POROSITY INTO POLYMER MICROSPHERES		
5.1	Aim of the Research	199
5.2	A Survey: Monodisperse Macroporous Polymer Microspheres	200
5.3	Experimental	202
5.3.1	Materials	202
5.3.2	Synthesis of Monodisperse Seed Particles	202
5.3.3	Polymerizations	203
5.3.4	Characterization	204
5.4	Results and Discussion	205
5.4.1	Dispersion Polymerization of 4-Methylstyrene	205
5.4.2	Porous Particles by Seeded Polymerization	207
5.4.3	Porous Particles by Dynamic Monomer Swelling	215
References		218
CHAPTER 6: FUNCTIONAL POLYMER MICROSPHERES		
6.1	Aim of the Research	219
6.2	Materials Used in This Study	220
6.3	Functional Micron-size Polymer Microspheres by Dispersion Polymerization	221
6.3.1	Experimental	222
6.3.2	Results and Discussion	223
6.4	Crosslinked Functional Copolymer Microspheres by Precipitation Polymerization	229
6.4.1	Experimental	229
6.4.2	Results and Discussion	231
6.4.2.1	Poly(DVB80-co-glycidyl methacrylate) microspheres	231

- xiv -

Table of Contents (continued)		Page
CHAPTER 6 (continued)		
6.4.2.2	Poly(DVB80-co-vinylbenzyl chloride) microspheres	232
6.4.2.3	Copolymerization of DVB80/4-vinylbenzenesulfonic acid sodium salt	236
6.4.2.4	Poly(bis(vinylphenyl) ethane-co-vinylbenzyl chloride)	240
6.4.3	Surface Modifications of Preformed Polymer Microspheres	241
6.4.3.1	Surface modification of poly(4-methylstyrene) microspheres	242
6.4.3.2	Surface modification of PPDVB microspheres	257
References		262

- xv -

LIST OF FIGURES		
		Page
Figure 1.1	Elution profile from the chromatography of phenyl- β -D,L-mannopyranoside on macroporous polymer imprinted with the D-enantiomer. (Mobile phase: acetonitrile with 4% concentrated ammonia solution and 5% water, flow rate 0.1 ml/min) (Ref. 18)	6
Figure 1.2	The structure of a nonchiral crown ether: dibenzo-18-crown-6	8
Figure 1.3	An example of a chiral crown ether. (a) Structure of the optically active crown ether used for optical resolution. (b) Chromatographic resolution of methyl phenylalaninate hydrochloride (Ref. 1). The chirality of the crown ether is due to the twist in the naphthyl rings	10
Figure 1.4	The interaction of an ammonium cation with a crown ether	11
Figure 1.5	200 MHz ^1H NMR spectra of (a) dibenzo-18-crown-6 (1) and (b) diacetyldibenzo-18-crown-6 (2). Solvent: CDCl_3	17
Figure 1.6	200 MHz ^1H NMR spectrum of (a) 3 , solvent: CD_3OD ; (b) 4 , solvent: CDCl_3	18
Figure 1.7	Statistical composition of BVPE isomers	25
Figure 1.8	200 MHz ^1H NMR spectrum of 1,2-bis(vinylphenyl) ethane. Solvent: CDCl_3	26
Figure 1.9	Reverse phase chromatography of the mixture of BVPE (5) isomers. peak 1: <i>m,m</i> - 5 ; peak 2: <i>m,p</i> - 5 ; peak 3: <i>p,p</i> - 5 . Solvent: methanol / water (85:15); Flow rate: 1 ml/min; Temp.: 20°C	27
Figure 1.10	SEM micrograph of template polymer	35
Figure 1.11	L-Lysine Methyl Ester Dihydrochloride	38

- xvi -

List of Figures (continued)	Page
Figure 1.12 (a) Static ¹ H NMR spectrum of poly(styrene-co-divinylbenzene); (b)-(d) The same polymer after incorporation of bis(hydroxyethyl) dibenzo-18-crown-6. (b) static ¹ H NMR spectrum, (c) direct polarization magic angle spinning ¹ H NMR spectrum, (d) static ¹³ C NMR spectrum	41 / 42
Figure 1.13 Static 500 MHz ¹ H NMR spectrum of poly(styrene-co-4-methoxystyrene-co-divinylbenzene) after incorporation of bis(acetoxyethyl)dibenzo-18-crown-6	43
Figure 1.14 Elution profile of <i>d</i> - and <i>l</i> -triflate applied on TP-07 polymer. Eluent: acetonitrile; Temperature: 25°C; flow rate: 0.4 ml/min	47
Figure 2.1 General kinetic features and particle size ranges of heterogeneous polymerization processes. (Ref. 20)	62
Figure 2.2 A schematic representation of particle formation and growth in nonaqueous dispersion polymerization of styrene in ethanol medium. (Ref. 7)	65
Figure 2.3 Comparison of rates of dispersion polymerization (A), precipitation polymerization (B) and solution polymerization (C) of methyl methacrylate at 80°C. (Ref.25)	66
Figure 2.4 Schematic representation of the close approach of sterically stabilized particles	67
Figure 2.5 Schematic of types of radiation emitted in scanning electron microscopy	77
Figure 2.6 Schematic of Coulter counter technique	79
Figure 3.1 Dispersion polymerization of DVB55	89
Figure 3.2 Effect of agitation method on particle size for 10 vol.% DVB55 in acetonitrile and ethanol	95
Figure 3.3 SEM micrographs of DPDVB55 particles prepared with: (a) 5%; (b) 10%;(c) 15%; (d) 20% DVB55 in acetonitrile.	98

List of Figures (continued)	Page
Figure 3.4 Particle size distributions of DPDVB55 microspheres prepared from (a)10%; (b) 15%; (c) 20% DVB55 in acetonitrile	100/101
Figure 3.5 Particles formed from a 5% solution in ethanol of: (a) 4-methylstyrene;(b) mixture of DVB55 and 4-methylstyrene, containing effective DVB of 30%; (c) DVB55. Reactions conditions: [PVP] = 16 g/L, [AIBN] = 1 wt%; 70°C for 24 h	105
Figure 3.6 PolyDVB55 particles obtained without PVP	108
Figure 3.7 DPDVB55 particles obtained in the scaled-up reaction using a 50-70°C temperature profile	109
Figure 3.8 Size-exclusion calibration of DPDVB55 particles. Conditions: narrow disperse polystyrene standards in tetrahydrofuran at 25°C; column bed length, 7 cm; flow rate, 0.5 ml/min	110
Figure 3.9 Surface structure of DPDVB55 particles	112
Figure 3.10 Stages of particle formation: (A) homogeneous solution of DVB55, PVP, AIBN; (B) formation of crosslinked oligomer radicals; (C) aggregation into primary particles, stabilized by PVP and/or crosslinking density; (D) particle grown by capture of oligomers, primary particles, and/or diffusion of monomer	114
Figure 4.1 A rotor plate used in precipitation polymerization of DVB55	123
Figure 4.2 Precipitation polymerization of DVB55 or DVB80	124
Figure 4.3 Photograph of the reactor used for precipitation polymerization of DVB55	129
Figure 4.4 SEM of PPDVB55 microspheres. Conditions: 2 vol.% DVB55; 2 wt% AIBN; 30 rpm; temperature: 20 to 70°C within 70 min., then at 70°C for 23 h.	130
Figure 4.5 Size histogram of PPDVB55 microspheres	131
Figure 4.6 SEM micrograph of PPDVB microspheres	133

List of Figures (continued)	Page
Figure 4.7 SEM micrograph of PPDVB55 microspheres with higher magnification	133
Figure 4.8 Size distribution pattern of DPDVB55 obtained under PPDVB55 conditions. Conditions: DVB55: 5 vol%; PVP: 16 g/L; acetonitrile; 70°C for 24 h.	137
Figure 4.9 Effect of initiator concentration on the size of PPDVB55 microspheres and DVB55 conversion.	140
Figure 4.10 Effect of initiator concentration on the size of PPDVB80 microspheres and DVB80 conversion.	141
Figure 4.11 Number of PPDVB80 microspheres and their spacing vs. initial initiator concentration.	143
Figure 4.12 Conversion of DVB55 at various temperatures in precipitation polymerization.	145
Figure 4.13 Conversion - time curve. Conditions: 70°C, 2 vol% of DVB55, 2 wt% of initiator (relative to DVB55)	150
Figure 4.14 Typical size distribution pattern of PPDVB55 microspheres obtained by using AIYP initiator	153
Figure 4.15 Effect of AIYP initial loading on PPDVB55 microspheres	157
Figure 4.16 Effect of propionitrile concentration on the precipitation polymerization of DVB55 in acetonitrile/propionitrile binary solvent system.	162
Figure 4.17 SEM micrograph of PPDVB55 microspheres. (dn=3.12 μm; CV=3.4%). Conditions: 2 vol% DVB55; 2 wt% BPO; acetonitrile/n-butanol=7/3 (v/v); 70°C for 24 h.	165
Figure 4.18 Higher magnification of PPDVB55 microspheres	165

List of Figures (continued)	Page
Figure 4.19 Effect of water content on PPDVB55 microspheres in the mixture of acetonitrile and water.	168
Figure 4.20 Effect of water on PPDVB55 particles. Water content (vol%): a) 1%; b) 2%; c) 3%; d) 4%; e) 5%; f) 6%; g) 7%; h) 8%; i) 9%	169/170
Figure 4.21 Kinetic curves for the polymerization of DVB55. Polymerization conditions: 2 vol% monomer; 2 wt% AIBN; acetonitrile as solvent	175
Figure 4.22 Reverse-phase HPLC profile of DVB55. Conditions: methanol/water = 70/30 (v/v); 1.0 ml/min., room temperature	177
Figure 4.23 Reverse-phase HPLC calibration curve for DVB55	178
Figure 4.24 Conversion curves of individual monomer in precipitation polymerization of commercial divinylbenzene (DVB55)	180
Figure 4.25 First order plots of the monomer consumption with the time of DVB55 in precipitation polymerization	181
Figure 4.26 Particle volume versus conversion during growth of PPDVB55 microspheres.	184
Figure 4.27 Solvent regains of different samples: PPDVB55 synthesized in (a) acetonitrile; (b) acetonitrile/1-propanol (70/30); (c) acetonitrile/n-butanol (70/30); (d) n-butanol; and (e) polyDVB55 particles obtained by suspension polymerization	185
Figure 4.28 Porosity of PPDVB55 determined by mercury porosimetry measurement	186
Figure 4.29 Optical photograph of PPDVB55 microspheres	189
Figure 4.30 SEM micrograph of PPDVB55 microspheres	190
Figure 4.31 Surface morphology of PPDVB55	192
Figure 4.32 Internal structure of PPDVB55 microspheres	193

List of Figures (continued)		Page
Figure 4.33	A schematic representation of microsphere formation and growth in precipitation polymerization of DVB55 in acetonitrile	195
Figure 5.1	Monodisperse polystyrene particles synthesized in the present system	206
Figure 5.2	SEM micrograph of poly(4-methylstyrene) microspheres.	209
Figure 5.3	Typical poly(4-methylstyrene) microsphere histogram.	210
Figure 5.4	SEM micrograph of poly(4-methylstyrene) seed particles	212
Figure 5.5	SEM micrographs of macroporous particles made by seeded polymerization utilizing linear poly(4-methylstyrene) and n-hexane as porogens. b) is higher magnification of a).	213
Figure 5.6	SEM of crushed hollow particles obtained in dynamic swelling method	216
Figure 6.1	Histogram of the size-distribution of poly(styrene-co-acrylamide) microspheres obtained with different monomer ratios as indicated on the top of each peak	224
Figure 6.2	FT-IR spectrum of poly(styrene-co-acrylamide) particles. Composition: a) styrene, ratio of styrene/acrylamide (w/w): b) 20/1; c) 10/1; d) 5/1	226
Figure 6.3	Histogram of the size-distribution of poly(styrene-co-hydroxyethyl acrylate) microspheres obtained with different monomer ratios	228
Figure 6.4	Surface morphology of poly(DVB80-co-glycidyl methacrylate) microspheres	234
Figure 6.5	Effects of crosslinker concentration on poly(DVB80-co-vinyl benzyl chloride) copolymer particles	235
Figure 6.6	SEM micrographs of poly(DVB80-co-vinylbenzyl chloride) microspheres (a) (sample FM8e"-3) and surface structure (b) (sample FM8e"-7)	237

- xxi -

List of Figures (continued)		Page
Figure 6.7	Conversion-time plot of polymerization of DVB80 and vinylbenzyl chloride	238
Figure 6.8	Spectrum of X-ray microanalysis for poly(DVB80-co-vinylbenzyl chloride) microspheres	239
Figure 6.9	SEM micrograph of poly(bis(vinylphenyl) ethane-co-vinylbenzyl chloride) microspheres. Conditions: BVE/VBC = 50/50 (w/w); acetonitrile, 2 wt% AIBN; 70°C; 24 h	240
Figure 6.10	Reaction setup for oxidation of P4MSt microspheres	243
Figure 6.11	Influence of [AcOH] on particle size and size distribution of oxidized P4MSt microspheres at 45°C for one-hour oxidation	245
Figure 6.12	Influence of [AcOH] on particle size and size distribution of oxidized P4MSt microspheres at 45°C for two-hour oxidation	245
Figure 6.13	SEM of P4MSt microspheres oxidized at 45°C for one-hour. Concentration of acetic acid (vol%): (b) 20; (c) 30; (d) 40; (e) 50. (a) is a SEM of P4MSt microspheres prior to oxidation	247/249
Figure 6.14	FT-IR of P4MSt microspheres before oxidation (a) and the microspheres oxidized with 50 vol% AcOH for two-hours (b). (specimens were prepared with casting solution of polymer particles in THF on NaBr disc)	250
Figure 6.15	Particle-size distribution of P4MSt microspheres oxidized. Reaction conditions: 10 vol% of AcOH; 45°C	251
Figure 6.16	SEM of P4MSt microspheres oxidized at different time: (a) 1 h; (b) 2 h; (c) 4 h; (d) 6 h; Reaction conditions: 10 vol% of AcOH; 45°C	253/254
Figure 6.17	GPC profile of P4MSt microspheres oxidized in 50 vol% AcOH solution at different time: (a) 1 h; (b) 4 h	255
Figure 6.18	A reactor for oxidation reaction of PPDVB55 microspheres with cobalt catalyst	258

- xxii -

List of Figures (continued)		Page
Figure 6.19	(a) FT-IR spectrum of PPDVB55 microspheres (b) FT-IR spectra of PPDVB55 microspheres after 0 h (A) and 18 h (B) oxidation	260
Figure 6.20	FT-IR spectra of oxidized PPDVB55 microspheres at different reaction times	261

- xxiii -

LIST OF SCHEMES

List of Schemes		Page
Scheme 1.1	The principle of molecular imprinting with formation of a defined arrangement of binding sites within the microcavity	4
Scheme 1.2	Synthesis of divinylidibenzo-18-crown-6 (4)	13
Scheme 1.3	Dehydration of diol crown ether	20
Scheme 1.4	Approach for synthesis of <i>l</i> -phenylalanine methylester (PAME) selective template polymer	29
Scheme 1.5	Incorporating crown ether into poly(styrene-co-4-methoxystyrene-co-divinylbenzene) matrix	39

- xxiv -

LIST OF TABLES		
		Page
Table 1.1	Syntheses of dibenzo-18-crown-6 derivatives	21
Table 1.2	Solubility of a template molecule and its precursor	33
Table 1.3	Template polymers synthesized in different porogens	34
Table 1.4	<i>l</i> -PAME selective template polymers: AcN as porogen	36
Table 2.1	Characteristics of free-radical heterogeneous polymerization processes	61
Table 2.2	Examples of stabilizers used in polar media	68
Table 2.3	Definition of symbols	71
Table 3.1	Crosslinked particles by dispersion polymerization	85
Table 3.2	Standard recipe for optimizing agitation method	93
Table 3.3	Effect of DVB55 concentration on DPDVB55 particles	97
Table 3.4	Dispersion polymerization of DVB55 in ethanol	102
Table 3.5	Solvent effect on the formation of DPDVB55 microspheres	103
Table 3.6	Effect of PVP concentration on DPDVB55 particles	106
Table 3.7	Relative radical reactivities of DVB55 components	113
Table 4.1	Initiators used in this research	122
Table 4.2	Conditions for monodisperse PPDVB55 microspheres	128
Table 4.3	Effects of DVB55 concentration on PPDVB55 microspheres	132
Table 4.4	Effects of DVB80 concentration on PPDVB80 microspheres	135
Table 4.5	Effect of crosslinker percentage in comonomer mixture on diameter	139
Table 4.6	Effect of initiator decomposition rate on microspheres	148
Table 4.7	Solubility of AIYP in some solvents	151
Table 4.8	Effect of <i>n</i> -butanol on PPDVB55 microspheres in the system using AIYP as initiator	152
Table 4.9	Hansen solubility parameters	155
Table 4.10	Solvent effect on PPDVB55 microspheres	159/160

- xxv -

List of Tables (continued)

		Page
Table 4.11	Effect of <i>n</i> -butanol on PPDVB55 microspheres in a binary solvent system	164
Table 4.12	Miscibility of 2 vol% DVB55 in the mixture of acetonitrile and water	166
Table 4.13	Solubility parameters for mixture of acetonitrile/water	166
Table 4.14	First-order kinetics of PPDVB55	174
Table 4.15	Apparent rate constant of individual monomer in PPDVB55	179
Table 4.16	Porosity data from nitrogen adsorption analyses	187
Table 4.17	Porosity data from mercury intrusion analyses	187
Table 5.1	Dispersion polymerization of 4-methylstyrene	208
Table 5.2	Recipes for preparation of porous particles with linear polymer seed	211
Table 5.3	Recipes for preparation of porous particles with crosslinked polymer seed	211
Table 6.1	Structures and sources of monomers	220
Table 6.2	Dispersion polymerization of styrene and acrylamide	223
Table 6.3	Monomer reactivity ratio for AAm (m_1)- <i>co</i> -St (m_2)	227
Table 6.4	Dispersion polymerization of styrene and 2-hydroxyethyl acrylate	228
Table 6.5	Precipitation polymerization of DVB80 and GMA	231
Table 6.6	Effect of AIBN loading on Poly(DVB80- <i>co</i> -GMA) microspheres	233
Table 6.7	Cobalt catalyzed oxidation of PPDVB55 microspheres	259

- xxvi -

2

CHAPTER 1

TEMPLATE POLYMERS BEARING CROWN ETHER USED AS CHIRAL SEPARATION MEDIA

1.1 INTRODUCTION

The need for optically pure materials in many fields continues to grow. In general, racemic mixtures consist of enantiomers which are optically active isomers with identical physical and chemical properties. The difference in their stereochemical structures can be identified only by measuring their rotation of plane-polarized light or by interaction with chiral reagents to form diastereomers which have different properties. However, the conventional methods of resolution, such as fractional crystallization of diastereomeric derivatives require the presence of specific functional groups in the enantiomers and in addition it is necessary to prepare and then to decompose the diastereomeric compounds.^{1,2,3} For these reasons, these methods are essentially restricted to racemic acids and bases, often involve high losses and do not always yield optically pure samples. In addition to the traditional methods of resolution of racemic mixtures, considerable progress has been reported on resolution by chromatographic methods using naturally occurring or synthetic polymers as stationary phases. In general, chromatographic resolutions are of two types. The first involves separation of diastereomers, formed by reaction with chiral compounds, on achiral stationary phases. The alternative method is the method of choice for direct resolution on a preparative scale

using either a chiral eluent or a chiral stationary phase. Resolution of racemic mixtures by liquid chromatography has been done using a wide variety of asymmetric stationary phases.

Recently, highly crosslinked polymers containing chiral cavities have been prepared and used for the resolution of racemic mixtures in a manner reminiscent of enzymatic processes. Names such as "template polymerization",^{4,5} "host-guest polymerization" or "imprinting"⁶ have been used to describe the technique of preparation of enzyme-like synthetic polymers containing asymmetric cavities with functional groups fixed in exact stereospecific positions. Crosslinked macromolecules, formed by polymerization around a template molecule, have been shown to exhibit an affinity for the original template molecules in subsequent batch competition rebinding studies⁷ and when the polymeric materials are used as chromatographic supports⁸. Apart from the general theoretical interest in this technique, potential applications are obvious, notably the use of such polymers for resolution of racemic mixtures⁹, for stereoselective control of organic chemical reactions,^{5,7,8} and possibly also as enzyme or receptor mimics.¹⁰

1.1.1 Molecular Recognition of Template Polymers

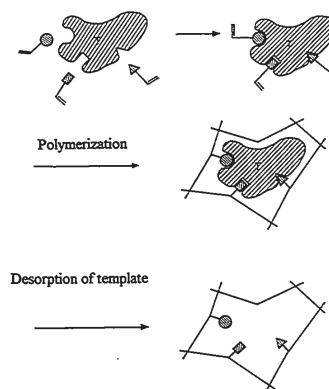
About four decades ago, a surface-imprinting technique was introduced by Dickey,¹¹ in which silica gel was produced in the presence of organic molecules. These molecules are later extracted, leaving 'footprints' or imprints of their shapes on the silica surface. Such surfaces may have a higher affinity to adsorb compounds of similar structures. At the same time, Pauling¹² presented the idea of constructing, by synthetic means, polymer network cavities which should fit only one of two enantiomers. Unfortunately, these studies did not receive much attention at that time.

During the 1970's, G. Wulff *et al.* introduced a new approach to the preparation of highly selective binding sites,^{4,7-13} which has some similarity with that of Dickey. The work showed that "in contrast to the usual resolution of racemates by interaction with a chiral molecule, no such species is required. Instead the resolution takes place in cavities, which are asymmetrical due to the particular spatial relationship of the functional groups".⁴ Basically, the principle rests on an imitation of an enzyme's binding site, which can usually be regarded as a chiral cavity or cleft in the protein, often highly specific with respect to binding of substrate enantiomers because of the precise steric requirements for multiple bond attachment. Because the experimental technique can be compared with making a plaster cast from an original template it has also been called 'molecular imprinting'. Thus, the molecules of a particular compound act as templates around which a rigid polymeric network is cast. This procedure, which is conceptually straightforward but quite delicate to carry out in practice, can be summarized in three distinct steps.

- (1) Formation of a complex between the compound used as template and a polymerizable monomer.
- (2) Polymerization with cross-linking to form a rigid matrix.
- (3) Removal of the template, either by washing, or, in the case of covalent attachment to the template, by means of a hydrolytic or similar reaction.

These steps are visualized in Scheme 1.1.

Polymerization by this template procedure results in the formation of a three-dimensional polymeric matrix interspaced by an occasional template assembly. After removal of the template molecule, free cavities result with a shape and an arrangement of



Scheme 1.1 The principle of molecular imprinting with formation of a defined arrangement of binding sites within the microcavity.

functional groups that correspond to those of the template. The functional groups on this polymer are located at quite different points of the polymer chain and are held in a spatial relationship by the crosslinking of the polymer. In most cases optically active template molecules were used. The resulting cavities, therefore, were chiral as well. Provided that the removal of the template by elution or hydrolysis does not introduce gross structural deformations in the macromolecule, the template-free polymer can exhibit a "memory" for the original template molecule. These polymers preferentially bind the exact configuration of the original template molecule, and may thus be used as batch or chromatographic separation media.⁹

To stabilize the asymmetric structure of the polymer and hence avoid the loss of the stereoregularity of the functional groups in the cavities after removal of the template molecules, the polymer is prepared under conditions that lead to a rigid low-swelling matrix which can be achieved by using a high degree of crosslinking. In addition, the functional groups of the cavities must undergo an easily reversible binding interaction with the template molecules that have been used in the preparation of the cavities, analogous to the active site in natural enzymes.

A typical example is G. Wulff's copolymerization of the tris-(4-vinylphenyl-boronic diester) of phenyl- β -D-mannopyranoside with excess ethylene glycol dimethacrylate in an equal volume of acetonitrile using 2,2'-azobis(isobutyronitrile) as initiator.¹⁴ In this case, the monomer units are covalently attached to the template. The chromatographic performance of this kind of sorbent is shown in Figure 1.1. The chromatogram illustrates one of the difficulties associated with the technique, viz. the necessity of fast reversible binding to reduce band broadening. Although boronic ester formation is a very fast process, it is still somewhat too slow for chromatographic purposes. It is important to keep in mind that most chromatographic sorption-desorption

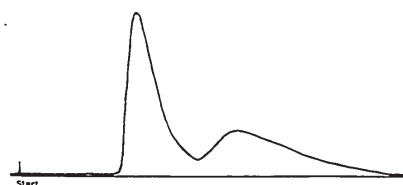
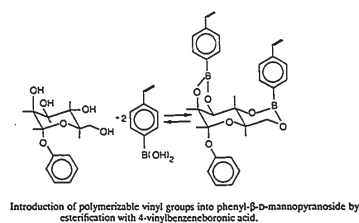


Figure 1.1 Elution profile from the chromatography of phenyl- β -D,L-mannopyranoside on macroporous polymer imprinted with the D-enantiomer. (Mobile phase: acetonitrile with 4% concentrated ammonia solution and 5% water, flow rate 0.1 ml/min.). (Ref. 18).

equilibria are based on non-covalent interactions, except for some protein separations by affinity chromatography where a thiol-disulphide interchange may contribute. Several template polymers of this type have been synthesized and used for the resolution of enantiomers of various racemic mixtures.

The free binding sites in Wulff's and similar covalently imprinted polymers sometimes show reasonable selectivity in rebinding the same template enantiomer from a solution of its racemate. The binding geometry was determined by covalent ester linkages between template and the polymerizable ligand. As a consequence, high activation energies are required to form or cleave the covalent (ester) bonds holding the template, and broad peaks were usually observed in chromatography using such imprinted polymers.¹⁸ These were concluded to be due to either (1) a slow binding reaction with a sterically hindered transition state of the covalent binding or (2) a slow orientation of the substrate in the cavity, when more than one binding interaction is possible. In addition, the template polymerization requires that the desired templates can be modified by vinyl substitution prior to their copolymerization with other vinyl monomers. Elaborate organic chemistry is often needed in this process, and this severely limits the application of covalent template polymers for chromatographic enantiomer separation. Therefore, a method which can obviate the need for both template modification and subsequent hydrolyses of polymers to remove polymer-bound template molecules is desired.

An alternative method of preparing substrate-selective polymers would be to utilize non-covalent (i.e., dipolar, electrostatic, hydrophobic, charge-transfer, hydrogen bonding) imprinting with the substrate in highly cross-linked polymers. In 1984, Mosbach and Sellergren *et al.*⁷ reported syntheses of *l*-phenylalanine ethyl ester-selective polymers. In this case, ion pairing between an amino acid ester and carboxylic acid groups of the monomer/polymer was utilized, resulting in macroporous polymers exhibiting substrate

selectivity and enantioselectivity when applied in a chromatographic procedure. The separation factor $\alpha = 1.04$ was obtained. The process since then has been optimized,^{8,15,16} and a separation factor $\alpha = 4.18$ has been achieved.¹⁷

1.1.2 Using Crown Ether Binding Sites in the Resolution of Enantiomers

Crown ethers are macrocyclic ring compounds containing several oxygens separated by ethylene moieties as shown in Figure 1.2. The term "crown ether" was coined in 1967 by Charles J. Pedersen because molecular models of these molecules, when viewed from the side, often resemble a crown in shape. Their ability to form strong complexes with metal cations as well as substituted ammonium ions has led to very

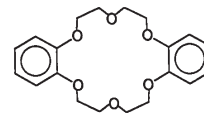


Figure 1.2 The structure of a nonchiral crown ether: dibenzo-18-crown-6

extensive research. In these early studies the cyclic compounds containing from five to ten oxygens atoms were shown to form stable complexes or "crown" a variety of cations.^{18,19} While working with the compounds, Pedersen recognized that the ability to form complexes between the various crown ethers and specific cations was size dependent. One interesting field is their use as phase-transfer agents, where the formation of lipophilic alkali-metal ion inclusion complexes is utilized for the transfer of alkali-metal

salts into organic solvents.²⁰ The field is now known as a branch of 'host-guest' complexation chemistry, mimicking Nature's principle for structural recognition, so common in biological regulatory systems.

Crown ethers and particularly 18-crown-6 derivatives form complexes with ammonium ion and protonated alkyl amines. By incorporating optically active ligands in the crown ether, optically active (chiral) 18-crown-6 molecules have been prepared.²¹ Stoddart and co-workers demonstrated a selective extraction-complexation property of this crown ether toward various racemic mixtures of chiral ammonium salts. In certain cases, the optically active ligands were able to complex one enantiomer of the amine salts more effectively than the other, thus leading the way for the application of suitable crown ethers to both solution and liquid-chromatographic resolutions of enantiomers.

The successful synthesis of optically active crown ethers led Cram and his collaborators to investigate their use for optical resolution purposes.²² Optically active crown ethers covalently attached to a polymeric support have been developed and used for the chromatographic separation of enantiomers of primary amine salts such as the salts of α -amino acids and their esters.²³ Figure 1.3(a) shows one of the chiral crown ethers synthesized by Cram *et al.*²⁴ and used to separate enantiomeric primary amines. In this type of separation, the degree of differentiation exhibited by a host molecule for a pair of enantiomers depends on the formation of temporary diastereomeric complexes usually held together by numerous hydrogen bonds. The phenomenon depends mainly on differences in steric relationships between the optically active crown ether and the two enantiomers being resolved. The situation is shown by Figure 1.3(b). The immobilized selector, the optically active crown ether of (R,R)-configuration, acts as the host, incorporating a guest, represented by the (S)-form of methyl phenylalaninate (as hydrochloride). All three protons of the ammonium group are hydrogen-bonded to crown

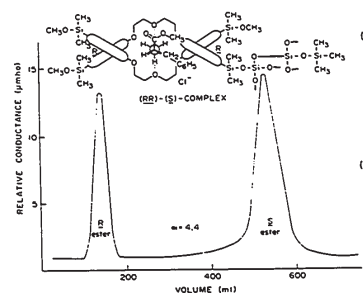


Figure 1.3 An example of a chiral crown ether. (a) Structure of the optically active crown ether used for optical resolution. (b) Chromatographic resolution of methyl phenylalaninate hydrochloride. (Ref. 24). The chirality of the crown ether is due to the twist in the naphthyl rings.

ether oxygen atoms. The conformational freedom within the complex is rather restricted and the geometry of the (S)-enantiomer permits an energetically more favorable conformation in the complexed form. Note that the crown ether, despite its apparent symmetry, can exist in four optically active forms because it is derived from the binaphthol units, which are resolvable owing to hindered rotation. The structure shown is obtained from the (R)-enantiomer. A relatively large number of racemates have been completely resolved by Cram's procedure, but thus far the approach has been found to be most effective for ammonium salts or amino ester salts.

Crown ethers selectively complex with cations. Ammonium ion has the proper ionic radius needed to fit into the 18-crown-6 cavity. The process of crown ether complexation with protonated amines is different than with metal ions because dipole-ion interactions are the only possible attractive forces in the metal ion case.^{25,26} However, in the case of 18-crown-6 polyethers different theories exist on the relative importance of the possible attractive forces between the host ether and guest ammonium ions. All six oxygens of the cyclic ether are interior to provide dipole to ion bonding as well as hydrogen bonding as visualized in Figure 1.4.²⁷ The gas phase association enthalpy of the 18-crown-6 ammonium cation complex has been calculated to be about 46 kcal/mol.²⁸

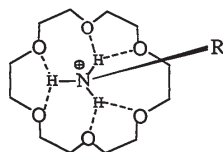


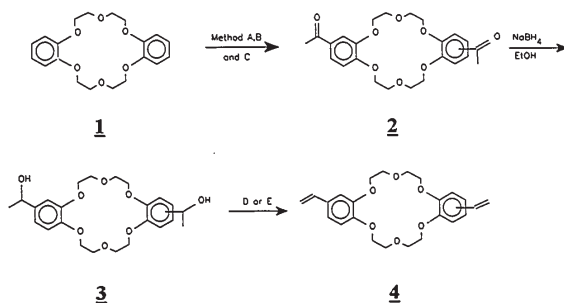
Figure 1.4 The interaction of an ammonium cation with a crown ether.

1.3 RESULTS AND DISCUSSION

1.3.1 Syntheses of Dibenzo-18-Crown-6 Derivatives

To introduce crown ether binding sites into the polymer network, we first had to synthesize vinyl substituted dibenzo-18-crown-6 as a polymerizable ligand. The aromatic rings of dibenzo-18-crown-6 are very reactive toward electrophilic substitution. Thus, a large number of substituted dibenzo-18-crown-6 crown ethers should be readily available from dibenzo-18-crown-6.

The general route to divinyl-dibenzo-18-crown-6 used in this work is outlined in Scheme 1.2, and discussed on the following page.



Scheme 1.2 Synthesis of divinyl-dibenzo-18-crown-6 (4).

1.2 AIM OF THE RESEARCH

As discussed above, essentially two different approaches have been used in the syntheses of template polymers: (a) reversible covalent binding of the print molecule to the monomers; (b) prearrangement of functionalized monomers around the print molecule by noncovalent interactions (i.e., electrostatic, hydrophobic, hydrogen bonding).^{7b,c} The covalent approach slows the removal of templates and the subsequent binding of the substrate molecules. The non-covalent approach has had some success so far, but has been limited by the weak binding energy of single, isolated hydrogen bonds (ca. 3 kcal/mol).

The focus of this research is to develop a template-ligand bonding that is intermediate in strength to covalent and individual non-covalent bonds. This non-covalent template approach will be based on the complex formation between chiral ammonium cations and vinyl-derivatized dibenzo-18-crown-6. A polymer embodying 18-crown-6 units would make an excellent anchor for templates containing at least one (primary) ammonium cation. The chiral binding sites form around the template-crown complex only during the polymerization step, which fundamentally differs from earlier work where inherently chiral crown ether derivatives serving as preformed chiral cavities were attached to insoluble supports.^{29,30,31,32} Such system would ideally allow rapid and spontaneous formation of the initial template complex, and efficient removal of the template after polymer formation. Template molecules amenable to recognition by these 18-crown-6 systems would include amino acids, oligopeptides with one or more free amino groups, substituted anilines, amino sugars and in general all primary ammonium compounds that are stable under the template polymerization conditions.

4,4'-diacetyldibenzo-18-crown-6 (2): A variety of methods have been developed for electrophilic acylation of reactive aromatic systems.³³ Nearly all of these methods involve catalysis by Lewis acids such as aluminum chloride, etc.

Although crown ethers are well known for their ability to form strong complexes with alkali metal and organic cations, no studies of complexes formed between crown ether and aluminum salts have been reported. It was suggested that the acylation of dibenzo-18-crown-6 catalyzed by AlCl₃ would be possible.³⁴ Efforts were made to synthesize 2 in this research by using 1 and acetyl chloride as reactants in methylene chloride in the presence of AlCl₃. A pink color solution was formed during the reaction. Only starting material 1 was recovered, which indicated that no acetylation of dibenzo-18-crown-6 had occurred. A similar situation had been encountered by Parish *et al.*³⁵ when they attempted the acylation of dibenzo-18-crown-6 with succinic anhydride. It is believed that the Lewis acid catalyst and/or the reactive electrophilic intermediate may be complexed and consequently deactivated by the crown ether.³⁵

When AlCl₃ was replaced by tin tetrachloride (SnCl₄), partial acylation of dibenzo-18-crown-6 was observed. In general, a cherry red solution was formed, followed by the formation of a dark red precipitate during the reaction. The final yield of total products was 99.5%, however, the selectivity toward 2 was low. ¹H-NMR indicated that the products were mixtures of 1 and 2, and the degree of acylation varied from about 15% to 40%, depending upon the amount of catalyst used. Zitsmanis³⁶ used SnCl₄ as catalyst in the reaction of dibenzo-18-crown-6 with succinic dichloride to synthesize polymer-bound dibenzo-18-crown-6. However, no information about the efficiency of acylation was given. The formation of precipitate and the low conversion in our case are presumably due to the same reason mentioned above, i.e., the formation of a complex between SnCl₄ and the crown ether. Since separation of 2 from the mixture was not practical, the conditions

of reaction were varied in an attempt to effect complete conversion of reactant. The reaction temperature was varied in increments of 10°C from 25°C to 65°C. No apparent improvement was observed. Attempts to vary the ratio of reactants to catalyst as well as their concentrations were essentially unsuccessful. A significant portion of the reactant remained in these reactions. The highest conversion in this reaction was about 40%.

The difficulties in acylation of dibenzo-18-crown-6 stems from the strong complexes of these metal-containing Lewis acids with the crown. A non metal-containing Lewis acid would be suitable for this acylation as indicated by Percec³⁷ who used polyphosphoric acid (PPA) as a catalyst in the acylation of dibenzo-18-crown-6 with 8-bromooctanoic acid to afford the bis(acetylated)dibenzo-18-crown-6 free of side products. Accordingly, PPA was chosen in this research.

Polyphosphoric acid (PPA) was used as both solvent and acylating catalyst for the acylation of DB18C6 with acetic acid. PPA is extremely viscous at room temperature, and requires higher reaction temperatures (90°C) to be handled easily. The reaction time was held to less than 1 hour after the temperature reached 90°C to avoid side reactions. A tiny amount of a white polymeric by-product was found under the conditions used, which was easily separated from the product. This procedure gave 89% conversion of **1** to **2**. The product has a melting range of 193-197°C. The broad range may in part stem from the formation of isomers in the diacylation of **1**. In addition, the product purity depends greatly upon the quality of the dibenzo-18-crown-6 starting material.

2 was also successfully synthesized according to the procedure described by Stott.³⁵ In this procedure, Eaton's reagent is used as acylating catalyst. Eaton's reagent is prepared by dissolving phosphorus pentoxide in anhydrous methanesulfonic acid.³⁸ It is a superior reagent for the acylation of benzo-crown ether compounds. Even though it has

been reported that this method leads to both acylation and glycol cleavage products, our experiments gave only acylation products.

Figure 1.5 shows the 200 MHz proton NMR spectra of, (a) precursor of **2** (dibenzo-18-crown-6), and, (b) compound **2**. The peak at 2.5 ppm is assigned to the methyl groups of **2**. Integration indicates that the reaction was complete within the accuracy of NMR.

4,4'-bis(1-hydroxyethyl)-dibenzo-18-crown-6 (3): The carbonyl groups of **2** were reduced to hydroxyl groups to give 4,4'-bis(1-hydroxyethyl)-dibenzo-18-crown-6 (**3**). The reaction was conducted in ethanol medium using NaBH₄ as reducing reagent at room temperature. The yield of the product was 85%. **3** was easily dissolved in methylene chloride. Upon standing in a refrigerator a crystalline compound precipitated from the solution. The crystal is presumably one of the two isomers of **3** and is soluble in methanol or ethanol.

Figure 1.6 (a) is the ¹H NMR spectrum of **3** taken in CD₃OD solvent. The integration of the spectrum and the complete disappearance of the peak at 2.5 ppm indicates that the conversion of carbonyl groups was complete.

4,4'-divinyldibenzo-18-crown-6 (4): The vinyl crown ether, 4,4'-divinyldibenzo-18-crown-6, was obtained in the last step in which two alternative methods were involved. In method D, thionyl chloride (SOCl₂) was added to a mixture of **3** and pyridine in chloroform at 0°C followed by refluxing. It was expected that 4,4'-dichloroethyldibenzo-18-crown-6 would be the product. However, the result showed that compound **4** was produced instead, which indicated the substitution of hydroxyl group by the chlorine followed by dehydrohalogenation. The workup of this product was made difficult because of emulsification, and led to 69% crude product. The final yield of **4** was

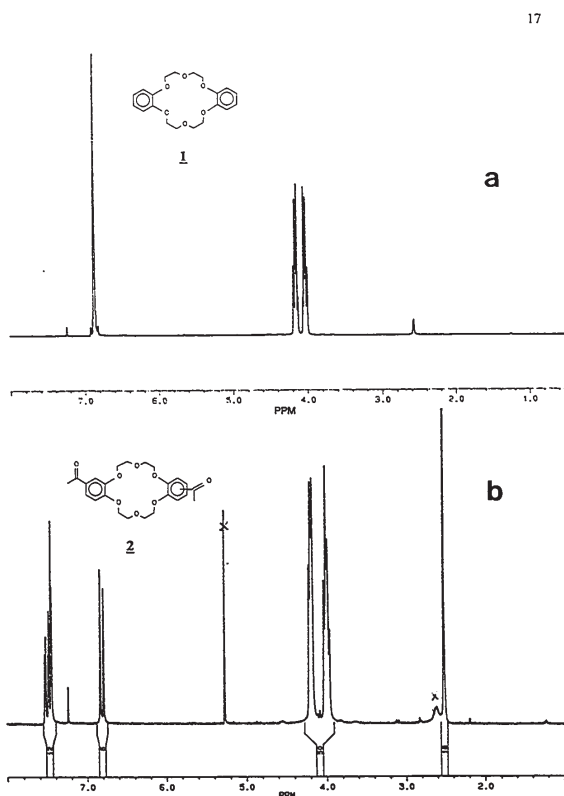


Figure 1.5 200 MHz ¹H NMR spectra of (a) dibenzo-18-crown-6 (**1**) and (b) diacetyldibenzo-18-crown-6 (**2**). Solvent: CDCl₃.

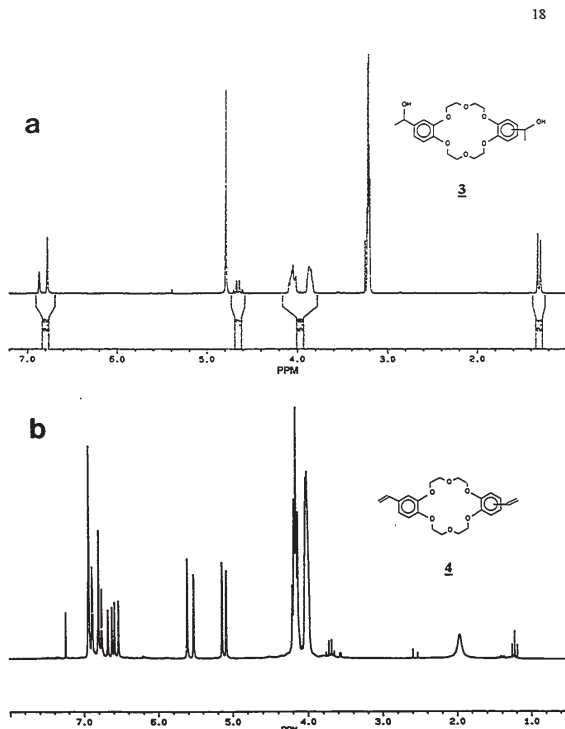


Figure 1.6 200 MHz ¹H NMR spectrum of (a) **3**, solvent: CD₃OD; (b) **4**, solvent: CDCl₃

32%. The reproducibility of this reaction was poor. Polymeric materials were observed during the reaction from time to time.

To achieve a high yield of divinylbenzo-18-crown-6, different solvents and catalysts were tried for the dehydration of **3**. Virtually only polymeric materials resulted upon heating for even short time except for the system of *p*-toluenesulfonic acid with dimethylsulfoxide (*p*-TSA/DMSO).

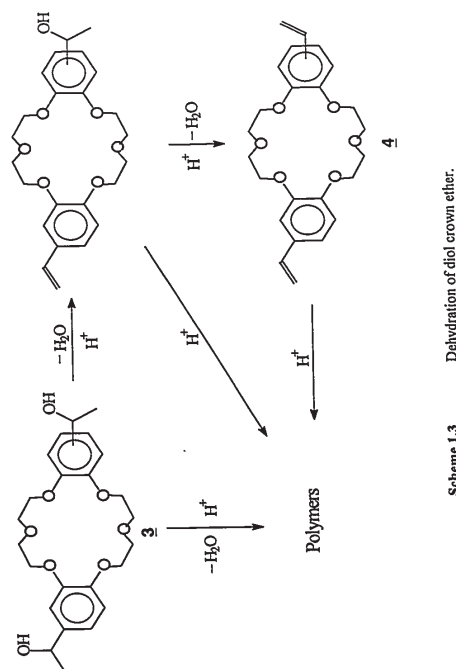
It is well known that dehydration of an alcohol is an efficient route to vinyl compounds. However, this method is limited to the preparation of volatile α -phenylethyl alcohol derivatives, since products must usually be distilled out during production, otherwise, cationic polymerization occurs rapidly. The dehydration of **3**, shown in Scheme 1.3, must compete with rapid cationic polymerization; normally the former is much slower than the latter. However, the *p*-TSA/DMSO system gave the desired product with high yield (85%) and without byproduct, even though a rather high reaction temperature (140-150°C) was used. DMSO probably here acts as a retardant for the cationic polymerization.³⁹

Figure 1.6(b) shows the ¹H NMR spectrum of this vinyl monomer. The results of syntheses of dibenzo-18-crown-6 derivatives are summarized in Table 1.1.

Table 1.1 Syntheses of Dibenzo-18-Crown-6 Derivatives

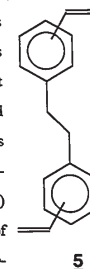
Compound	Method	Conditions	Time (hr.)	Temp. (°C)	m.p. (°C)	Yield (%)
2	A	$\text{SnCl}_4/\text{CH}_3\text{COCl}/\text{CH}_2\text{Cl}_2$	20	25		
	B	PPA* + AcOH	1	90		89.2
	C	AcOH, P_2O_5 / $\text{CH}_3\text{SO}_3\text{H}$	24	25	193-197	98.3
3		a) $\text{NaBH}_4/\text{EtOH}$	24	25	166-169	94.8
		b) $\text{H}_2\text{SO}_4(\text{aq})$				
4	D	SOCl_2 , Pyridine / CHCl_3	24	80		32.0
	E	<i>p</i> -TSA* / DMSO	0.25	140	146-148	85.0

* PPA = Polyphosphoric Acid, *p*-TSA = *para*-Toluene Sulfonic Acid.

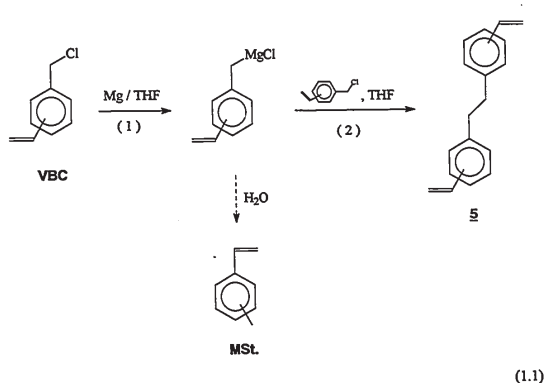


1.3.2 Novel Crosslinking Agent

In order to get template polymers with high matrix rigidity, a large amount of a bifunctional crosslinking agent is required. As a preliminary study, we have chosen commercial divinylbenzene (DVB55) as a crosslinking agent because of its availability and low cost. Commercial divinylbenzene consists of a mixture of four main isomers: *para*- and *meta*-divinylbenzene (55%), *para*- and *meta*-ethylstyrene (42%). Each of these isomers has a different radical reactivity as reported by Walcznski.⁴⁰ It is also well known that the reactivities of the two vinyl groups in *p*-divinylbenzene are quite different. The reactivity of the second double bond of the divinylbenzene isomers is different from that of the first one after the molecule has been incorporated into the polymer. These reactivity differences stem from the conjugation of the two vinyl groups through the benzene ring. Therefore, in addition to functionality that is intentionally introduced by the template synthesis method, the polymer also contains a large number of unsaturated groups as a result of only partially polymerized divinylbenzene. As well, the crosslink sites are inhomogeneously distributed in the polymer network.^{41,42,43} The resulting polymer resin is structurally and chemically heterogeneous. This can give rise to gradations in chemical reactivity over regions of the polymer. As a result of this inhomogeneity, the distribution of functionality at the polymer-solvent interface is poorly defined. In contrast to divinylbenzene, the two vinyl groups in **5** are electronically isolated from each other, and are thus expected to show identical reactivities. Actually, the reactivity ratios in free-radical copolymerization of styrene with *p,p'*-**5** ($r_1=1.06$, $r_2=0.87$, $r_1r_2=0.92$) manifest more uniformly distributed crosslinkages as compared with those of styrene and *m*-DVB ($r_1=0.65$, $r_2=0.60$, $r_1r_2=0.39$) or those of styrene and *p*-DVB ($r_1=0.14$, $r_2=0.50$, $r_1r_2=0.07$).^{44,45}



The synthesis of compound $\underline{5}$ is based on the Grignard coupling of two equivalents of vinylbenzyl chloride (VBC) with magnesium turnings (Mg) in tetrahydrofuran (THF). Commercial VBC which contains 70% *meta*- and 30% *para*-vinylbenzyl chloride was used as starting material. Two steps are involved in the formation of $\underline{5}$ (reaction 1.1). The Grignard reagent was formed relatively slowly in the first step, and then reacted rapidly with more vinylbenzyl chloride in the second step to produce bisvinylphenyl ethane, $\underline{5}$.



One of the by-products in this reaction is 4 (or 3)-methylstyrene which is formed by reaction of the Grignard reagent with a trace of water. Even under anhydrous

conditions we observed a small amount of methylstyrene that was already present in the starting material, vinylbenzyl chloride.

The synthesis was initially conducted with 15.26g (0.1 mol) of starting material at 5 to 10°C. $\underline{5}$ was produced as well as a noticeable amount of polymeric materials. At or below 0°C, reactions gave products without these polymeric materials. It was found that a starting temperature of -5°C and maintenance of the reaction temperature at 0°C was sufficient to give both high yield (84%) and high purity (96%) of $\underline{5}$. Recently, this reaction has been scaled up to 91.57g of starting material (VBC) with yield and purity of $\underline{5}$ both better than 95%.⁴⁶

Commercial VBC contains 70% *meta*- and 30% *para*-vinylbenzyl chloride. The Grignard coupling of this material is expected to produce three isomers, *m,m*- $\underline{5}$, *m,p*- $\underline{5}$ and *p,p*- $\underline{5}$. They should be produced in the relative amounts expected assuming equal reactivities for both starting isomers, viz, *m,m*- $\underline{5}$: *m,p*- $\underline{5}$: *p,p*- $\underline{5}$ = 49 : 42 : 9 (Figure 1.7).

Figure 1.8 shows the ¹H NMR spectrum of the products. The expanded benzylic region reveals the isomeric composition. The three singlets for the ethylene protons (around 2.9 ppm) correspond to the *m,m*- (2.89ppm), *m,p*- or *p,m*- (2.88ppm), and *p,p*- (2.87ppm) isomers of $\underline{5}$. In addition, a small peak at 2.35 ppm is assigned to the methyl group of methylstyrene which is present in traces in the starting material. In fact, methylstyrene may also be produced during the reaction (equation 1.1).

The product was analyzed by using reverse phase HPLC (high performance liquid chromatography). Base line resolved chromatograms were obtained using a SEPARON C18 column and a mixture of 85% methanol / 15% water as eluent. A UV detector operating at 254 nm was used. Figure 1.9 is an example of the reverse phase HPLC profile of the product. The peaks eluted at retention times of 30, 33 and 38 minutes

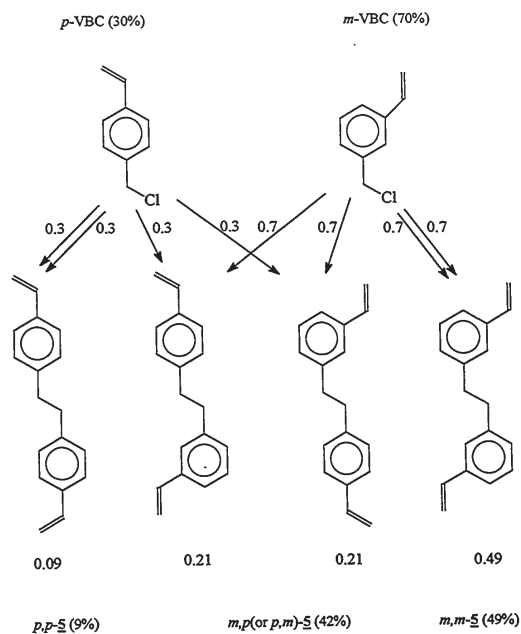


Figure 1.7 Statistical composition of BVPE isomers

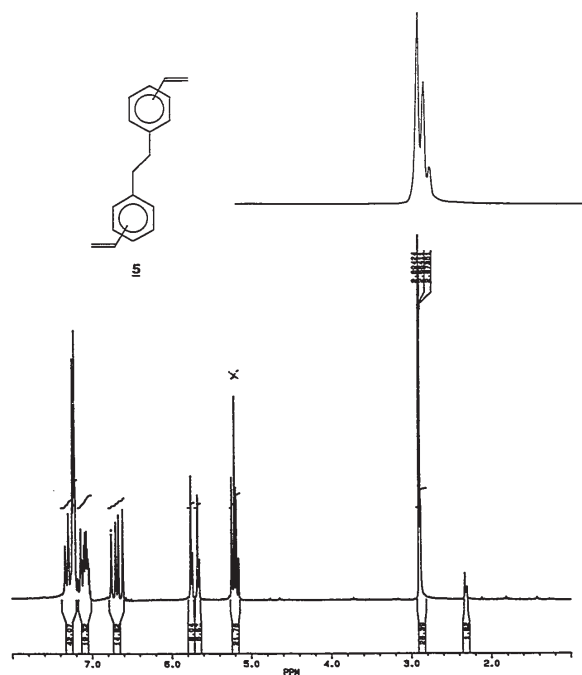


Figure 1.8 200 MHz ¹H NMR spectrum of 1,2-bis(vinylphenyl) ethane ($\underline{5}$). Solvent: CDCl₃.

correspond to *m,m*-, *m,p*- and *p,p*-**5**. Two small peaks around the retention time of 8-10 minutes arise from methylstyrenes. It was noticed that they were present even in the starting material. Area normalization was used for the peak integration according to the following equation:⁴⁷

$$X\% = \frac{f_i \cdot A_i \cdot 100}{\sum_j f_j \cdot A_j} \quad (1.2)$$

Where X is the concentration of compound x ; and f_i is the response factor of compound i in the mixture. If we assume that each isomer of BVPEs has the same f value, a calculation gives the composition of the isomers: *m,m*-**5** : *m,p*-**5** : *p,p*-**5** = 47 : 45 : 8, which is close to the expected statistical distribution of these isomers in the product.

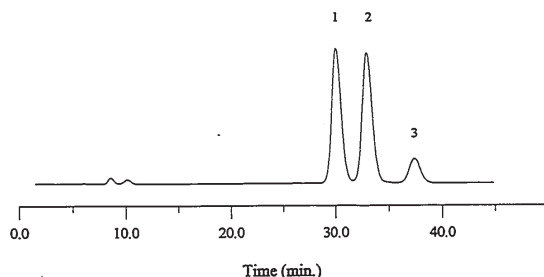
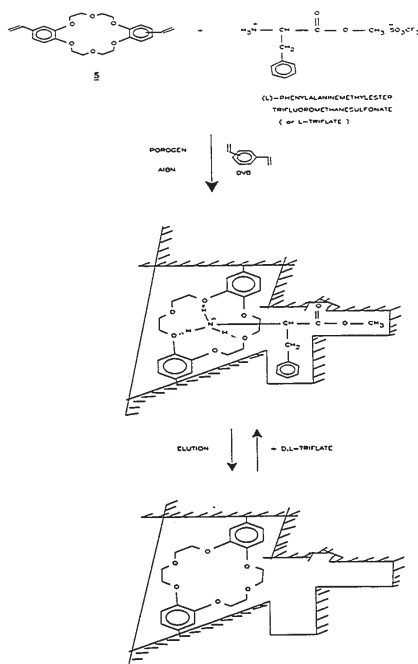


Figure 1.9 Reverse phase chromatography of the mixture of compound **5** isomers. peak 1: *m,m*-**5**; peak 2: *m,p*-**5**; peak 3: *p,p*-**5**. Solvent: methanol / water (85:15); Flow rate: 1 ml/min; Temp.: 20°C.



Scheme 1.4 Approach for synthesis of phenylalanine methylester (PAME) selective template polymer.

It was noticed that white crystals separated from the initial viscous product upon storing in a refrigerator for several hours. They have been identified as *p,p*-**5** which is the most symmetrical of the three isomers. No attempt was made to separate each individual isomer from the mixture in this research. The crosslinker synthesized, **5**, was used in related suspension polymerization,⁴⁶ while the template polymerizations described below were carried out with DVB55 as crosslinker.

1.3.3 Synthesis of *L*-Phenylalanine Methyl Ester (PAME)

Selective Template Polymer

In the light of the principle we have discussed above, our synthetic approach for a phenylalanine methyl ester (PAME) selective template polymer is schematically outlined in Scheme 1.4.

Dibenzo-18-crown-6 is used as a receptor, which is bound to an appropriate ammonium cation to form a polymerizable template complex as described earlier. As a model reaction we chose a UV detectable chiral starting material (*L*-phenylalanine methyl ester salt) which binds to divinylbenzo-18-crown-6 to form a polymerizable complex. This is then copolymerized using radical initiation in the presence of an inert solvent with a high amount of a bifunctional crosslinking agent. During polymerization, the complexed ammonium cation will occupy a position slightly above the plane of the crown, with its motion largely restricted to rotation around an axis perpendicular to the plane of the crown. After polymerization, the resulting polymer is continuously washed by solvent. Elution of the template from the formed matrix should be rapid and complete. The template polymer is packed into an HPLC column, which is then tested for separation of *d*- and *l*-phenylalanine methyl ester salt.

1.3.3.1 Choice of crosslinking reagent and porogen

There are several factors influencing the quality of the imprinted polymers.¹⁴ To maintain the stability of the specific cavity after removal of the template, the polymer should possess high rigidity. This can be achieved by applying a large amount of crosslinking reagent during the polymerization. For covalent bond template polymers, it should also possess some degree of flexibility⁷⁶ in order to enable a fast reversible binding of the substrates to the transition state. In contrast, the matrix of non-covalent template polymers may be made more rigid through the use of more and shorter crosslinkers, because these cavities do not have to undergo configurational changes during binding and release as transition state to binding should closely mimic the binding geometry.

In this research, technical grade divinylbenzene (DVB55) was chosen as crosslinking reagent due to its availability and low cost as well as a number of other desirable properties. PolyDVB55, synthesized by free-radical initiated polymerization, is a highly cross-linked three-dimensional network of styrene-type polymer. It is a brittle, glassy, amorphous substance that is insoluble in all organic solvents and chemically inert to most reagents.^{48,49} Divinylbenzene is a rigid crosslinker which is able to produce a material capable of sustaining permanent porosity.⁵⁰

For molecular recognition, the macroporous structure of the template polymer is desirable since it gives access to a large number of binding sites. It is known that the microphase separation that takes place during polymerization leads to the macroporosity of the polymer. The precipitated polymer particles aggregate and, depending upon the porogen, can further agglomerate to produce materials with a permanent porosity.^{51,52} The porosity in these materials arises from the interstitial voids between the precipitated polymer particles. There are a number of variables that influence the formation of

macroporous materials including the nature and the percent of cross-linker, also the type and amount of porogen as pointed out by Li, Stöver and Hamielec⁵³ and others.^{54,55,56}

Our selection of a porogen was made from the consideration of the solubility behavior of the template molecule. *l*-Phenylalanine methyl ester hydrochloride was initially tried as the template molecule. The high polarity of this compound makes it soluble in water, methanol and ethanol, however, only slightly soluble in other polar solvents such as acetonitrile (AcN), dimethylsulfoxide (DMSO), and dimethylformamide (DMF), etc. It was our intention to use acetonitrile as a porogen for the following reasons: it has been demonstrated that polydivinylbenzene with reasonable porosity can be obtained in the presence of acetonitrile;⁵ AcN is a proper solvent for HPLC analysis, and it also has a better compatibility toward polydivinylbenzene resin (compared with ethanol); most importantly, divinyl crown ether **4** is soluble in acetonitrile.

1.3.3.2 Solubility of the template molecule

To increase the solubility of the template molecule in acetonitrile, *l*-phenylalanine methyl ester hydrochloride was converted to *l*-phenylalanine methyl ester trifluoromethanesulfonate (*l*-triflate) (equation 1.3). *l*-Triflate is completely soluble in AcN, DMSO, and DMF. The solubilities of *l*-phenylalanine methyl ester hydrochloride and *l*-triflate in different solvents are listed in Table 1.2. They were measured by mixing 0.1 g of each salt with 5.0 ml of solvent. *l*-Triflate was insoluble in CH₂Cl₂, but soluble in CH₂Cl₂ in the presence of **4** due to the formation of the complex between ammonium cation and the crown ether. The same phenomenon was observed for toluene at temperatures above 60°C.

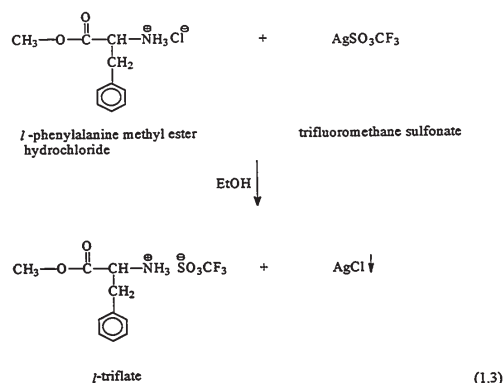


Table 1.2 Solubility of Template Molecule and Its Precursor

Solvent	<i>l</i> -PAME-HCl	<i>l</i> -Triflate
AcN	ss	cs
DMSO	ss	cs
DMF	ss	cs
CH ₂ Cl ₂	is	is
toluene	is	is
EtOH	cs	cs
MeOH	cs	cs
H ₂ O	cs	cs

is = insoluble; ss = slightly soluble; cs = completely soluble;
l-PAME-HCl = *l*-phenylalanine methyl ester hydrochloride;

1.3.3.3 Polymerization

Polymerization was initiated by a free-radical initiator (AIBN) was used for most of the experiments) at reaction temperatures of 60 to 70°C. In some preparations azobis(2,4-dimethylvaleronitrile) was used as the initiator. Since this initiator decomposes at lower temperatures (see Chapter 3), polymerizations were carried out at 40°C for 24 hours. These *l*-phenylalanine methyl ester selective polymers were prepared with a low fraction of template monomer in DVB in order to avoid the possibility of site-site interactions.

In order to test the reactivity of divinylbenzo-18-crown-6, the copolymerization of styrene with the template monomer complex using acetonitrile as solvent was conducted; a gel polymer was obtained (TP-01). The swellability of TP-01 was 4.75 in CHCl₃. ¹H NMR analysis of the residual showed the complete conversion of

crown ether. This indicates that compound **4** will copolymerize with other vinyl monomers smoothly under the conditions used.

To examine the effect of the porogen on the molecular recognition of PAME selective template polymers, polymerizations were performed in acetonitrile as well as in other solvents (or porogens). Table 1.3 lists the results of these polymerizations in different porogens other than in acetonitrile. In all cases, about equal weights of porogen and monomer mixtures were used.^{7a} Polymerization in a good solvent, toluene, led to a gel type of polymer (TP-04-4) which will shrink in a poor solvent such as methanol, and

Table 1.3 Template polymers synthesized in different porogens

TP Code	Solvent 6 ml	DVB55 (g)	4 (g)	<i>l</i> -triflate (g)	Time (hr)	Comment
TP-04-1	DMSO	4.0	0.31	0.25	12	Block
TP-04-2	DMF	4.0	0.31	0.25	24	Block
TP-04-3	EtOH	4.0	0.31	0.25	12	Block
TP-04-4	toluene	4.0	0.31	0.25	36	Gel

polymerization was initiated by 0.04g AIBN (1.0 wt.%) at 70°C.

swell in a good solvent such as methylene chloride. The volume swellability was 3.23 as determined in chloroform. In terms of molecular recognition, TP-04-4 is therefore not suitable because the shapes of specific cavities would probably not be preserved upon removal of template molecules. Template polymers obtained in any of the other porogens were hard blocks of polymer. The conversions of these polymerizations were nearly quantitative.

The morphologies of the template polymers depend greatly on the amount of acetonitrile (Table 1.4). TP-02 was synthesized with a large amount of DVB55 relative to acetonitrile. The resulting polymer formed one block which was hard, rigid and therefore had very good mechanical stability. When the amount of porogen was increased from 6 to 20 ml, the appearance of the polymer changed to irregularly shaped particles such as those indicated in Figure 1.10. These particles were formed by the aggregation of primary particles during the polymerization.^{52,57} This polymer could take up quite a large amount of non-solvent because of its porosity. Even though these particles had high crosslinking densities, the mechanical strength of the aggregates was low. The aggregates easily broke

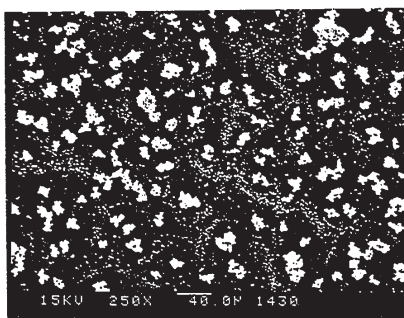


Figure 1.10 SEM micograph of template polymer.

upon touching either in dry or wet state, due to the loose adhesion between the aggregated primary particles. It was noticed that the sizes of these particles decreased with increasing amount of porogen. At the ratio of DVB55 : AcN = 1 : 5, hard particles with more regular shape were obtained from time to time (TP-03 in Table 1.4). Polymerization under these conditions falls into the category of precipitation polymerization, which will be discussed in detail in Chapter 4. When a polymeric stabilizer, such as polyvinylpyrrolidone (PVP), was used in the system, spherical hard particles were produced. TP-07 was synthesized under the same conditions as TP-03, but in the presence of PVP. The polymer obtained was in form of small particles with a narrow size distribution (around 2-3µm, optical microscopy). This polymerization is a dispersion polymerization (see Chapter 3).

1.3.4 *L*-Lysine Methyl Ester Dihydrochloride Selective Template Polymer

PAME template polymers were formed usually in the form of large, hard blocks or as loose aggregates, which led to some difficulties during HPLC tests (see section 1.3.5). With respect to HPLC, uniform spherical resins are desired. We therefore tried to incorporate crown ether binding sites, as well as the crown-template complex, directly into preformed polymer beads. The polymer beads were formed by the suspension polymerization of commercial divinylbenzene, and had an optimal spherical shape for chromatographic applications. *L*-Lysine methyl ester dihydrochloride was used as a template molecule (Figure 1.11). This molecule contains two ammonium cations. By introducing its crown complex into the polymer, the template polymer thus obtained may have specific cavities containing two crown binding sites instead of one as is the case with the PAME selective template polymer.

Table 1.4 PAME selective template polymers: AcN as porogen

Sample	Styrene (g)	DVB55 (g)	4 (g)	<i>r</i> -iriflate (g)	AIBN (g)	AcN (ml)	Temp. (°C)	Time (hr)	PVP (g)	Comment
TP-01	4.0	—	0.34	0.25	0.05	20	75	24	—	Gel
TP-02	—	4.0	0.31	0.25	0.1	6	60	24	—	C*
TP-03	—	4.0	0.31	0.25	0.05	20	60	24	—	particles (2.5-3µm)
TP-07	—	4.0	0.31	0.25	0.05	20	60	24	0.4	particles (2-3µm)

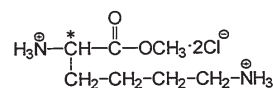
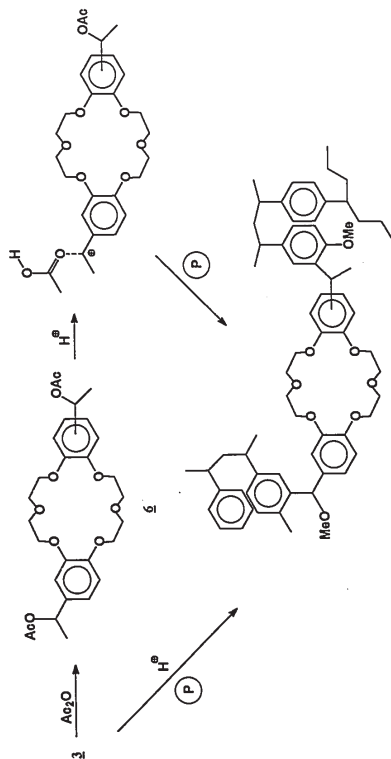


Figure 1.11 *L*-Lysine Methyl Ester Dihydrochloride

The process of incorporation is illustrated in Scheme 1.5. The diol, **3**, was acetylated to form bis(acetoxyethyl)dibenzo-18-crown-6 (**6**). Both the hydroxyethyl groups in **3** and the acetoxyethyl groups in **6** easily generate benzylic cations in the presence of a strong acid such as trifluoromethanesulfonic acid. These cations can then undergo electrophilic aromatic substitution on neighboring aromatic rings.⁵⁸ Difunctional crowns in the presence of linear polystyrene chains may thus act as a crosslinking agent, by reacting with aromatic rings situated on two different polymer chains. In the case of the diacetoxy crown, **6**, the electrophilic aromatic substitution regenerates an acid proton at the end of each reaction cycle, thus making the reaction catalytic with regards to the acid.

We introduced the reactive crown ether into both linear and crosslinked polymers based on styrene and 4-methoxystyrene. Poly(styrene-co-4-methoxystyrene-co-divinylbenzene) was not reactive towards electrophilic aromatic substitution, and showed higher compatibility with the ionic ammonium and metal templates.

The diol crown **3** was incorporated into linear polystyrene using traces of triflic acid to give the expected crosslinked polymer in high yield. The poly(styrene-co-divinylbenzene) and the poly(styrene-co-4-methoxystyrene-co-divinylbenzene) beads were swollen in a small amount of methylene chloride containing one of the two crown ether derivatives **3** or **6**. Small amounts of neat triflic acid were added, and the mixtures were



Scheme 1.5 Incorporating crown ether into a poly(styrene-co-4-methoxystyrene-co-divinylbenzene) matrix.

Scheme 1.5

stirred at 20°C for 1 to 3 days. After washing with methylene chloride, *N,N*-dimethylformamide, and methanol, and Soxhlet extraction with methylene chloride, the polymers were swollen with excess deuterio chloroform, and characterized by ^1H and ^{13}C NMR.

Figures 1.12a and 1.12b show the static ^1H NMR spectra of poly(styrene-co-divinylbenzene) before and after reaction with 10 wt.% of **3**. In order to eliminate some of the homogeneous broadening imposed by the crosslinking, the chloroform swollen sample was spun at the magic angle in a Doty MAS probe. The resulting direct polarization magic angle spinning (DP/MAS) 500 MHz ^1H NMR spectrum (Figure 1.12c) of the polymer incorporating diol **3** clearly shows a baseline resolved signal for the crown ether attached to the polymer. The corresponding DP/MAS ^{13}C NMR spectrum (Figure 1.12d) shows the crown ether carbon signals at 65 ppm.

Figure 1.13 shows the ^1H NMR spectrum of poly(styrene-co-4-methoxystyrene-co-divinylbenzene) after reaction with 10 wt% of diacetoxymethyl crown **6**. The small broad signal at 3.75 ppm indicates the incorporated crown ether. Incorporation even of the diacetoxymethyl crown ether into this activated methoxy polymer is low, suggesting substantial homopolymerization of the crown.

Of the two crown ether derivatives, the diacetoxymethyl crown **6** proved more reactive than the diol crown **3**. These results correspond with the better leaving group ability (nucleofugicity) of acetic acid compared to water, as well as the rapid deactivation of the trifluoromethanesulfonic acid catalyst by the water eliminated from the diol crown. Both diol and diacetoxymethyl crowns were more easily incorporated into the crosslinked polystyrenes that contained 4-methoxystyrene units. The polar nature of the methoxystyrene copolymers facilitated diffusion of the crown ether and of the acid catalyst through the polymer beads. As well, the 4-methoxy styrene units are best able to compete

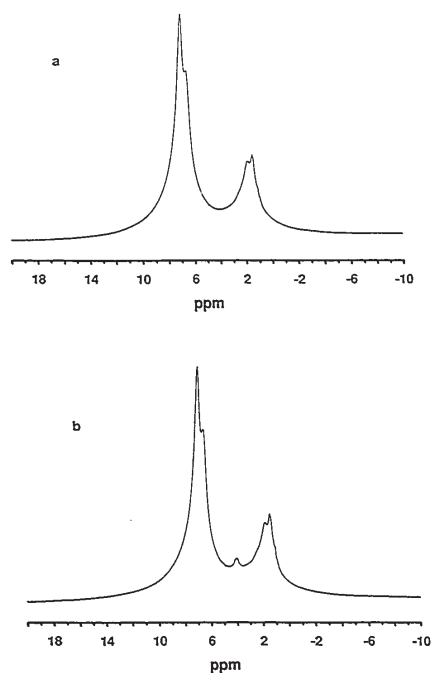


Figure 1.12 (a) Static ^1H NMR spectrum of poly(styrene-co-divinylbenzene); (b)-(d) The same polymer after incorporation of bis(hydroxyethyl)dibenzo-18-crown-6. (b) static ^1H NMR spectrum, (cont. on next page).

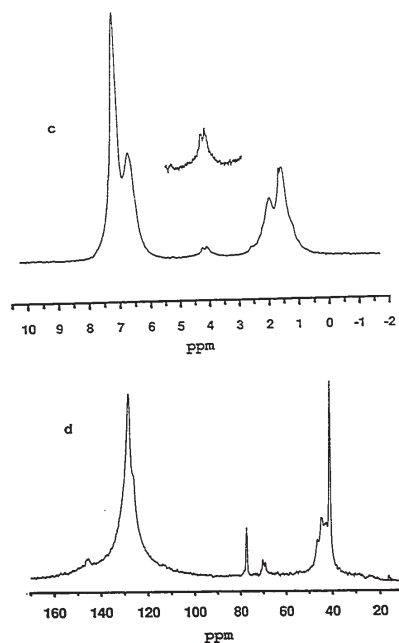


Figure 1.12 (cont.) (c) direct polarization magic angle spinning ^1H NMR spectrum. (d) static ^{13}C NMR spectrum.

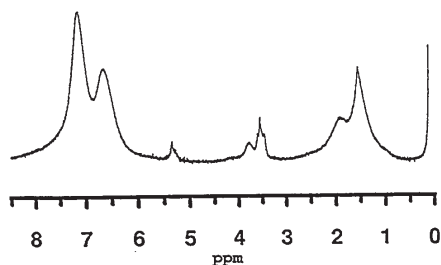


Figure 1.13 Static 500 MHz ^1H NMR spectrum of poly(styrene-co-4-methoxystyrene-co-divinylbenzene) after incorporation of bis(acetoxyethyl)dibenzo-18-crown-6.

with other crown ether molecules for the benzylic cations formed in the reaction. The incorporation into both polymers increased with reaction time from 1 to 3 days. Higher crown ether concentrations also led to higher incorporation.

It is conceivable that if two crown ethers, both complexed to the same diammonium cation such as *l*-lysinemethylester dihydrochloride, are attached to such a network, they may carry their spatial relationship from the complex over into the polymer. The resulting polymer would then show a high affinity for the *l*-lysine based diammonium cations over other dications or monocations. Accordingly, *l*-lysinemethyl ester dihydrochloride was first complexed with two equivalents of diol crown **3**, and the resulting complex incorporated into the crosslinked polymer as described above. In this case, six cooperative hydrogen bonds should provide enough binding energy to hold the template molecule in place. The resulting crown ether crosslinked polymer should contain permanent molecular cavities reflecting the shape of the template molecule. The incorporation of the crown ether was verified by ^1H NMR of the deuteriochloroform swollen gel. No further tests were performed on this polymer.

1.3.5 Characterization of PAME Selective Template Polymers

Template polymers are highly crosslinked and, thus, insoluble in all solvents. In addition, the presence of a wide distribution of pore sizes results in opacity. Therefore, the chiral cavities cannot be characterized by direct spectroscopic methods. Instead techniques that have to be employed give indirect information. Since the specific chiral cavities formed inside the polymer matrix will preferentially take up the original template enantiomer, the resolution of the racemate of the template, therefore, can be used for evaluating the molecular recognition abilities of the template polymers.^{4,7,59,60} High

performance liquid chromatography (HPLC) was used to test PAME template polymers for the resolution of PAME racemate.

The template polymers obtained were extracted on a Soxhlet apparatus with acetonitrile for 24 hours, then slurry-packed into a 1x10 cm adjustable glass HPLC column. The glass column had a 0.25 μm filter on the outlet. HPLC experiments were conducted with a Waters pump Model 590 and a 441 UV detector (254 nm). Acetonitrile was used as the mobile phase. The selectivity of the template polymer is expressed as the separation factor α , which is the ratio of the distribution coefficients between solution and polymer of *l*- and *d*-PAME-TR. The calculation of α is based on equation 1.4.

$$\alpha = \frac{v_{R2} - v_0}{v_{R1} - v_0} \quad (1.4)$$

v_{R2} and v_{R1} - retention volume of *l*- and *d*-template molecule;
 v_0 - void volume (determined by the retention volume of toluene).

α is a measure of relative peak separation and is constant under given analytical conditions (stationary and mobile phase, temperature, etc.). It is independent of factors that do not affect the equilibrium constants of the system, such as flow-rate, column dimensions, particle size, etc. Such factors, on the other hand, are of fundamental importance for the column efficiency.⁶¹

Four template polymers were packed into a glass column and tested as described above. The retention volumes of *l*- and *d*-triflate were identical on a column except polymer TP-07. TP-02 was in the form of a block, which was grounded to fine particles. The particles of less than 75 μm diameter were collected by sieving, and fines were removed by repeated sedimentation in methanol. The top portion of the solution

containing extremely fine particles was discarded. The lower portion of the solution was mixed with more pure methanol and this procedure repeated twice. The particles left were then packed into the column. Initially, some fine particles of size less than 0.25 μm were eluted out with acetonitrile. The back pressure of this column was initially low (200 psi), but it kept increasing to above 1200 psi, beyond the capacity of the glass column. To avoid this difficulty, a stainless steel column (4.6x250 mm) was used instead of the glass column. A slurry was made by mixing the particles with a solvent mixture of methylene chloride and acetone balanced to match the density of the particles. The column was packed using a Shandon HPLC packing pump operated at a constant pressure of 1600 psi. A similar situation occurred. With a flow rate of 0.2 ml/min, the back pressure was relatively low at the beginning, but gradually went up beyond the limitation of HPLC system. Apparently, the high back pressure was due to the broad distribution of the TP-02 particles.

TP-07 was synthesized under the conditions of dispersion polymerization. The polymer was in the form of small particles with relative narrow size distribution. TP-07 particles were packed into the glass column and gave a moderate back pressure of 1000 psi when the flow rate of eluent was 0.4 ml/min. For this column, a separation factor of $\alpha = 1.03$ was obtained. Figure 1.14 shows the elution profile of *l*- and *d*-triflate on TP-07.

The selectivity of 1.03 is not very marked. However, considering the separation was obtained without any optimization, the result is promising. In template polymerization, in general, the lack of separation ability may be attributed to a number of factors including:

- shrinking and swelling of the polymer may deform the chiral cavities. Molecular recognition of the template polymer is based on the specific binding sites and the shape of the chiral cavities; it only happens if the shape of the cavity can be preserved

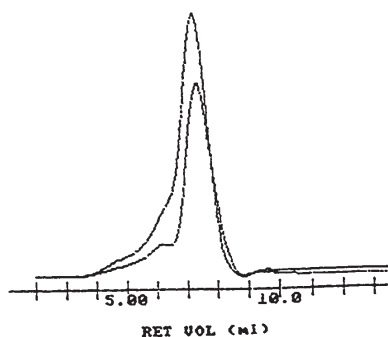


Figure 1.14 Elution profile of *d*- and *l*-triflate applied on TP-07 polymer. Eluent: acetonitrile; Temperature: 25°C; flow rate: 0.4 ml/min.

throughout the process. Any physical changes of the polymer matrix, including the high pressure in the HPLC process, may impact on the properties of these cavities, and may jeopardize the ability of template polymer to separate enantiomers of the template.

- technical grade divinylbenzene contains at least four components. The differences of these monomers and reactivities of two vinyl groups in divinylbenzene result in inhomogeneous polymerization. The macroporous polymers produced contain regions of different density of cross-linking. It is possible that the specific cavities (or anchoring sites) might be located in the dense and highly crosslinked parts of the polymer (the so-called nuclei)⁶². In this case, removing and binding new templates will be difficult. The actual number of binding sites or cavities would be reduced dramatically, which would lead to lower separation ability of the polymer.
- not enough macropores were created on the polymer bead surface. This would also limit the number of accessible binding sites.

Probably, the factors mentioned above could be optimized to increase the efficiency of molecular recognition on our PAME selective template polymers. However, another problem lies in the morphology of the template polymers. HPLC column packings of 3-10 μm spherical particles are known to show acceptable back pressures and less peak broadening compared with irregular shaped particles. Our attention, therefore, focused on synthesizing highly crosslinked polystyrene-type particles in the range of 3 to 8 micron diameter under conditions which are suitable for our template polymerization process. This will be described in Chapters 3 and 4.

1.4 EXPERIMENTAL

General. Dibenzo-18-crown-6, acetyl chloride, acetic acid, polyphosphoric acid, tin tetrachloride and all other reagents were obtained from Aldrich; *l*- and *d*-phenylalanine methyl ester hydrochloride, and *l*- and *d*-lysine methyl ester dihydrochloride were purchased from Sigma. 2,2'-Azobis(isobutyronitrile) (AIBN, Eastman Kodak) and 2,2'-azobis(2,4-dimethylvaleronitrile) (ADVN, Polysciences) were used without further purification. DVB55 and styrene monomers were passed through neutral alumina columns to remove the phenolic inhibitor.

¹H NMR spectra were recorded using a Bruker AC 200 spectrometer. ¹³C NMR were measured at 125.7 MHz on a Bruker AM 500 spectrometer. ¹H and ¹³C chemical shifts are reported relative to tetramethylsilane. Where necessary, peaks attributable to the minor impurities are marked with an asterisk (*). HPLC tests of template polymers and reversed-phase HPLC were carried out on a Waters model 590 pump with a model 441 UV detector. A Separon C18 column (4.6 x 250 mm) was used as reversed-phase column, and the mobile phase was a mixture of 85% methanol and 15% water at a flow rate of 1 ml/min.

4,4'-diacetyldibenzo-18-crown-6 (2) **Method A:** Acetyl chloride (1.54 g, 20 mmol) and tin tetrachloride (5.12 g, 20 mmol) were added dropwise to a stirred solution of **1** (3.60 g, 10 mmol) in 75 ml of methylene chloride at 0°C. Then, stirring was continued for 20 h at room temperature, during which time the reaction mixture turned cherry red and a precipitate was formed. After adding 30 ml of cold dilute HCl(aq), the mixture was refluxed until all the precipitate was dissolved. The organic phase was removed by a separatory funnel and washed three times with water; and then was separated from the

water phase, and dried over magnesium sulfate. Evaporation of the solvent gave 4.41g (99.5%) of brown product. The NMR spectrum showed that the product was a mixture of **1** and **2**.

Method B: Compound **1** (3.60 g, 10 mmol) and acetic acid (25 mmol) were added to polyphosphoric acid (39.83 g). The mixture was heated to about 90°C for 1 h under strong stirring. After pouring the mixture onto 50 g of ice, an equal volume of water was added and the mixture was stirred for another 8 h. The crude brown product was removed by filtration, dissolved in 75 ml of methylene chloride, and washed three times with dilute sodium hydroxide solution and then with water. The organic phase was separated and dried over anhydrous magnesium sulfate. The solvent was evaporated and the solid recrystallized from ethanol to give 3.96 g (89.2%) of a light tan product.

Method C: Diacylation of DB18C6 by using Eaton's reagent; This method was described by P.E. Stott in 1978⁵⁵. **Preparation of Eaton's reagent:** A mixture of 8.5 g of phosphorus pentoxide and 100.0 g of anhydrous methanesulfonic acid was stirred for about 30 h until all of the solids were dissolved. **Diacylation reaction:** Compound **1** (15.0 g, 41.5 mmol) and acetic acid (6.45 g, 107.5 mmol) were added to the reagent, respectively. The solution turned to cherry red. The reaction mixture was stirred overnight at room temperature, poured into 500 g ice water, and stirred overnight. Methylene chloride (200 ml) was used to extract the product from the solution. The organic phase was washed three times with dilute sodium hydroxide solution and water, respectively, then dried over anhydrous magnesium sulfate. Evaporation of the solvent gave 18.18 g (98.3%) of light tan product. m.p.: 193-197°C.

¹H NMR (200 MHz, CDCl₃, ppm): δ 2.52 (s, 6H, -CH₃), 3.97-4.21 (m, 16H, CH₂O), 6.8-7.54 (m, 6H, aromatic -CH-).

4,4'-bis(1-hydroxyethyl)-dibenzo-18-crown-6 (**3**): To 4.55 g (0.01 mol) of **2** and 100 ml of ethanol was added 2 g (0.05 mol) of sodium borohydride (NaBH₄), the mixture was stirred overnight, and the excess of NaBH₄ was destroyed with dilute sulfuric acid (H₂SO₄). Water (200 ml) was added and the mixture was extracted four times with 25 ml portions of methylene chloride. Upon removal of the methylene chloride 4.35 g (94.8%) of crude product was obtained. The crude product (4.15 g) was extracted with methylene chloride in the Soxhlet apparatus for 6 h and 1.83 g of white solid was obtained after evaporation of methylene chloride. It is one of the isomers of **3**, m.p. 166-169°C. ¹H NMR (200 MHz, CD₃OD, ppm): δ 1.30 (d, 6H, -CH₃), 3.84-4.05 (m, 16H, CH₂O), 4.65 (q, 2H, -CH-CH₃), 6.78-6.87 (m, 6H, aromatic -CH-).

4,4'-divinyldibenzo-18-crown-6 (**4**). Attempted preparation: *para*-toluenesulfonic acid (*p*-TSA) catalyzed dehydration in benzene gave only polymer. Similarly, attempted reaction with PCl₃/pyridine to form the di(chloroethyl)dibenzo-18-crown-6 also resulted in the formation of polymers.

The successful synthesis of the monomer (**4**) was achieved by the following two procedures: a) 0.8 ml (11.0 mmol) of thionyl chloride was added dropwise to a mixture of 0.97 g (2.17 mmol) of **3**, 1.0 ml (12.36 mmol) of pyridine and 50 ml of chloroform, with stirring at 0°C. The mixture then was heated to reflux (ca.80°C). Gas evolution began (SO₂). The solution turned red and the reaction continued overnight. After pouring into 300 ml of water, the mixture was extracted with methylene chloride, and separated. The organic phase was washed several times with water, then dried over MgSO₄. Evaporation of solvent gave 0.62 g (69.5%) of crude product. Crude product (0.13 g) was recrystallized from ethanol to give 0.06 g of product. m.p. 146-148°C, yield 32%.

for another 4 h. The solution was decanted from unreacted magnesium, the solvent evaporated at room temperature, and the residue treated with a mixture of 150 ml hexanes and 100 ml ice water. The aqueous layer was acidified with dilute HCl and then removed. The organic phase was washed three times with 100 ml distilled water, separated, and dried with anhydrous magnesium sulfate. The solvent was evaporated to give 11.63 g light yellow oily product, a statistical mixture of *m,m*-, *m,p*-, and *p,p*- isomers of **5**. The color was eliminated by passing the product dissolved in hexanes through a short column packed with silica gel under nitrogen, and 9.87 g (84%) of a white oily product was obtained after evaporation of the hexanes. White crystalline flakes were formed upon storing the oily product at 0°C. m.p. 92.5-93.5°C. ¹H NMR (200 MHz, CDCl₃): δ 7.1-7.35 (m, aromatic -CH-); 6.7 (dd, -CH=CHH); 5.7 (dd, -CH=CHH); 5.2 (dd, -CH=CHH); 2.9 (s, -CH₂-CH₂-).

Synthesis of *l*-PAME selective template polymers (general). Compound **4** (0.31 g, 0.75 mmol) and *l*-phenylalanine methyl ester trifluoromethane sulfonate (0.25 g, 0.75 mmol) were dissolved in varying amounts of porogen in a glass bottle (size of the bottle depends the amount of porogen). Commercial divinylbenzene (4.0 g) and AIBN (0.05 g) were added. The mixture was stirred with a magnetic stirrer at 70°C. The polymerization usually was stopped after 24 h. The polymer obtained was ground if it was in the form of a block. Polymer particles were then extracted with acetonitrile in a Soxhlet apparatus for 24 h.

Incorporation of *l*-lysine methylester dihydrochloride into polystyrene. Compound **3** (0.2 g, 0.4 mmol) was dissolved in an acetone/chloroform (vol. ratio 3:1) solution with *l*-lysine methylester dihydrochloride. The solvent was removed under

b) Trace of *p*-toluene sulfonic acid was added to the mixture of **3** (4.14 g) and dimethylsulfoxide (100 ml) in an open 250 ml round bottom flask. The temperature was increased to ca.140-150°C for 10 min and some moisture was evolved. The mixture was then poured into water with stirring and extracted into methylene chloride (three times, 50 ml each). The methylene chloride phases were washed twice with water, then the solution was concentrated under vacuum and poured into petroleum ether. The precipitate was filtered and dried in vacuum to afford 3.24 g product. m.p. 146-148°C, yield 85%. ¹H NMR spectrum are identical for both a) and b). ¹H NMR (200 MHz, CDCl₃, ppm): δ 4.00-4.19 (m, 16H, CH₂O), 5.08-5.13 (dd, 2H, -CH=CHH), 5.52-5.61 (dd, 2H, -CH=CHH), 6.53-6.67 (dd, 2H, -CH=CH₂), 6.75-6.92 (m, 6H, aromatic -CH-).

4,4'-bis(1-acetoxyethyl)dibenzo-18-crown-6 (**6**). The diol crown **4** (8.18 g, 18.2 mmol) was dissolved in 90 ml of acetic anhydride, and the solution was stirred for 24 h at 60°C. After the solvent was removed under reduced pressure, the residual solid was recrystallized from ethyl acetate, and dried under vacuum for 24 h. Yield: 7.63 g (81%). ¹H NMR (200 MHz, CDCl₃): δ 1.44 (d, 6H, CH₃), 2.17 (s, 6H, -CO-CH₃), 3.9-4.2 (m, 16H, CH₂O), 5.75(q, 2H, CH), 6.7-6.9 (m, 6H, aromatic -CH-).

1, 2-bis(vinylphenyl) ethane (5**).** THF was dried by refluxing over potassium and distilled. Commercial chloromethylstyrene is inhibited by *tert*-butylcatechol and nitromethane. These inhibitors were removed by vacuum distillation at 2 mbar.

Oven-dried magnesium (1.26 g, 0.06 mol) covered with 100 ml THF in a 250 ml round bottom reactor was cooled to 0°C under nitrogen. Chloromethylstyrene (15.26 g, 0.1 mol) was added slowly with stirring (color of the solution changed to green). The reaction was kept at 0°C for 20 h, then 0.35 g Mg was added to the solution, and reacted

vacuum and the remaining solid complex dried on a vacuum line for 2 h. This complex was redissolved in chloroform together with 2 g of polystyrene. Triflic acid (15 mol %) was used to catalyze the reaction at room temperature for 2 h. The resulting polymer gel was purified by exhaustive washings with methanol, acetone, chloroform methylene chloride and acetonitrile. ¹H NMR (CDCl₃): δ 1.2-2.4 (m, CH₃ of hydroxyethyl, CH and CH₂ of polystyrene); 3.6-4.4 (s, CH₂ of crown ether); 6.3-7.3 (aromatic -CH- of **3** and polystyrene).

Copolymerization of styrene with the complex of **4 and *l*-triflate.** Compound **4** (divinyldibenzo-18-crown-6, 0.49 g) and template (*l*-triflate) (0.25 g) were dissolved in 20 ml of acetonitrile in a 100 ml round bottle. Styrene (4.0 g) and AIBN (0.05 g) were added. Polymerization was conducted at 70°C under nitrogen for 24 h. The crosslinked polymer was ground and washed with methylene chloride in a Soxhlet apparatus. Swellability of this polymer was 4.75 in chloroform.

Chromatographic Experiments. The polymers were ground mechanically. The fraction having diameters smaller than 75 μm was collected by sieving. Fines were removed by repeated sedimentation in methanol. The following conditions were used in the chromatographic investigations: acetonitrile was used as eluent; the amount of *l*-PAME triflate used was varied between 3 and 30 mmol, in a volume of 20 μl; the flow rate was 0.4 ml/min or less depending upon the back pressure; the elution was monitored at 254 nm; the enantiomers were injected separately, and the retention times were determined by measurement of the peak maxima elution times; the void elution time (or column dead volume) was determined by injecting a small amount of toluene.

Determination of Polymer Swellability: For some polymers, the process of swelling in chloroform was observed in a thin walled 5 mm NMR tube. The extent of swelling was described as a specific volume change defined as V / V_0 , where V and V_0 are the average volume of polymer particles after and before the swelling test, respectively.

REFERENCES

- 1 R.M. Sekor, *Chem. Rev.*, **63**, 297 (1963).
- 2 S.H. Wilen, *Topics in Stereochemistry*, Vol. 6, Wiley Interscience, New York and London, p. 107, 1973.
- 3 R. Audebert, *J. Liq. Chromatogr.*, **2**, 1063 (1979).
- 4 G. Wulff, A. Sarhan, and K. Zabrocki, *Tetrahedron Lett.*, 4329 (1973).
- 5 K.J. Shea; E.A. Thompson; S.D. Pandey; and P.D. Beauchamp, *J. Am. Chem. Soc.*, **102**, 3149 (1980).
- 6 R. Arshady; and K. Mosbach, *Makromol. Chem.*, **182**, 687 (1981).
- 7 a) A. Sarhan; and G. Wulff, *Makromol. Chem.*, **183**, 1603 (1982).
b) G. Wulff; R. Kemmerer; J. Vietmeier; and H.-G. Poll, *J. Chim.*, **6**, 681 (1982).
c) G. Wulff; W. Vesper; R. Grobe-Einsler; and A. Sarhan, *Makromol. Chem.*, **178**, 2799 (1977).
d) G. Wulff; J. Gimpel, *Makromol. Chem.*, **183**, 2469 (1982).
- e) K.J. Shea, and E.A. Thompson, *J. Org. Chem.*, **43**, 4255 (1978).
- f) J. Damen; and D.C. Neckers, *Tetrahedron Lett.*, 1913 (1980).
- g) J. Damen; and D.C. Neckers, *J. Am. Chem. Soc.*, **102**, 3265 (1980).
- h) B. Anderson; B. Sellergren; and K. Mosbach, *Tetrahedron Lett.*, **25**, 5211 (1984).
- 8 a) G. Wulff; and W. Vesper, *J. Chromatography*, **167**, 171 (1978).
b) G. Wulff; and M. Minarik, *J. High Res. Chrom.*, **9**, 607 (1986).
c) B. Sellergren; B. Ekberg; and K. Mosbach, *J. Chromatogr.*, **347**, 1 (1985).
d) B. Sellergren; M. Lepistö; and K. Mosbach, *J. Am. Chem. Soc.*, **110**, 5853 (1988).
e) M. Glad; O. Norrlov; B. Sellergren; N. Siegbahn; and K. Mosbach, *J. Chromatogr.*, **347**, 11 (1985).
- 9 G. Wulff, *J. Liq. Chromatogr.*, **9**, 385 (1986).
- 10 G. Wulff, *Biomimetic Reactions Using Organized Polymeric Supports, in Biomimetic Polymers*, C.G. Gebelein (Ed.), p1, Plenum Press, New York, 1990.
- 11 F.H. Dickey, *Proc. Natl. Acad. Sci.* **35**, 227 (1949).
- 12 L. Pauling, *Chem. Eng. News.*, **27**, 313 (1949).
- 13 G. Wulff, A. Sarhan, *Angew. Chem.*, **84**, 364 (1972); *Angew. Chem. Int. Ed. Engl.*, **11**, 341 (1972).
- 14 G. Wulff, *Molecular recognition in polymers prepared by imprinting with templates*, ACS Symp. Ser. No.308, American Chemical Society, Washington, DC, 1986.
- 15 L. Andersson, *Reactive Polymers*, **9**, 29 (1988).
- 16 B. Sellergren, M. Lepistö, and K. Mosbach, *J. Am. Chem. Soc.*, **110**, 5853 (1988).
- 17 M. Lepistö, and B. Sellergren, *J. Org. Chem.*, **54**, 6010 (1989).
- 18 C. Pedersen, *J. Am. Chem. Soc.*, **89**, 2495 (1967).
- 19 C. Pedersen, *J. Am. Chem. Soc.*, **89**, 7017 (1967).
- 20 G.W. Gokel, and H.D. Durst, *Aldrichim. Acta*, **9**, 3 (1976).
- 21 W.D. Curtis, D.A. Laidler, J.F. Stoddart and G.H. Jones, *Chem. Commun.*, **833**, 835 (1975).
- 22 E.P. Kyba, G.W. Gokel, F. de Jong, K. Koga, L. R. Sousa, M. G. Siegel, L. Kaplan, G.D.Y. Sogah and D.J. Cram, *J. Org. Chem.*, **42**, 4173 (1977).
- 23 a) G. Dotsevi, Y. Sogah, and D.J. Cram, *J. Am. Chem. Soc.*, **97**, 1259 (1975);
b) G. Dotsevi, Y. Sogah, and D.J. Cram, *J. Am. Chem. Soc.*, **98**, 3038 (1976).
- 24 L.R.Sousa, G.D.Y. Sogah, D.H. Hoffman and D.J. Cram, *J. Am. Chem. Soc.*, **100**, 4569 (1978).
- 25 D.J. Cram, *Science*, **183**, 803 (1974).
- 26 A. Hamilton, 'Comprehensive Heterocyclic Chemistry' Vol. I, A. Katritzky, C. Rees, eds., Pergamon Press, New York, 1984.
- 27 M. Hilton, and D.W. Armstrong, *J. Liq. Chrom.*, **14**, 3673 (1991).
- 28 D. Gehin, P.A. Collman, G. Wipff, *J. Am. Chem. Soc.*, **111**, 3011 (1989).
- 29 W. Bussmann, J.-M. Lehn; U. Oesch; P. Plumere and W. Simon, *Helv. Chim. Acta*, **64**, 657 (1981).
- 30 V. Prelog, *Pure Appl. Chem.*, **50**, 893 (1978).
- 31 G. D. Y. Sogah and D. J. Cram, *J. Am. Chem. Soc.*, **101**, 3035 (1979).
- 32 T. Kakuchi, T. Takaoka and K. Yokota, *Polym. J.*, **22**, 199 (1990).
- 33 L.G. Wade, Jr.; *Organic Chemistry*, Prentice-Hall, Inc., 1987.
- 34 C.J. Pedersen, *U.S. Patent* 3 687 978, 1972.
- 35 W.W. Parish, P.E. Stott, and C.W. McCausland, *J. Org. Chem.*, **43**, 4577 (1978).
- 36 A. Zitsmanis, A. Roska and M. Klyavinsh, *Reactive Polymer*, **9**, 59 (1988).
- 37 V. Percec, and R. Rodenhouse, *Macromolecules*, **22**, 2043 (1989).
- 38 P.E. Eaton, G.R. Carlson, and J.T. Lee, *J. Org. Chem.*, **38**, 4071 (1973).
- 39 J. Nishimura; Y. Ishida; K. Hashimoto; Y. Shimizu; A. Oku and S. Yamashita, *Polym. J.*, **13**, 635 (1981).
- 40 B. Walcznski, B. N. Kolazz, and H. Galina, *Polym. Commun.*, **26**, 276 (1985).
- 41 O. Okay, *Makromol. Chem.*, **189**, 2201 (1988).
- 42 G. Hild, R. Okasha, *Macromol. Chem.*, **186**, 93 (1985).
- 43 D. R. Miller, C. W. Macosko, *J. Polym. Sci., Polym. Phys.*, **26**, 1 (1988).
- 44 R.H. Wiley, G.L. Mayberry, *J. Polym. Sci., Part A*, **1**, 217 (1963).
- 45 R.H. Wiley, J.K. Allen, S.P. Chang, K.E. Musselman, and T.K. Venkatachalam, *J. Phys. Chem.*, **68**, 1776 (1964).
- 46 W. H. Li, K. Li, H.D.H. Stöver, and A.E. Hamielec, *J. Polym. Sci., Polym. Chem.*, **32**, 2023 (1994).
- 47 K.A. Rubinson, *Chemical Analysis*, by Little, Brown & Company Limited, 1987.
- 48 J. L. Amos, L. C. Rubens, and H. G. Hornbacker, *ACS Monogr.*, No. 115, 709 (1970).
- 49 W. Funke, *Chimia*, **22**, 111 (1968).
- 50 K.J. Shea, G.J. Stoddard, D.M. Shavelle, F. Wakui, and R.M. Choate, *Macromolecules*, **23**, 4497 (1990).
- 51 M. Bartholin, G. Boissier, and J. Dubois, *Makromol. Chem.*, **182**, 2025 (1981).
- 52 A. Guyot, *Synthesis and Separations Using Functional Polymers*; D.C. Sherrington, P. Hodge, Eds.; John Wiley & Sons: New York, p1, 1989.
- 53 W.H. Li, H.D.H. Stöver, and A.E. Hamielec, *J. Polym. Sci. Polym. Chem.*, in press.
- 54 J. Seidl, J. Malinsky, K. Dusic, and W. Heitz, *Adv. Polym. Sci.*, **5**, 113 (1967).
- 55 J.R. Millar, D.G. Smith, W.E. Marr, and T.R.E. Kressman, *J. Chem. Soc.*, 218 (1963).
- 56 J.R. Millar, *J. Polym. Sci., Polym. Symp.*, **68**, 167 (1980).
- 57 K.A. Kun, and R. Kunin, *J. Polym. Sci. Part A-1*, **6**, 2689 (1968).
- 58 J.M.J. Fréchet, S. Matuszczak, B. Reck, H.D.H. Stöver, and C.H. Willson, *Macromolecules*, **24**, 1746 (1991).
- 59 G. Wulff, W. Best, and A. Akelah, *React. Polym. Ion Exch., Sorbents*, **2**, 167 (1984).
- 60 K.J. Shea, E.A. Thompson, S.D. Pandey, and P.S. Beauchamp, *J. Am. Chem. Soc.*, **102**, 3149 (1980).
- 61 L.R. Snyder, J.J. Kirkland, *Introduction to Modern Liquid Chromatography*, 2nd ed., Wiley, New York, 1979.
- 62 G. Wulff, R. Grobe-Einler, W. Vesper, and A. Sarhan, *Makromol. Chem.*, **178**, 2817 (1977).

CHAPTER 2

AN INTRODUCTION TO THE METHODS OF SYNTHESIS AND CHARACTERIZATION OF POLYMER MICROSPHERES

For several decades, heterogeneous polymerization processes have been used to obtain different polymers. Suspension and emulsion polymerizations have become the most popular techniques for the production of polymers with particular properties and morphologies. Recently, some new polymerization processes have been developed in order to synthesize monodisperse crosslinked polymer particles of micron-size for chromatography packing and other purposes.

In this chapter, a critical summary concerning the synthesis and characterization of micron-size polymer particles in general will be given.

2.1 GENERAL FEATURES OF HETEROGENEOUS POLYMERIZATION PROCESSES

Heterogeneous polymerization processes have been known for more than fifty years. In general, two basic types of heterogeneous polymerization processes can be distinguished: 1) the initial reaction mixture consists of two-phase systems in which the starting monomer(s) is in the form of a fine dispersion in an immiscible liquid, as in emulsion or suspension polymerization; and 2) the reaction mixture is initially

59

61

Our aim was to synthesize micron size polymer particles with very narrow particle size distribution (PSD) for chromatographic application. Therefore, the following discussion will be focused mainly on the processes which are able to give size of particles in the range of 1 to 10 μm . These include dispersion and precipitation polymerizations.

Table 2.1 Characteristics of free-radical heterogeneous polymerization processes.¹

Type of polymerization	Continuous phase	Characteristics
Precipitation	Water, organic liquids	Monomer and initiator soluble in continuous phase; autoaccelerated polymerization due to gel effect.
Dispersion	Organic liquids	Monomer and initiator soluble in continuous phase; polymeric stabilizer; gel effect.
Emulsion	Water	Low monomer solubility, initiator soluble in continuous phase; ionic/non-ionic surfactants; high rates due to radical isolation.
Suspension	Water	Low monomer solubility, initiator soluble in monomer; low level of ionic surfactant; gel effect.

homogeneous but as polymerization proceeds, polymer separates out and the reaction then continues in a heterogeneous manner, as in dispersion or precipitation polymerization. Table 2.1 summarizes the characteristics of these various types of heterogeneous free-radical polymerizations. In these processes, the polymerization initiator may be soluble in the monomer or in the continuous phase, and it may or may not be present within the polymer particles during their formation. In addition to monomer(s), polymerization medium and initiator, one or more additives is also added to the polymerization mixture to emulsify the monomer, and/or to stabilize the monomer droplets and the resulting polymer particles.

The four heterogeneous polymerization processes mentioned in Table 2.1 are employed for the manufacture of particulate polymer products. Each of the techniques is able to give polymer particles within a certain range of particle size as indicated in Figure 2.1. In general, both emulsion and emulsifier-free emulsion polymerization processes are suitable for syntheses of submicron size particles with narrow or even monodisperse particle size distribution (PSD) (under certain conditions, latex (particles) of 2 μm can be formed with emulsifier-free emulsion polymerization¹¹). Suspension polymerization is well known for syntheses of packing materials such as GPC and HPLC resins, etc. The size of particles obtained by this technique is in the range from 10 up to 1000 μm with typically broad size distribution. Precipitation polymerization is rarely used because the products are in the form of a coagulum, except for a few monomer systems such as vinyl chloride or acrylonitrile. Dispersion polymerization is a recent technique, which has proven suitable to produce monodisperse micron-size polymer particles (microspheres).

62

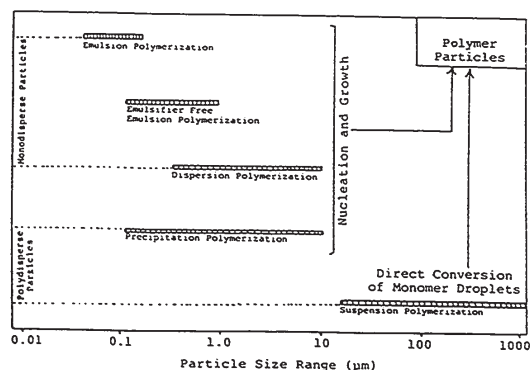


Figure 2.1 General kinetic features and particle size ranges of heterogeneous polymerization processes. (Ref. 22).

2.2 SYNTHESIS OF POLYMER MICROSPHERES

The research into monodisperse polymer microspheres for use in coatings, biotechnology, and as chromatographic packing materials has seen important advances in recent years. Emulsion polymerization, for example, is used to prepare monodisperse polymer spheres in the submicron range in a single step.² Larger diameter particles up to around 50 μm can be made from emulsion seed particles using stepwise swelling processes originally developed by Ugelstad.^{3,4} On the other hand, dispersion polymerization can lead in a single step to monodisperse polymer particles in the diameter range of 0.1-18 μm .^{5,6,7} Both emulsion and dispersion polymerization methods require additives to prevent coagulation.^{2,8} Emulsifier-free emulsion polymerization is used to prepare polymer latices in the submicron range that are stabilized by ionic charges derived from the initiator, usually a persulfate.^{9,10} This process has been limited to low monomer loading (ca. 10%).¹¹ Recently, Rudin *et al.*^{12,13} reported that, with semi-batch procedure, high solid content of polymer latices (above 40%) can be synthesized in the absence of emulsifier. Fréchet *et al.*¹⁴ used emulsifier-free emulsion polymerization technique to synthesize polystyrene microspheres with diameters up to 2.46 μm . It is also suitable to prepare monodisperse crosslinked styrene-divinylbenzene latices with diameters up to 640 nm diameter.¹¹ Larger diameter monodisperse crosslinked microspheres have to be made using multistage emulsion polymerizations.^{15,16} However, our recent reports have revealed that narrow and monodisperse crosslinked polystyrene type microspheres can be synthesized in a single step by dispersion and precipitation polymerization, respectively.^{17,18} These processes will be described in Chapter 3 and Chapter 4.

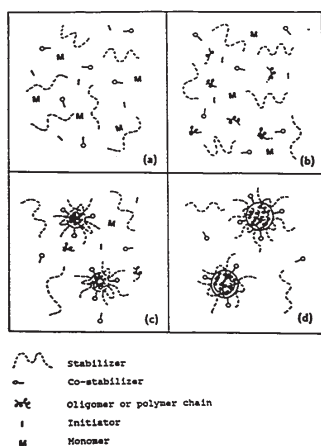


Figure 2.2 A schematic representation of particle formation and growth in nonaqueous dispersion polymerization of styrene in ethanol medium. (Ref. 7)

2.3 A CRITICAL REVIEW ON DISPERSION POLYMERIZATION

In non-aqueous dispersion polymerization, a monomer is reacted in an organic liquid to produce an insoluble polymer in the form of a stable colloidal dispersion. The colloidal stability is provided by the adsorption on the particle surface of an amphiphatic polymeric stabilizer. Dispersion polymerization is really a modified precipitation polymerization except that flocculation is prevented and particle size is controlled.¹⁹

The research of dispersion polymerization has been summarized in a number of excellent reviews. The early studies in dispersion polymerization and its development up until 1975 has been reviewed by Barrett,²⁰ and the recent developments in this field have been reviewed by Croucher and Winnik,^{6,21} as well as by Arshady,²² Ober²³ and Walbridge.²⁴

2.3.1 Process Description

In a typical dispersion polymerization, monomer, stabilizer and initiator are soluble in the homogeneous polymerization medium, which is a poor solvent for the resulting polymer. Upon heating to the reaction temperature, polymerization starts in solution to form oligomeric radicals. Depending on the solvency of the medium for the resulting oligomeric radicals and macromolecules, phase separation occurs which leads to nucleation and the formation of primary particles. These primary particles adsorb stabilizer from the medium onto their surface, such that the forming particles become sterically stabilized. The resulting particles are significantly swollen by the monomer. As a result, polymerization proceeds largely within the individual particles, leading to the formation of spherical particles in the diameter region of ca. 0.1 to 20 μm . This situation is schematically outlined in Figure 2.2.

As polymerization proceeds within the swollen particles, the viscosity within each particle increases and the reaction rate accelerates rapidly due to the reduction in the diffusion-controlled termination rate. Figure 2.3 shows a plot of conversion versus time for three polymerizations of methyl methacrylate at 80°C.²⁵ A dispersion polymerization (A) was performed in dodecane using AIBN initiator with a hydrocarbon polymer as stabilizer. A precipitation polymerization (B) was carried out under identical conditions except that no stabilizer was present. Finally, a solution polymerization (C) was done in benzene again with no stabilizer present. The dispersion polymerization process was shown to be the fastest of the three, exhibiting a pronounced gel effect.

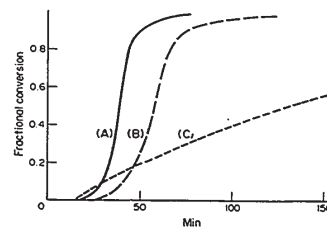


Figure 2.3 Comparison of rates of dispersion polymerization (A), precipitation polymerization (B) and solution polymerization (C) of methyl methacrylate at 80°C. (Ref.25).

2.3.2 Steric Stabilization and Stabilizers

The theoretical background of steric stabilization in dispersion polymerization has been comprehensively discussed by Osmond and Waite.²⁶ It is believed that the colloidal stabilization conferred by adsorbed polymer molecules is due to the local increase in polymer segment density resulting from the interpenetration or compression of the polymer sheaths when two particles approach one another (Figure 2.4).²⁴ The osmotic diffusion of solvent into the region of increased polymer concentration generates a repulsive force, causing the particles to separate.

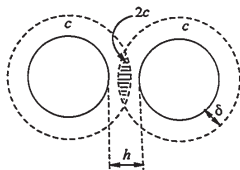


Figure 2.4 Schematic representation of the close approach of sterically stabilized particles. *c*: concentration of polymer chains.

Compared with electrostatic stabilization (for example, in emulsion polymerization), there is no long-range repulsion and the particles are subject only to attractive forces until the outer fringes of the adsorbed molecules are in physical contact. The stability of the particles is thus decided by the dimensions and the solution properties of the adsorbed polymer as well as the size and nature of the particle core.

Steric stabilizers used in dispersion polymerization have been based on block,

or graft copolymers, and homopolymers. These copolymers consist of segments of polymer which are soluble in the reaction medium and joined to segments of polymer with a composition similar to the particles being formed. The latter segments are believed to act as anchors to the particles while the former act as the dispersant component. Some commonly used polymeric stabilizers for dispersion polymerization in polar media are listed in Table 2.2.

Table 2.2 Examples of Stabilizers used in Polar Media.

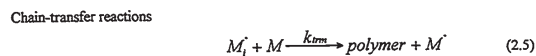
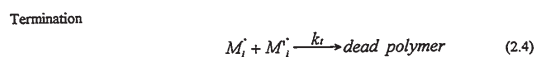
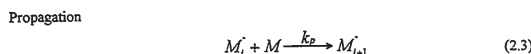
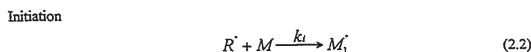
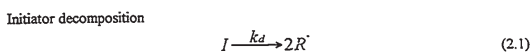
Polymeric Stabilizer	Disperse polymer	Medium	Ref.
poly(acrylic acid)	PS	ethanol	27
		isopropanol/water	28
poly(N-vinylpyrrolidone)	PS	ethanol	7, 29
		PMMA	methanol
hydroxypropyl cellulose	PS	methyl cellosolve/alcohol	31
poly[(propionylimino)ethylene]	PMMA	methanol	32

2.3.3 Initiation and Polymerization

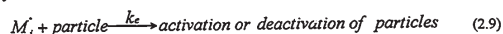
Two types of initiators, solvent soluble and oil soluble initiators, have been employed in dispersion polymerization. For dispersion polymerization in polar solvents, the thermal decomposition of the continuous phase soluble initiator generates primary radicals in the continuous phase. However, the major locus of polymerization was suggested to be the interior of the polymer particles.⁷ The oil-soluble initiator (or monomer soluble initiator) is supposed to generate radicals also in the monomer/polymer phase.^{33,34}

The following reaction schemes have been proposed for dispersion polymerization in polar medium.

a) with continuous phase soluble initiator:

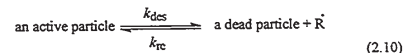


Entry



b) with oil-soluble initiator: The polymerization principally includes the kinetic events given by eq 1-8 (for the monomer/polymer phase) and also the following steps.

Radical desorption and re-entry



The definition of these symbols used in the above equations are listed in Table 2.3.

The overall rate for a dispersion polymerization has been given by Barrett (eq. 2.11).

$$R_p = \alpha [M_d] k_p (\Phi R_i / k_t)^{1/2} \quad (2.11)$$

where α is the partition coefficient of monomer between the diluent phase $[M_d]$ and the particle phase $[M_p]$, which is defined as $\alpha = [M_p]/[M_d]$. Φ is the volume fraction of particles in the dispersion.

2.3.4 Comparison of Dispersion and Precipitation Polymerization

As mentioned earlier, dispersion polymerization can be viewed as a type of precipitation polymerization in which flocculation is prevented by stabilizer, and particle size is controlled.² In the process of precipitation polymerization, the initial state of the reaction mixture is also a homogeneous solution. Precipitation or at least coalescence takes place as soon as the polymerization reaction has started. In these systems, initiation and polymerization proceed largely in the continuous medium. This leads to continuous nucleation and the coagulation of the resulting nuclei to form larger and larger particles. Usually, particles produced in precipitation polymerization are irregularly shaped and polydispersed.

Table 2.3 Definition of Symbols

character	meaning
I	initiator
R [•]	primary radical formed by the decomposition of initiator
M	monomeric unit
M [•]	monomeric radical
P [•]	polymeric radical
I [•]	radical formed by the chain-transfer to initiator
S [•]	radical formed by the chain-transfer to solvent
M _i [•] or M _i [•]	growing radical with chain length i
j	number of monomer units in oligomer radical before it enters the particle
M _j	continuous phase free radical
k _d	the first-order initiator decomposition rate constant
k _i	initiation rate constant
k _p	propagation rate constant of the polymeric radical
k _t	termination rate constant of the polymeric radical
k _{trm}	monomer chain-transfer rate constant
k _{trp}	polymer chain-transfer rate constant
k _{tri}	initiator chain-transfer rate constant
k _{des}	desorption rate constant
k _e	entry rate constant
k _{re}	re-entry rate constant

where V_m = total volume of mixture (ml), ΔE = energy of vaporization of component 1 or 2 (cal), V = molar volume of component 1 or 2 (ml), ϕ = volume fraction of component 1 or 2 in the mixture (dimensionless).

The expression $(\Delta E/V)$ is termed "cohesive energy density" (CED) which is the molar energy of vaporization per unit volume.

The solubility parameter (δ) is defined as³⁷

$$\delta = \left(\frac{\Delta E}{V} \right)^{1/2} \quad (2.13)$$

Therefore, equation 2.12 can be written as:

$$\Delta H_m = V_m \phi_1 \phi_2 (\delta_1 - \delta_2)^2 \quad (2.14)$$

In this case, the heat of mixing of a solute and a solvent is proportional to the square of the difference in solubility parameters.

As can be seen from eq. 2.14, the Hildebrand theory predicts only endothermic (positive) heats of mixing. The heat of mixing is zero when δ_1 and δ_2 are equal; the solution process becomes more endothermic as the difference between δ_1 and δ_2 becomes greater. Increasing endothermicity means increasing opposition to the process of solution. Consider the formula

$$\Delta F_m = \Delta H_m - T\Delta S_m \quad (2.11)$$

The process of solution is increasingly favored as the value of ΔF_m becomes increasingly negative. The value of ΔS_m is always positive, which favors the solution

2.4 SOLUBILITY AND SOLUBILITY PARAMETERS OF POLYMER

When a polymer dissolves, the first step is a slow swelling process called solvation. Linear and branched polymers dissolve in a second step, but network polymers remain in a swollen condition. The Gibbs free energy equation is used to describe the process of mixing or dissolving a polymer in a solvent.

The entropy of a solution is always larger than the sum of the entropies of the unmixed components; this excess entropy is called the entropy of mixing (ΔS_m). Similarly the free energy of a stable solution is always less than the free energy of the unmixed components; this difference is called the free energy of mixing (ΔF_m). For nonideal solutions there is also a nonzero enthalpy (heat) of mixing (ΔH_m). Quite obviously,

$$\Delta F_m = \Delta H_m - T\Delta S_m \quad (2.11)$$

The magnitude of the term ΔF_m is the deciding factor in the sign of the free energy change and, in consequence, the solubility of a polymer in a given solvent.

Hildebrand³⁵ and Scatchard³⁶ have presented a more general formula for the heat of mixing for molecules of unequal volume. The history and the development of the theory are fully presented by Hildebrand and Scott.³⁵ The result is

$$\Delta H_m = V_m \left[\left(\frac{\Delta E_1}{V_1} \right)^{1/2} - \left(\frac{\Delta E_2}{V_2} \right)^{1/2} \right]^2 \phi_1 \phi_2 \quad (2.12)$$

process. However, ΔS_m for polymer solutions is smaller than ΔS_m for a solution in which the polymer segments are separated from each other, i.e., a monomer solution. A positive value of ΔH_m opposes the process of solution because it makes ΔF_m less negative.

In general liquids of low molecular weight are miscible even if $|\delta_1 - \delta_2|$ is reasonably large. However, polymers will generally not dissolve appreciably in a solvent if $|\delta_1 - \delta_2|$ is as great as 2.0.³⁸

During 1960's, Hansen³⁹ introduced a three-dimensional solubility parameter that appears to give very good agreement with experimental data on solubility of polymers. It is assumed that the energy of vaporization of a liquid can be divided into contributions from van der Waals dispersion forces E_d , dipole-dipole forces E_p , and hydrogen-bonding forces E_h :

$$E = E_d + E_p + E_h \quad (2.15)$$

Dividing by the molar volume of the solvent gives

$$\frac{E}{V} = \frac{E_d}{V} + \frac{E_p}{V} + \frac{E_h}{V} \quad (2.16)$$

$$\delta^2 = \delta_d^2 + \delta_p^2 + \delta_h^2 \quad (2.17)$$

and

$$\delta_d = \left(\frac{E_d}{V} \right)^{1/2}; \quad \delta_p = \left(\frac{E_p}{V} \right)^{1/2}; \quad \delta_h = \left(\frac{E_h}{V} \right)^{1/2} \quad (2.18)$$

With Hansen's method, one can obtain for any liquid a solubility parameter composed of three parameters, δ_d , δ_p , and δ_h . The solubility of a polymer can also be represented by three parameters δ_d , δ_p , and δ_h .

Hansen parameters have been utilized to account for the observations in dispersion polymerization of styrene by Paine,⁴⁰ and better correlation has been obtained compared with using a single overall solubility parameter (or Hildebrand solubility parameter).⁴¹

2.5 CHARACTERIZATIONS OF POLYMER MICROSPHERES

The techniques which may be employed to determine average particle diameters include electron microscopy (also used for determining the morphology of particles), light scattering, ultra centrifugation, small angle X-ray scattering, and photon correlation spectroscopy. For particles of more than 1 μm diameter, optical microscopy and electronic particle counting by a Coulter counter (Coulter Multisizer) are additional possibilities. Here we will briefly discuss scanning electron microscopy (details see ref. 42) and Coulter Multisizer techniques which have mainly been used to characterize the morphology and size of polymer particles throughout this thesis.

2.5.1 Scanning Electron Microscopy (SEM)

The electron microscope provides a narrow beam of electrons that can be focused on a sample for the purpose of image formation or elemental analysis. The beam may be moved or scanned across the sample surface, or fixed at one point. The formation

of an image depends on the detection of a signal that varies with the topography or composition of the sample.

The interaction of the electron beam with the sample results in several different emissions that can be detected for the purposes of image formation or elemental analysis. Figure 2.5 shows schematically the types of radiation emitted when an electron beam impinges on the sample surface and gives rough estimates for the depths from which each type of radiation escapes the surface. This figure shows that both the escape depth and radial resolution are most favorable for secondary electrons which can only escape from the first 50-500 Å.

Back scattered electrons are those electrons from the incident beam which are reflected by inelastic collisions with nuclei of atoms near the surface. Secondary electrons are electrons which are ejected from the outer shells of atoms near the surface due to inelastic collisions with beam electrons. Both backscattered and secondary electrons "illuminate" the surface (bright areas correspond to areas from which more electrons are emitted and subsequently detected) and therefore can be used to create a map of surface texture. X-rays are emitted when an electron from the beam inelastically collides with and causes the ejection of an electron from one of the inner shells. Subsequently an electron from an outer shell replaces it and in doing so loses energy equivalent to the difference in energy between the two shells.

Each x-ray photon has a wavelength (and hence energy) characteristic of the electron transition made between the two atomic states and is specific to the element in which it is produced. Thus by measuring the wavelength or the energy of the photon, the element can be identified. The characteristic x-ray of light elements cannot be measured with accuracy (or cannot be measured at all in some cases) with the detectors currently available in electron beam machines. Therefore, SEM microanalysers cannot be used for

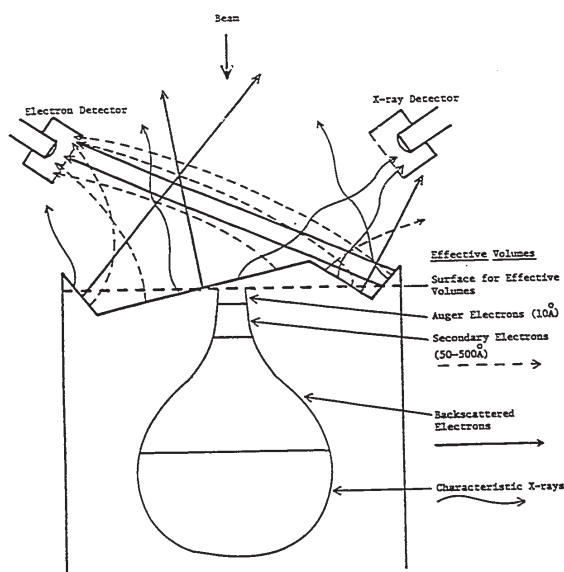


Figure 2.5 Schematic of types of radiation emitted in scanning electron microscopy

compositional analysis of polymers. However, they can be used to detect heavy atoms present as substituents.

Microscopy represents the only method of obtaining particle size and size distribution by direct measurement of individual particles. However, microscopic methods are typically slow and tedious except if modern image analyzers are used. Systems of this type can however be quite costly.

2.5.2 Coulter Multisizer

The Coulter Multisizer (or Coulter counter) is a particle sizing instrument that operates by measuring the electrical current through an aperture. In this instrument, the particles are diluted in an electrolyte and passed through a fine capillary that connects two larger chambers containing immersed electrodes. A potential difference is applied between the electrodes. The resistance change that occurs when a particle passes through the orifice between the plates is proportional to the amount of electrolyte displaced and therefore to the size of the particle. A wide range of orifice sizes is available to cover size ranges from 0.4 μm to about 1000 μm . Figure 2.6 shows a schematic of a typical experimental setup.

This device can be used for the analysis of particle samples that can be put into the electrolyte solution without producing any undesirable effects on the particles themselves. Dilution of the dispersion is often required because the appearance of two particles in the sensing zone at one time would be measured as a single larger particle. The size range analyzed is also limited because particles on the order of 40% of the aperture diameter lead to blockage, and particles smaller than about 2% of the aperture diameter do not produce a signal above the noise (background) and are effectively invisible.

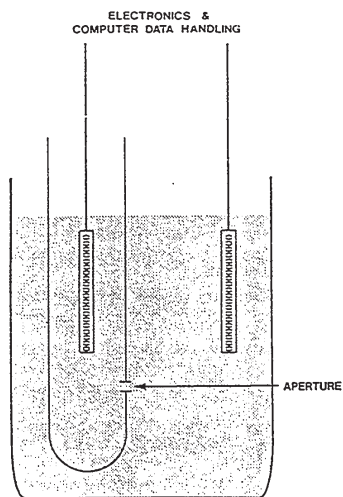


Figure 2.6 Schematic of Coulter counter technique.

REFERENCES

- 1 C.E. Schildknecht, *Polymer Processes*, Interscience Publishers Inc., New York, 1956.
- 2 D. Bassett, and A.E. Hamielec, Eds., *Emulsion Polymers and Emulsion Polymerization*, *ACS Symposium Series*, Vol. 165, American Chemical Society, Washington, D.C., 1981.
- 3 J. Ugelstad, and P.C. Mørk, *Adv. Colloid Interface Sci.*, **13**, 101 (1980).
- 4 J. Ugelstad, H.R. Mfutakamba, P.C. Mørk, T. Ellingsen, A. Berge, R. Schmid, L. Holm, A. Jørgedal, F. K. Hansen, and K. Nustad, *J. Polym. Sci. Polym. Symp.*, **72**, 225 (1985).
- 5 C.K. Ober, K.P. Lok, and M.L. Hair, *J. Polym. Sci. Polym. Lett. Ed.*, **23**, 103 (1985).
- 6 M.D. Croucher, and M.A. Winnik, "Control of Particle Size in the Dispersion Polymerization of Sterically Stabilized Polymer Colloids", in *Future Directions in Polymer Colloids*, M.S. El-Aasser and R.M. Fitch, ed., NATO ASI Series, Martinus Nijhoff Publishers, Boston, 1987.
- 7 C.M. Tseng, Y.Y. Lu, M.S. El-Aasser, and J.W. Vanderhoff, *J. Polym. Sci. Polym. Chem. Ed.*, **24**, 2995 (1986).
- 8 A.J. Paine, and J. McNulty, *J. Polym. Sci. Polym. Chem.*, **28**, 2485 (1990).
- 9 A.R. Goodall, M.C. Wilkinson, and J. Hearn, *J. Polym. Sci. Polym. Chem.*, **15**, 2193 (1977).
- 10 Z. Song, and G.W. Poehlein, *J. Polym. Sci. Polym. Chem.*, **28**, 2359 (1990).
- 11 D. Zhou, V. Derlich, K. Gandhi, M. Park, L. Sun, D. Kriz, Y. D. Lee, G. Kim, J.J. Aklonis, and R. Salovey, *J. Polym. Sci. Polym. Chem.*, **28**, 1909 (1990).
- 12 S.T. Eckerley, and A. Rudin, *J. Appl. Polym. Sci.*, in press.
- 13 S.T. Eckerley, and A. Rudin, *Progress in Organic Coatings*, in press.
- 14 V. Smigol, F. Svec, K. Hosoya, Q. Wang, and J.M.J. Fréchet, *Die Angew. Makromol. Chem.*, **195**, 151 (1992).
- 15 M. Okubo, M. Shiozaki, M. Tsujihira, and Y. Tsukuda, *Colloid Polym. Sci.*, **269**, 222 (1991).
- 16 D. Zou, L. Sun, J.J. Aklonis, and R. Salovey, *J. Polym. Sci. Polym. Chem.*, **30**, 1463 (1992).
- 17 K. Li, and H.D.H. Stöver, *J. Polym. Sci. Polym. Chem.*, **31**, 2473 (1993).
- 18 K. Li, and H.D.H. Stöver, *J. Polym. Sci. Polym. Chem.*, **31**, 3257 (1993).
- 19 K.E.J. Barrett, *Br. Polym. J.*, **5**, 259 (1973).
- 20 K.E.J. Barrett (ed.), *Dispersion Polymerization in Organic Media*, Wiley, London, 1975.
- 21 M.D. Croucher, M.A. Winnik, "Preparation of Polymer Particles by Dispersion Polymerization", in *Scientific Methods for the Study of Polymer Colloids and Their Applications*, NSTO ASI Series, 1990.
- 22 R. Arshady, *Colloid Polym. Sci.*, **270**, 717 (1992).
- 23 C.K. Ober, *Makromol. Chem., Macromol. Symp.*, **35/36**, 87 (1990).
- 24 R.H. Ottewill, and T. Walker, *Kolloid-Z. Z. Polymere*, **227**, 108 (1968).
- 25 K.E.J. Barrett, and H.R. Thomas, *J. Polym. Sci., Part A-1*, **7**, 2627 (1969).
- 26 D.W.J. Osmond, and F.A. Waite, The Theoretical Basis for the Steric Stabilization of Polymer Dispersions Prepared in Organic Media, in *Dispersion Polymerization in Organic Media*, K.E.J. Barrett, ed., Wiley, London, 1975.
- 27 T. Corner, *Coll. Surf.*, **3**, 119 (1981).
- 28 A. Tuncel, R. Kahraman, and E. Piskin, *J. Appl. Polym. Sci.*, **51**, 1485 (1994).
- 29 A.J. Paine, W. Luymes, and J. McNulty, *Macromolecules*, **23**, 3104 (1990).
- 30 S. Shen, E.D. Sudol, and M.S. El-Aasser, *J. Polym. Sci. Polym. Chem.*, **31**, 1393 (1993).
- 31 C.K. Ober, F.V. Grunsven, M. Mcgrath, and M.L. Hair, *Colloids and Surfaces*, **21**, 347 (1986).
- 32 S. Kobayashi, H. Uyama, Y. Matsumoto, and I. Yamamoto, *Makromol. Chem.*, **193**, 2355 (1992).
- 33 J.A. Alduncin, J. Forcada, M.J. Barandiaran, J.M. Asua, *J. Polym. Sci. Polym. Chem.*, **29**, 1265 (1991).
- 34 J.M. Asua, V.S. Rodrigues, E.D. Sudol, and M.S. El-Aasser, *J. Polym. Sci., Polym. Chem.*, **27**, 3569 (1989).
- 35 J.H. Hildebrand, and R.L. Scott, *Solubility of Non Electrolytes*, Reinhold, New York, 1950.
- 36 G. Scatchard, *Chem. Revs.*, **8**, 321 (1931).
- 37 A.D. Jenkins, *Polymer Science*, A.D. Jenkins, Ed., North-Holland, Amsterdam and London, 1972.
- 38 A.V. Tobolsky, and I.V. Yannas, Thermodynamics of Polymer Solutions. in *Polymer Science and Materials*. A.V. Tobolsky and H.F. Mark, ed., Wiley-Interscience, New York, 1971.
- 39 C.M. Hansen, *J. Paint Technol.* **39**, 104 (1967).
- 40 A.J. Paine, *J. Polym. Sci. Polym. Chem.*, **28**, 2485 (1990).
- 41 K.P. Lok, and C.K. Ober, *Can. J. Chem.*, **63**, 209 (1985).
- 42 M.A. Hayat, *Introduction to Biological Scanning Electron Microscopy*, University Park Press, Baltimore, 1978.

CHAPTER 3

NARROW DISPERSE POLYDIVINYLBENZENE
PARTICLES BY DISPERSION POLYMERIZATION3.1 RECENT RESEARCH ON THE SYNTHESIS OF NARROW
DISPERSE CROSSLINKED POLYMER PARTICLES

The synthesis of crosslinked polymer particles has been the subject of much research. In many cases, suspension polymerization is used to obtain polymer particles in the micron range¹. A drawback of this method is that it leads to broad particle size distributions, even if the polymerization conditions are strictly controlled.² For many practical applications such as liquid chromatographic packing materials, narrow or monodispersity is highly desirable. Many approaches have been explored recently for the preparation of such crosslinked polymer particles.

More than a decade ago, Ugelstad *et al.*^{3,4} invented a method, called the activated swelling method, for the production of monodisperse particles with crosslinked structure. This procedure allows preparation of uniform beads up to 100 μm in size from different monomers. Although the theory of this method has been described in several publications since 1979,^{4,5} the process was never published in detail. Fréchet *et al.*^{6,7,8} recently reported their work on the syntheses of monodisperse polymer particles with crosslinked structure by a multi-step swelling process and the application of these particles as packing materials. In this process, monodisperse polymer particles obtained by emulsion

83

polymerization were used as seeds. They were swollen by a mixture of a second monomer (containing crosslinker) and porogenic solvent to afford monodisperse crosslinked porous polymer particles in the 5–6 μm size range. Adopting a similar approach, El-Aasser *et al.*^{9,10} synthesized monodisperse crosslinked polystyrene particles which had diameters above 10 μm . The polystyrene seeds of 8.7 μm diameter used were synthesized by a method called successive seeded emulsion polymerization, in which small size latexes were swollen with monomer and polymerized in a series of growth cycles. To avoid the multi-step seeded polymerization required to synthesize large polymer seeds, 4.5 to 12 μm diameter monodisperse polystyrene seeds were prepared in a single step by dispersion polymerization by Kobayashi and Senna.¹¹ The subsequent seeded polymerization led to non-porous, highly crosslinked and monodisperse polystyrene particles.

The processes mentioned above require a multi-step procedure, or at least two steps. In contrast, the direct synthesis of narrow or monodisperse crosslinked particles by a single-step method would be very interesting. Zou and Salovey^{12,13,14} described the syntheses of monodisperse crosslinked polystyrene, polymethacrylate and polymethacrylonitrile microspheres directly by adding a crosslinking agent to the reaction mixture during emulsion polymerization. The sizes of these microspheres, however, were less than 0.7 μm . An attempt to obtain crosslinked polystyrene particles within a single-step was reported by Fréchet *et al.*⁶ They added 0.5 to 10 vol% of divinylbenzene to the styrene in an emulsifier-free emulsion polymerization, but obtained only aggregated product.

Since dispersion polymerization is capable of giving monodisperse polymer microspheres from 0.1 to 18 μm , the direct synthesis of narrow or even monodisperse crosslinked particles from this system seems even more attractive. Tseng, Lu, El-Aasser and Vanderhoff¹⁵ studied the effect of crosslinker in the preparation of monodisperse

85

polystyrene microspheres in alcoholic media. They found that as the DVB concentration was increased from 0 to 0.3 wt% (relative to styrene), the particle dispersity remained narrow. When 0.6 wt% DVB was used, the final particles had irregular shapes, and coagulation occurred upon further increasing the DVB concentration. Ober and Lok¹⁶ observed a similar phenomenon. Table 3.1 lists their results of making crosslinked polystyrene particles produced by dispersion polymerization in alcohol. It shows that broadening of the particle size distribution occurs with increased DVB concentrations. SEM indicated that when higher concentrations of DVB were used (>0.7 wt%), the particles obtained had irregular shapes.¹⁷

Table 3.1 Crosslinked Particles by Dispersion Polymerization¹⁶

Monomer	DVB (wt%)	Diameter (μm)
Styrene	0.3	7
	0.5	7
	0.75	3-9
	1.0	1-10

Similar situations were encountered in other monomer systems. Margel *et al.*¹⁸ observed broadening of the size distribution upon adding 2 vol% of DVB to chloromethylstyrene monomer in a dispersion polymerization process. Recently, Shen, Sudol and El-Aasser *et al.*¹⁹ reported the dispersion polymerization of methyl methacrylate which gave monodisperse poly(methyl methacrylate) particles. They observed that adding a small amount of crosslinking monomer (DVB or ethylene glycol dimethacrylate, <0.3 wt%) did not show any significant effect on the particle size or distribution. However,

86

higher concentrations of crosslinking agent (0.3 wt%) led to partial flocculation or severe coagulation (0.6 wt%).

In addition to these attempts to synthesize crosslinked polymer microspheres by the dispersion polymerization method mentioned above, efforts have also been made by other researchers.^{20,21} All these results had similarities. In general, when a crosslinker such as divinylbenzene is added, the sphericity and the monodispersity of the microspheres prepared by conventional dispersion polymerization are seriously affected giving deviations from spherical shape and monodispersity. To maintain monodispersity of particle size, a divinylbenzene concentration of less than 0.6% must be used. No explanations have been given thus far to account for this phenomenon. The fact that only particles of linear or very slightly crosslinked polymers can be produced by dispersion polymerization has been a big limitation of this method.

3.2 AIM OF THE RESEARCH

Due to the high pressure drop in the HPLC test of the template polymers (see Chapter 1), it became necessary to produce PAME selective template polymers of spherical shape and with a narrow size-distribution in the five micron range. As discussed in Chapter 2, four heterogeneous polymerization processes can be used to synthesize polymeric particles. For our purpose, both emulsion and suspension polymerizations have to be excluded because all of the template molecules (e.g., *l*-triflate) would be extracted into the water phase. The *l*-triflate-crown ether complex is only stable and soluble in polar aprotic solvents such as acetonitrile, ethanol, etc. The problem to be tackled is then whether highly crosslinked polystyrene-type microspheres can be obtained by dispersion polymerization in such solvents.

More generally, past attempts to prepare crosslinked narrow or monodisperse polymer particles in a single step were largely unsuccessful. It would be theoretically and practically interesting to find a route to such particles.

In this chapter, experiments for preparing narrow disperse crosslinked polymer microspheres by means of dispersion polymerization are described. Commercial divinylbenzene was used as monomer. The experimental parameters that affect particle size and size distribution were studied. A formation mechanism for these crosslinked microspheres is proposed.

3.3 EXPERIMENTAL

3.3.1 Materials and Their Purification

In this study, technical-grade divinylbenzene (DVB55, Aldrich) was used as monomer. It was purified by passing it through an alumina column to eliminate the phenolic inhibitor. Polyvinylpyrrolidone (PVP, $M_w = 40,000$; Aldrich) was used as steric stabilizer. Acetonitrile (HPLC grade) and absolute ethanol were purchased from BDH and used without further purification. 2,2'-Azobis(isobutyronitrile) (AIBN) initiator was purchased from Kodak and purified by recrystallization from methanol.

3.3.2 Dispersion Polymerization of DVB55 (DPDVB55, General Procedure)

Most of the experiments described in this chapter were performed in 20 ml glass vials which were fixed on the bottom of a low power ultrasonic cleaning bath. Commercial divinylbenzene (DVB55) was used as monomer. Polymerization was initiated by radical initiator (AIBN). The polymer obtained, therefore, had a highly crosslinked structure (Figure 3.1). In general, initiator, PVP, and DVB55 were weighed into 20 ml glass vials, and the mixtures made up to 10 ml with acetonitrile (or ethanol). The capped and sealed vials were then placed in a thermostated low-power ultrasonic bath. The ultrasound supplied the necessary vibration to prevent sedimentation and coagulation of the forming microspheres during the polymerization. The temperature of the ultrasonic bath was controlled to $\pm 0.5^\circ\text{C}$ by circulating water from a thermostated water bath.

Alternatively, the capped and sealed vials were fixed onto an umbrella-shaped rotor which was slowly rotated at 30 rpm around its stem axis. The rotor was submerged in a thermostated water bath, with a notch causing mild additional agitation at every revolution. In either agitation mode, polymerizations were carried out for 24 h at 70°C .

89

90

The obtained microspheres were dispersed in methanol and centrifuged for 10 min (at 6000 rpm), then placed under acetone overnight. This was followed by two more redispersions/centrifugations. The microspheres were then dried under vacuum at ambient temperature. For all polymerizations, concentrations of DVB55 are given as volume percent (vol%) in the DVB55/solvent mixture at room temperature. AIBN concentrations are given as weight percent (wt%) relative to DVB55. PVP concentrations are given in g of solution (solvent plus monomer). All polymerization mixtures contained 16 g L⁻¹ PVP and 1.0% AIBN, unless otherwise specified.

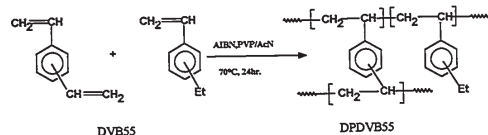


Figure 3.1 Dispersion polymerization of DVB55

3.3.3 Conversion of Monomer

The conversion of monomer was determined gravimetrically. A 2 ml sample was taken from the reaction mixture, which was mixed with a trace of inhibitor (benzoquinone) in a preweighed glass dish. The mixture was weighed, and then put in a refrigerator for at least 15 min. The volatile fraction was evaporated to constant weight under vacuum at 50°C (about 48 h), and the dish with the dry residue was weighed again. The solid fraction was calculated as:

$$F_{\text{Solid}} = \frac{(W_{\text{dish}} + W_{\text{dry}}) - W_{\text{dish}}}{(W_{\text{dish}} + W_{\text{sample}}) - W_{\text{dish}}} \quad (3.1)$$

The conversion of monomer was then given by:

$$x\% = \frac{F_{\text{Solid}} - F_{\text{Init}} - F_{\text{Stab}}}{F_{\text{Mono}}} \quad (3.2)$$

Where F_{Init} is the weight fraction of initiator; F_{Stab} is the weight fraction of stabilizer; and F_{Mono} is the weight fraction of monomer initially present.²²

3.3.4 Size and Size Distribution of the Microspheres

Particle size and size distribution were determined using a 256-channel Coulter Multisizer II. An orifice tube with a 30 μm aperture was used. Before the measurement, a drop of the particle suspension in methanol was diluted with Isoton II electrolyte. A drop of this dilute suspension was then placed into the measurement chamber. Even though the Coulter Multisizer is able to count up to 10,000 particles per second, it was noticed that too high a concentration of particles can cause problems such as aggregation of particles. These aggregates can clog the aperture or generate secondary peaks. For some measurements, the Isoton suspension was sonicated for up to 10 seconds. A personal computer interfaced to the Coulter Multisizer was used to calculate and plot the size, size distribution of the particles, and other parameters.

Optical microscopy was also used for the determination of particle size, especially for those samples which contained microspheres less than 1 μm in diameter. In this case, about 200 individual particle diameters were measured from optical micrographs and averaged to give the particle diameters.

The number average diameter d_n and the standard deviation σ , are defined as follows:

$$d_n = \frac{\sum n_i d_i}{\sum n_i} \quad (3.3)$$

and

$$\sigma = \sqrt{\frac{\sum n_i (d_i - d_n)^2}{\sum n_i}} \quad (3.4)$$

where n_i is the number of particles with diameter d_i . The standard deviation was divided by the number-average diameter of the particles to give the coefficient of variation (CV), i.e. $CV = \sigma / d_n$. CV was used as an index for the size dispersity.

3.3.5 Morphology of DPDVB55 particles

The morphology of DPDVB55 particles were studied with an ISI DC-130 scanning electron microscope (SEM). SEM specimens were prepared by redispersing the cleaned particles in methanol and placing a drop of the suspension on a piece of cover glass, which was mounted with double adhesive tape on an aluminum stud. The drop was dried in clean air at room temperature and then sputter-coated under vacuum with a thin layer (12 ~ 15 nm) of gold. Acceleration potentials of up to 15 kv were used during the SEM measurements.

3.3.6 Determination of Porosity of DPDVB55 Particles

Size-exclusion Chromatography (SEC) was used to measure the porosity of the DPDVB55 particles. The particles were slurry packed into a Millipore/Waters adjustable glass column by the technique previously described (see Chapter 1, Experimental section). The packed column had bed dimensions of 10 mm i.d. \times 70 mm. The column was calibrated with a series of narrow disperse polystyrene standards (Polysciences, molecular weight range $1.32 \times 10^3 - 2.02 \times 10^7$) in HPLC grade tetrahydrofuran (THF) at 25°C. The setup involved a Waters Model 590 programmable pump equipped with a Rheodyne 20 μ l loop injector. A Waters 441 UV detector (254 nm) was used to monitor the peaks which were recorded on a computer running Viscotek's GPC-PRO software. The flow rate of THF was 0.5 ml / min. Toluene was used to determine the total inclusion volume, V_{toluene} . The porosity of the microspheres was assessed using the following equation:

$$\text{Porosity (\%)} = 100 \frac{V_{\text{toluene}} - V_0}{V_{\text{total}} - V_0} \quad (3.5)$$

where V_{total} is the total volume of the column bed; V_0 is the dead volume (or void volume).

3.4 RESULTS AND DISCUSSION

3.4.1 Choice of Agitation Method

In the presence of crosslinker, the process of dispersion polymerization becomes more complicated. In order to obtain crosslinked polymer particles by this process, we used commercial divinylbenzene containing 55% crosslinker. Initial experiments were conducted to find a proper agitation method for our system. The standard recipe used in this study is given in Table 3.2.

Table 3.2 Standard Recipe for Optimizing Agitation Method^a

Materials	Concentration	Amount
DVB55	10 vol% (based on total)	1.010 g
Acetonitrile or Ethanol	90 vol% (based on total)	10.0 ml
PVP	16 g L ⁻¹	0.180 g
AIBN	1.0 wt% (based on monomers)	0.010 g

^a Polymerization at 70°C for 24 h.

In dispersion polymerization, the particles are formed from an initially homogeneous reaction mixture, and are stabilized by a suitable steric stabilizer. The process is generally less sensitive to the type and rate of agitation compared with suspension polymerizations. This situation may change, however, if crosslinker is present. The dispersion system becomes unstable, probably because stabilizer is incorporated into the interior of the crosslinked polymer matrix during the particle growth which leads to a loss in the effectiveness of the stabilizer.

Initial experiments were conducted using conventional magnetic and mechanical stirring methods. Highly coagulated particles were observed with magnetic stirring using a teflon-coated stirring bar at different spin rates. A similar observation was made in a reactor with a mechanical overhead paddle stirrer at 300 rpm. The enforced contact between the forming microspheres, caused by the stirring, apparently resulted in the coagulation of these microspheres. It seemed that a milder agitation would be necessary.

The first observation of spherical DPDVB55 particles was made during a static, unstirred polymerization reaction. Coulter Multisizer measurements indicated that the particles had bimodal distributions: a main peak centered at 2.9 μ m beside some particles less than 1 μ m when acetonitrile was used as polymerization solvent; and a main peak of 2.2 μ m beside some particles less than 1 μ m in ethanol. The bimodal distribution pattern was due to the sedimentation of polymer microspheres during the reaction. Better results were achieved by using either lower power ultrasonic agitation or rotor agitation as described in the experimental section. Figure 3.2 shows the effects of different types of agitation on the formation of DPDVB55 particles.

Unimodal distribution pattern of DPDVB55 particles were obtained in the ultrasonic and rotor agitation systems. As indicated in Figure 3.2, by using either acetonitrile or ethanol as solvent, relative narrow distribution with coefficient variation of about 20 % were obtained. Under the same conditions, the microspheres synthesized in acetonitrile were larger than those obtained in ethanol. It was also noticed that the ultrasonic agitation system gave larger particles compared with the rotor system. Since the ideal particle size for our HPLC application is about 5 μ m, most of the subsequent experiments, therefore, were performed in the ultrasonic water bath.

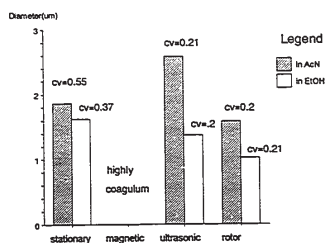


Figure 3.2 Effect of agitation method on particle size for 10 vol% DVB55 in acetonitrile and ethanol.

3.4.2 Parameters Influencing the Formation of DPDVB55 Particles

The initial success in synthesizing highly crosslinked DPDVB55 particles by dispersion polymerization prompted us to study this reaction further. For this new process, many basic questions need to be answered:

- why the crosslinked polystyrene microspheres could not be obtained when earlier researchers used low levels of crosslinker?
- how high a level of the crosslinker has to be used in order to obtain microspheres?
- how do the microspheres form and how do they grow during the polymerization?

In order to elucidate the mechanism of DPDVB55 particle formation, the influence of

different factors (concentration of actual crosslinker, stabilizer and initiator, solvents and temperature) on the size and size distribution of DPDVB55 particles was studied.

3.4.2.1 Effect of initial monomer concentration

In dispersion polymerization, the initial monomer concentration is important because the final number of particles is determined at a very early stage.²³

In this set of experiments, DVB55 was polymerized to poly(divinylbenzene) particles in acetonitrile at 70°C for 24 h. Table 3.3 shows the average particle sizes and size distributions obtained at initial DVB55 concentrations of 5, 10, 15, and 25 vol%.

As the monomer concentration was increased from 5% to 20%, the conversion increased from 68 to 89%. At the same time the average particle diameter changing from less than 1 µm to about 9 µm for the main peak, with particle shapes changing from spherical to popcorn. At DVB55 concentrations of 25%, particles are formed initially but then coagulated into one polymeric block.

Increasing the monomer concentration increases the solution polymerization rate. The major effect of monomer concentration, however, is to change the initial solvency of the reaction medium.²⁴ Because the monomer (DVB55) is a good solvent for the polymer being formed, the solvency of the medium for the polymer will improve with increasing monomer concentration. This causes swelling of the forming network oligomer and permits more early coalescence to generate fewer larger particles. In addition, the mature particle surface will remain sticky longer in the presence of high monomer concentration. This extends the period during which same size particles can aggregate, and results in the roughness of particle surface as seen in Figure 3.3. Figure 3.3 shows SEM micrographs of three polydivinylbenzene dispersions prepared with 5, 10, 15, and 20 vol%

Table 3.3 Effect of DVB55 Concentration on DPDVB55 Particles*

Sample	DVB55 (vol.%)	Particle Size (µm)		CV (%)	Conversion (%)	Comment
		$d_{(0.05)}$ ^b	d_n			
DDVB-5(a)	5	< 1	< 0.89	—	68	Spherical
DDVB-5(b)	10	2.68	2.58	21	80	Spherical, unimodal
DDVB-5(c)	15	5.02	6.12 (73%)	13	81	Bimodal, rough surface
DDVB-5(d)	20	> 7	1.86 (27%) 9.40 (61%)	13	89	Bimodal, rough surface
DDVB-5(e)	25	—	< 6.0 (39%)	—	—	Congulum

* [PVP] = 1.6 g/L; [AIBN] = 1.0 wt%.

^b $d_{(0.05)}$ = diameter determined by optical microscopy

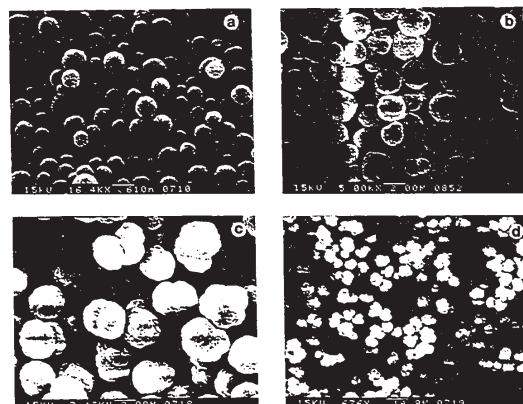


Figure 3.3 SEM micrographs of DPDVB55 particles prepared with: (a) 5%; (b) 10%; (c) 15%; (d) 20% DVB55 in acetonitrile. (Each of the four micrographs has different magnification as indicated by the scale-bar).

DVB55 in acetonitrile. It clearly shows that the surface roughness increases with particle size.

On the other hand, large particles, obtained at higher DVB55 concentrations, capture oligomers in solution less efficiently due to the smaller total surface area. The oligomeric radicals in solution can continue to aggregate (nucleate) to generate new primary particles. These new primary particles are produced faster than they can be captured by the initially formed particles, especially if these initial particles have now grown past their sticky phase. The particles generated at a later time grow to form smaller final particles, and result in a broader size distribution or even bimodal particle size distributions as seen in Table 3.3 for 15 and 20 vol% of DVB55. Figure 3.4 shows the particle size distributions measured by a Coulter Multisizer. The particles obtained from 15 and 20% of DVB55 concentrations gave bimodal distributions due to the secondary nucleation.

With 25 vol% DVB55 concentration, the free space among the forming particles was further reduced due to the high population of the particles, leading to coagulation during the final stage of polymerization. This situation will be discussed further in the next Chapter.

3.4.2.2 Solvent effects

The dispersion polymerization of DVB55 in different solvents was also explored. Generally, the criteria for choosing a solvent are that the solvent should be miscible with the monomer, and at the same time precipitate the polymer formed. The initiator must also be soluble in the dispersion medium. Aliphatic alcohols such as ethanol and other polar organic solvents are commonly used as reaction media for the dispersion

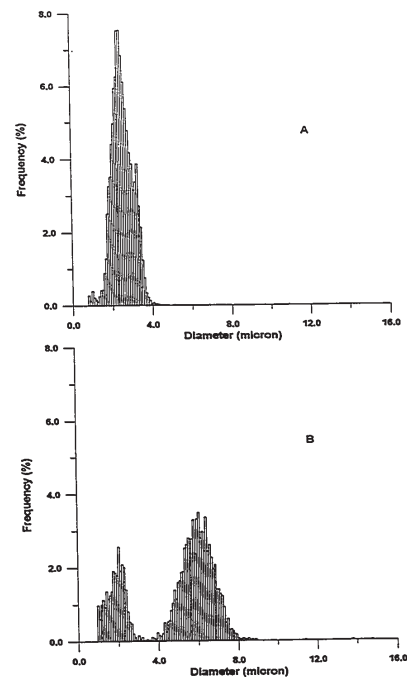


Figure 3.4 (continues on the next page)

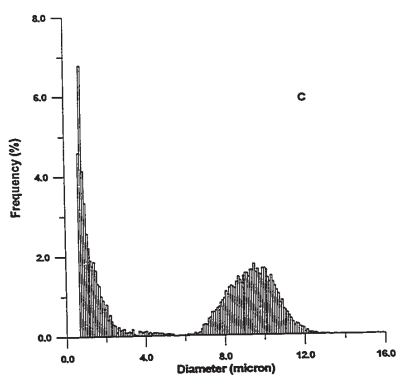


Figure 3.4 (cont. from previous page) Particle size distributions of DPDVB55 microspheres prepared from (a) 10%; (b) 15%; (c) 20% DVB55 in acetonitrile.

polymerization of styrene.^{15,25,26,27,28,29,30,31} In this study, we also found that using ethanol as a polymerization solvent resulted in narrow disperse DPDVB55 particles (Table 3.4). The size of the particles increased from submicron to 2.77 μm when the concentration of DVB55 increased from 5 to 15 vol%. It was noticed that the average particle diameters of DPDVB55 particles synthesized in ethanol were smaller compared with the particles obtained in acetonitrile (Table 3.3, also see Figure 3.2), using otherwise identical reaction conditions. The larger size of the DPDVB55 particles in acetonitrile was probably due to the relatively higher solvating power ($\delta = 12.1 \text{ cal}^{1/2} \text{ cm}^{-3/2}$) of acetonitrile compared with that of ethanol ($\delta = 12.8 \text{ cal}^{1/2} \text{ cm}^{-3/2}$) (Table 3.5). Lok and Ober²⁸ revealed, however, that the effect of a solvent is not only dependent on its solubility parameter. We observed (Table 3.5) odd-shape particles and even coagulum during polymerizations in *N,N*-dimethylformamide (DMF) and dimethylsulfoxide (DMSO), even though they have solubility parameters close to that of acetonitrile. Plausibly, the high viscosity of these solvents has an important effect on the aggregation.

In our experiments, DPDVB55 particles obtained are highly crosslinked. They will not be dissolved in any organic solvent. Because of the crosslinked structure, the polymer formed during the reaction should precipitate out in both "poor" and "good"

Table 3.4 Dispersion Polymerization of DVB55 in Ethanol

DVB55 (vol%)	d_n (μm)	CV (%)	Comment
5	< 1	—	Spherical
10	1.37	20	Spherical
15	2.77	16	Deformed
20	—	—	Coagulum

solvents. A reaction was therefore conducted in a good solvent. Dispersion polymerization of DVB55 in toluene (Table 3.5), however, gave only a gel. This is due to the surface stickiness. Although the forming particles will not be dissolved, they will be swollen by the solvent, which makes the particle surface more sticky as in the case of high concentration of monomer. In addition, toluene reduces the crosslink density by chain transfer, further increasing the particle stickiness. As described earlier, the sticky surface of the microspheres will then lead to coagulation.

Table 3.5 Solvent Effect on the Formation of DPDVB55 Microspheres^a

Solvent	δ^b (cal ^{1/2} cm ^{3/2})	η^b [cP]	Particle Shape
Acetonitrile	12.1	0.341	Spherical
Ethanol	12.8	1.080	Spherical
N,N-Dimethylformamide	12.1	0.802	Deformed
Dimethylsulfoxide	12.0	1.991	Coagulum
Toluene	8.91	0.553	Gel

^a [DVB55] = 5 vol.%; [PVP] = 16 g/L; [AIBN] = 1.0 wt.%; 70°C; 24 h.

^b δ = solubility parameter; η = viscosity³²

3.4.2.3 Effective Crosslinker Concentration

Attempts to synthesize crosslinked polystyrene microspheres by means of dispersion polymerization have been reported in several papers as described in section 3.1. All these attempts were conducted in the similar fashion, *i.e.*, a low level of crosslinker was added to the reaction mixture under standard dispersion polymerization conditions. Our approach was based on the idea that a highly crosslinked structure may give some

special properties, such as enhancement of the stability of forming microspheres, to the polymer microspheres. As well, our ultimate application of these particles as HPLC resins incorporating rigid chiral cavities required very high crosslink densities. We started with commercial divinylbenzene which contains 55% of actual crosslinker (*m*-DVB, *p*-DVB) in addition to 45% ethylstyrenes, and observed that spherical particles having highly crosslinked structure were indeed formed.

In order to test the influence of the actual crosslinker/monovinyl ratio, we diluted commercial divinylbenzene with 4-methylstyrene (MSt) to cover the range of effective crosslinker content from 0 to 55% at a constant total monomer loading of 10 vol%. PVP and AIBN concentrations were held constant at 16 g/L and 1 wt%, respectively. The reactivities of MSt and of the ethylstyrene were considered equivalent. In this set of experiments, narrow disperse particles were formed both in complete absence of crosslinker (Figure 3.5a), and at an effective divinylbenzene content of 55% (Figure 3.5c). Coagulation occurred progressively when the actual crosslinker concentration fell below 50% (Figure 3.5b, 30% (*m+p*)-divinylbenzene).

This result indicates that a high level of effective crosslinker is indeed crucial for forming crosslinked polystyrene-type microspheres by dispersion polymerization. In this case, at the same concentration of total monomer (*i.e.*, solvency of the medium is same), reactions containing less crosslinker will give larger, swollen particles. Compared with the particles formed in the presence of high levels of crosslinker, these swollen particles are prone to aggregate due to the sticky surfaces. A ratio of 50% actual divinylbenzene isomers to 50% mono vinylbenzenes seems to be the minimum level of crosslinker necessary to get spherical crosslinked polystyrene-type particles by dispersion polymerization.



Figure 3.5 Particles formed from a 5% solution in ethanol of: (a) 4-methylstyrene; (b) mixture of DPDVB55 and 4-methylstyrene, containing effective DVB of 30%; (c) DPDVB55. Reactions conditions: [PVP] = 16 g/L, [AIBN] = 1 wt.%, 70°C for 24 h.

3.4.2.4 Effect of Stabilizer Concentration

In all experiments described in this chapter, poly(*N*-vinylpyrrolidone) was used as a stabilizer. Table 3.6 shows the effect of stabilizer (PVP) concentration on particle size. For PVP concentrations below 16 g/L substantial amounts of coagulum were obtained. Dispersions became stable at PVP concentrations of 16 g/L or higher. At a PVP concentration of 48 g/L spherical submicron particles were formed. Such a strong dependence of particle size on stabilizer concentration has already been observed in linear polymer microspheres, and is thought to reflect the larger particle surface area that can be stabilized at higher PVP concentrations.²⁴ A PVP concentration of 16 g/L appears well suited for the formation of narrow disperse micron size DPDVB55 particles under the conditions used.

Table 3.6 Effect of PVP Concentration on DPDVB55 Particles^a

PVP (g/L)	d_n (μm)	Conversion (%)	Comment
0	2.1	—	spherical, narrow disperse
1.6	—	85	Coagulum
4.8	—	89	Coagulum
8.0	—	76	Coagulum
16.0	2.68	80	Spherical
32.0	<1 ^b	88	Spherical
48.0	0.1-0.9 ^b	88	Spherical

^a Conditions: 10 vol.% DPDVB55 in acetonitrile; 1 wt% AIBN; 70°C for 24 h.

^b Optical microscopy, average of 200 particles.

There was an unexpected result in this set of experiments. When we changed the concentration of PVP from 1.6 to 48 g/L to study the stabilizer effect on the particle formation, we also performed a reaction in the complete absence of stabilizer. The result was astonishing. Spherical particles were obtained. Duplicate experiments showed that this experiment was reproducible in acetonitrile. However, under the same conditions, only coagulum was obtained in ethanol. When the polymerization was done using the rotor stirring method described in section 3.3.2, the microspheres obtained had even narrower size dispersity. Figure 3.6 shows the optical micrograph of polyDVB55 particles synthesized without using PVP in acetonitrile.

This result was very interesting to us. As there was no PVP stabilizer involved, this polymerization falls into the category of precipitation polymerization. The microspheres obtained had a clean surface which is attractive for many applications. The fact that these polyDVB55 particles were formed in the absence of stabilizer suggests a different mechanism of particle formation and stabilization compared to dispersion polymerization. Efforts have been made to study this new process and will be described in Chapter 4.

3.4.3 Scale-up of DPDVB55 Microspheres Production

Spherical particles were obtained in the reaction of 10% DVB55 in acetonitrile at 70°C. However, a strong influence of temperature on DPDVB55 particle morphology was observed upon scale-up. Linear scale-up to 5 g DVB55 in 50 ml acetonitrile, under otherwise identical conditions, required lower reaction temperatures to yield spherical particles. Figure 3.7 shows DPDVB55 particles prepared using a step-wise temperature rise from 50 to 70°C. The polymerization temperature was initially held at 50°C for 20 h, then raised to 60°C for 4 h, and finally increased to 70°C for the last 2 h.

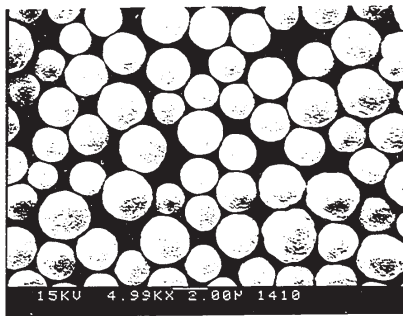


Figure 3.7 DPDVB55 particles obtained in the scaled-up reaction using a 50-70°C temperature profile.

3.4.4 Porosity of DPDVB55 Particles

To evaluate their potential as chromatographic supports, the DPDVB55 particles prepared in the scaled-up reaction (see next section) were slurry packed into a column as described previously in Chapter 1. The plot of retention volumes versus molecular weight of the narrow disperse polystyrene standards (Figure 3.8) shows the particles to have an exclusion limit at a molecular weight of 9.8×10^6 , giving a void volume (V_0) of 3.12 ml. The elution volume for toluene (or total inclusion volume, V_{toluene}) is ca. 3.8 ml. The particle porosity is then given by eq. (3.5), and amounts to 29%

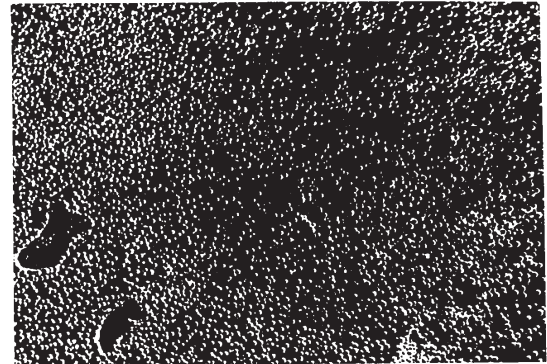


Figure 3.6 PolyDVB55 particles obtained without PVP

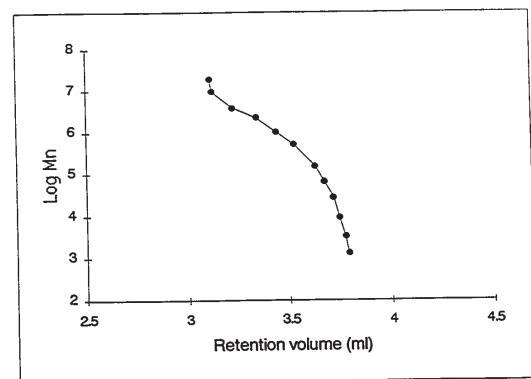


Figure 3.8 Size-exclusion calibration of DPDVB55 particles. Conditions: narrow disperse polystyrene standards in tetrahydrofuran at 25°C; column bed length, 7 cm; flow rate, 0.5 ml/min.

of the total particle volume. No macropores are noticeable in the scanning electron micrograph of these particles (Figure 3.9). It is plausible that most of this pore volume is due to micropores, e.g., the interstitial volume between primary and secondary clusters within the particles.

3.4.5 Morphology of DPDVB55 Particles

The surface morphology of polystyrene microspheres synthesized by dispersion polymerization has been described by many researchers. Narrow or even monodisperse microspheres with very smooth surface are commonly observed. In contrast, the DPDVB55 particles prepared in this research usually have rough surfaces. This unique feature is due to the different particle formation process. Diffusion of monomer into the stabilized microspheres followed by polymerization inside the microspheres is believed to be the process of particle growth in the dispersion polymerization of styrene (and other monovinyl monomers).¹⁵ In our present system, the diffusion of monomer, DVB55, into the stabilized particles is probably limited, especially when the crosslinking density increases. The growth of particles is then largely due to the absorption and binding of small entities (oligomeric radicals, primary particles, unstable small particles *etc.*) onto the existing stable larger particles. These small entities are surface active. They keep growing by absorbing further oligomers, and lead to final particles with a rough surface structure.

It is conceivable that the observed porosity is caused by the interstitial spaces between these deposited small entities. The subsequent growing process, i.e., by incorporating oligomers or monomer, will fill in the macropores. This will diminish the porosity and results in the lack of macropores as seen above in Figures 3.8 and 3.9.

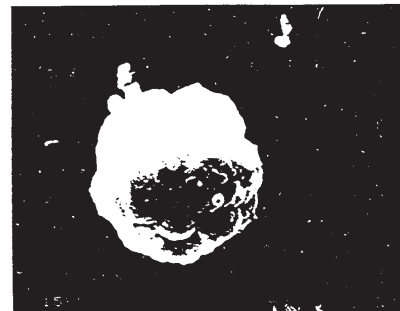


Figure 3.9 Surface structure of DPDVB55 particles

One can expect to see radial growth of these particles, especially at later stages when the particle cores have become highly crosslinked and glassy. This radial polymerization may offer a means of incorporating functional comonomers into the surface near the end of the polymerization. In principle, core-shell particles may be obtained by this method. A composition gradient may even exist within particles prepared from DVB55. As we have mentioned earlier, commercial divinylbenzene is a mixture of *meta*- and *para*-divinylbenzene (55%) and monofunctional ethylvinylbenzenes (EVB, 42%). The individual isomers have different relative radical reactivities as reported by Walczynski³³ (Table 3.7).

Table 3.7 Relative Radical Reactivities of DVB55 Components³³

DVB55 Component	Relative Reactivities
p-Divinylbenzene	7
m-Divinylbenzene	4
m-Ethylstyrene	1.4
p-Ethylstyrene	1

As the two divinylbenzene isomers are more reactive than either ethylstyrene, they should be preferentially incorporated at early stages of polymerization, i.e., into the primary particles. This would lead to highly crosslinked primary particles that would form the cores of the final particles. The final particle surfaces form at higher monomer conversions, when the system is partially depleted of crosslinker. These surfaces should therefore be less highly crosslinked than the particle cores. This has been confirmed by using reverse phase HPLC in monitoring the conversion of individual DVB55 components during polymerization (see Chapter 4).

3.4.6 Proposed Mechanism of DPDVB55 Particle Formation

The mechanism for formation and growth of dispersion polymer particles from monofunctional monomers has become reasonably well understood, at least in its general principles. In analogy, we can propose the mechanism shown in Figure 3.10 for the formation of the DPDVB55 particles.

At the start of the process, DVB55, PVP and AIBN form a homogeneous solution in the reaction medium (A). Upon heating to the reaction temperature, the initiator decomposes and the free radicals react with divinylbenzene to form insoluble oligomeric network radicals (B). These oligomers aggregate quickly to form the primary

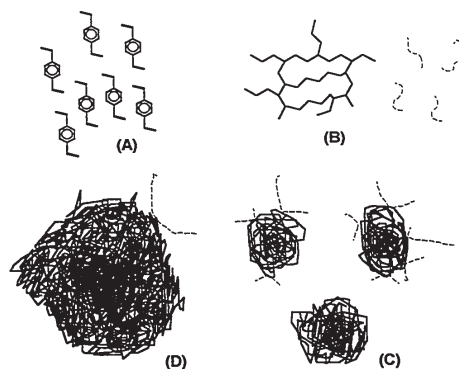


Figure 3.10 Stages of particle formation: (A) homogeneous solution of DVB55, PVP, AIBN; (B) formation of crosslinked oligomer radicals; (C) aggregation into primary particles, stabilized by PVP and/or crosslinking density; (D) particle grown by capture of oligomers, primary particles, and/or diffusion of monomer.

solid particles (C). These may then grow further by either DVB55 absorption, or by oligomer capture, or by aggregation with other primary particles, to form the final stable particles (D). As in linear dispersion polymerization of styrene, the primary particles should be very efficient at removing newly formed oligomers from solution.

The stability of the forming particles are controlled by two factors. PVP stabilizer certainly contributes to stabilize the forming particles. In fact, we have seen that the number of particles increased with increasing concentration of PVP. However, the question is to what extent the stabilizing effect of PVP is affected by the crosslinking. As pointed out by Barrett and Thompson, the effectiveness of the stabilizer may be lost due to its incorporation into the interior of the crosslinked polymer matrix during growth in dispersion polymerization.³⁴ In stage (C), the forming primary particles incorporate PVP, but are not stable enough because of the low efficiency of PVP. They will aggregate with other primary particles, oligomer radicals or newly formed primary particles to produce larger particles. This trend would keep on going indefinitely provided no other factors contribute to stabilize these particles. Since spherical DPDVB55 particles can only be obtained in the presence of large amounts of crosslinker, the high crosslinking density is therefore thought to be the main reason for the stability of larger DPDVB55 particles. Due to the high level of crosslinker, a high crosslinking density is soon built up both inside and on the surface of the particles. Particles become hard and rigid, and hence stable. In addition, there was relatively little adsorption of monomer into the particles because of the highly crosslinked structure. The major locus of polymerization was in the liquid phase. The progressive nucleation during the polymerization made DPDVB55 particles narrow disperse, not monodisperse.

117

- 18 S. Margel, E. Nov, and I. Fisher, *J. Polym. Sci. Polym. Chem.*, **29**, 347 (1991).
- 19 S. Shen, E.D. Sudol, and M.S. El-Aasser, *J. Polym. Sci. Polym. Chem.*, **31**, 1393 (1993).
- 20 M. Okubo, Y. Katayama, and Y. Yamamoto, *Colloid Polym. Sci.*, **269**, 217 (1991).
- 21 Y. Almog, S. Reich, and M. Levy, *Br. Polym. J.*, **14**, 131 (1982).
- 22 A. Penlidis, Ph.D. thesis, McMaster University.
- 23 A.J. Paine, *Macromolecules*, **23**, 3109 (1990).
- 24 A.J. Paine, W. Luymes, and J. McNulty, *Macromolecules*, **23**, 3104 (1990).
- 25 F. Winnik and C.K. Ober, *Eur. Polym. J.*, **23**(8), 617 (1987).
- 26 C.K. Ober, K.P. Lok and M.L. Hair, *J. Polym. Sci. Polym. Letters Ed.*, **23**, 103 (1986).
- 27 C.K. Ober and K.P. Lok, *Macromolecules*, **20**, 268 (1987).
- 28 K.P. Lok, and C.K. Ober, *Can. J. Chem.*, **63**, 209 (1985).
- 29 C.K. Ober, and M.L. Hair, *J. Polym. Sci. Polym. Chem. Ed.*, **25**, 1395 (1987).
- 30 T. Corner, *Colloids Surf.*, **3**, 119 (1981).
- 31 Y.Y. Lu, M.S. El-Aasser, and J.W. Vanderhoff, *J. Polym. Sci. Polym. Phys. Ed.*, **26**, 1187 (1988).
- 32 J.A. Riddick, W.B. Bunger, and T.K. Sakano, *Organic Solvents-Physical Properties and Methods of Purification*, 4th ed., Wiley, New York, 1986.
- 33 B. Walczynski, B.N. Kolazz, and H. Galina, *Polym. Commun.*, **26**, 276 (1985).
- 34 K.J. Barrett, and M.W. Thompson, The Preparation of Polymer Dispersions in Organic Liquids, in *Dispersion Polymerization in Organic Media*, K.J. Barrett, ed., Wiley, London, p232, 1975.

REFERENCES

- 1 A. Guyot, Synthesis and Structure of Polymer Supports, in *Syntheses and Separations Using Functional Polymers*, D.C. Sherrington and P. Hodge, Ed., p1, John Wiley & Sons, 1988.
- 2 S.M. Ahmed, *Dispersion Sci. Technol.*, **5**, 421 (1984).
- 3 J. Ugelstad, H.R. Mfutakamba, P.C. Mørk, T. Ellingsen, A. Berge, R. Schmid, L. Holm, A. Jorgedal, F.K. Hansen, and K. Nustad, *J. Polym. Sci. Polym. Symposium*, **72**, 225 (1985).
- 4 J. Ugelstad, K.H. Kaggerud, F.K. Hansen, A. Berger, *Makromol. Chem.* **180**, 737 (1979).
- 5 J. Ugelstad, A. Berge, T. Ellingsen, R. Schmid, T.-N. Nilsen, P.C. Mørk, P. Stenstad, E. Hornes, and Ø. Olsvik, *Prog. Polym. Sci.*, Vol. **17**, 87 (1992).
- 6 V. Smigol, F. Svec, K. Hosoya, Q. Wang, and J.M.J. Fréchet, *Angew. Makromol. Chem.*, **195**, 151 (1992).
- 7 K. Hosoya, and J.M.J. Fréchet, *J. Liq. Chromat.*, **16**(2), 353 (1993).
- 8 K. Hosoya, and J.M.J. Fréchet, *J. Polym. Sci. Polym. Chem.*, **31**, 2129 (1993).
- 9 C.M. Cheng, F.J. Micala, J.W. Vanderhoff, and M.S. El-Aasser, *J. Polym. Sci. Polym. Chem.*, **30**, 235 (1992).
- 10 C.M. Cheng, J.W. Vanderhoff, and M.S. El-Aasser, *J. Polym. Sci. Polym. Chem.*, **30**, 245 (1992).
- 11 K. Kobayashi, and M. Senna, *J. Appl. Polym. Sci.*, **46**, 27 (1992).
- 12 D. Zou, V. Derlich, K. Gandhi, M. Park, L. sun, D. Kriz, Y.D. Lee, G. Kim, J.J. Aklonis, and R. Salovey, *J. Polym. Sci. Polym. Sci.*, **28**, 1909 (1990).
- 13 D. Zou, S. Ma, R. Guan, M. Park, L. Sun, J.J. Aklonis, and R. Salovey, *J. Polym. Sci. Polym. Chem.*, **30**, 137 (1992).
- 14 D. Zou, J.J. Aklonis, and R. Salovey, *J. Polym. Sci. Polym. Chem.*, **30**, 2443 (1992).
- 15 C.M. Tseng, Y.Y. Lu, M.S. El-Aasser, and J.W. Vanderhoff, *J. Polym. Sci. Polym. Chem.*, **24**, 2995 (1986).
- 16 C.K. Ober, and K.P. Lok, *U.S. Patent #4,617,249*.
- 17 C.K. Ober, *Makromol. Chem., Macromol. Symp.*, **35/36**, 87 (1990).

CHAPTER 4

MONODISPERSE POLYDIVINYLBENZENE
MICROSPHERES BY PRECIPITATION POLYMERIZATION

4.1 POLYMER PARTICLES BY PRECIPITATION POLYMERIZATION

The work described in this chapter stems directly from the intriguing observation that DVB55 forms narrow disperse microspheres during polymerization in complete absence of steric or ionic stabilizers (page 107 in Chapter 3). The process involves only DVB55, AIBN initiator, and acetonitrile solvent, and should be classified as a precipitation polymerization. Similar to dispersion polymerization, precipitation polymerization starts off in a homogeneous solution. As soon as polymer chains are formed, and grow to exceed their critical chain length, precipitation takes place. Usually, precipitation polymerization produces polymers in the state of coagulum or aggregates instead of fine microspheres.

In addition to the well known precipitation polymerizations of acrylonitrile¹ and vinyl chloride,^{2,3} which are two examples in which polymer particles can be produced, several other systems have recently been reported. Pelton⁴ found that monodisperse hydrogel microspheres were produced in the polymerizations of some N-substituted acrylamide. Kawaguchi *et al.*⁵ obtained monodisperse 1 μm size particles in the

precipitation copolymerization of acrylamide with other comonomers. They found that methacrylic acid as comonomer was very effective in producing small, monodisperse microspheres. This was attributed to the contribution of methacrylic acid units to the stabilization of the particles formed at the initial stage of polymerization.⁶ Naka and Yamamoto *et al.*⁷ reported the synthesis of monodisperse poly(diethylene glycol dimethacrylate) microspheres. Diethylene glycol dimethacrylate was used as monomer, and reactions were carried out in different organic solvents. The process was a precipitation polymerization in nature, and the polymerization was initiated with ⁶⁰Co gamma rays at room temperature. Monodisperse microspheres in the range of 0.4 - 4.8 μm were obtained. The stability of the particles was thought to be due to their crosslinked structure. This process most closely resembles the precipitation polymerization described here.

The synthesis of polystyrene type particles by means of precipitation polymerization has not been described yet, although extensive studies on the formation of polystyrene-type particles have been carried out for many years.

4.2 AIM OF THE RESEARCH

The synthesis of monodisperse crosslinked polydivinylbenzene microspheres by means of precipitation polymerization is a new process. The process may have significant practical implication, since the resulting particles have several unusual properties. As well, the process may have theoretical implications with regard to particle formation, growth and stabilization. Information on this novel system is largely unknown. For application purposes as well as for understanding the mechanism of particle formation, the following experiments were conducted.

First, the optimum conditions for synthesizing monodisperse polydivinylbenzene microspheres were studied. Subsequently, several experimental parameters that influence the particle formation and growth during the polymerization were evaluated. The microspheres obtained were characterized by different techniques. Finally, a mechanism for the formation of monodisperse polydivinylbenzene microspheres in this system was proposed.

4.3 EXPERIMENTAL

4.3.1 Materials

In addition to the materials described in the experimental section of Chapter 3, the following materials were used. Technical-grade divinylbenzene containing 75 to 85 wt% of *p*-DVB and *m*-DVB was purchased from Fluka. ¹H NMR analysis indicated the product we used contained 80.1% of divinylbenzenes and 19.9% of ethylstyrenes. The material was accordingly called DVB80. Initiators used in this research along with their structures and suppliers are listed in Table 4.1. These initiators were used as received. Acetonitrile was obtained from BDH and ethanol from Aldrich. Both were HPLC grade. All other solvents were used without further purification.

4.3.2 Description of the Reactor

Since precipitation polymerizations of commercial divinylbenzene were conducted in absence of stabilizer, it was found that the formation of particles was even more sensitive to the agitation method. The reactor was designed to permit a very gentle, even agitation during the polymerization. A rotor plate with ten holes to hold bottle reactors was used (Figure 4.1). The rotor plate was submerged in a thermostatted water bath and rotated around the long axis horizontally at 30 rpm.

A version of the setup for the precipitation polymerization of DVB55 is shown in Figure 4.3. The rotor plate was driven by a motor via a flexible cable, and the speed of the rotor plate was controlled by a transformer. The temperature was controlled to better than ±1°C for all polymerizations.

Initiators	Abbr.	Structure	Source
2,2'-Azobis(isobutyronitrile)	AIBN		Kodak
Benzoyl peroxide	BPO		Aldrich
2,2'-Azobis(2,4-dimethylvaleronitrile)	ADVN		Polysciences Inc
2,2'-Azobis[2-(2-imidazolin-2-yl) propane]	AIYP		Polysciences Inc

Table 4.1 Initiators used in This Research

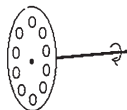


Figure 4.1 A rotor plate used in precipitation polymerization of commercial divinylbenzene.

4.3.3 Typical Precipitation Polymerization of DVB55 (PPDVB55)

Polymerizations were carried out in sets of 8-10 parallel experiments. AIBN (0.011 g, 2 wt% relative to DVB55) was added to a solution of DVB55 (0.6 ml, 0.56 g; 2 vol% relative to total volume) in acetonitrile (29.4 ml) in a 30 ml polypropylene screw-cap bottle. The polymerization process was identical to dispersion polymerization of DVB55 discussed in the last chapter, except that no PVP was used (Figure 4.3). The bottles were attached to the rotor plate which was submerged in the water bath and rotated around the long axis at 30 rpm as described above. The temperature of the water bath was increased from ambient to 70°C within 50 min. The initially homogeneous reaction mixtures turned milky white within 1-2 hours after reaching 70°C, depending on the initiator and monomer concentrations. All reactions were run for 24 h, unless otherwise stated. At the end of the reaction, unreacted monomer and any traces of soluble polymer and initiator residues were removed by centrifuging and resuspending the microspheres twice each in ethanol and tetrahydrofuran. The microspheres were then left under acetone overnight, resuspended twice in ethanol, and centrifuged. The cleaned microspheres were kept in ethanol (or methanol) solution, or dried under vacuum if necessary. In some reactions, a small amount of hydroquinone was added to each bottle at the end of the reaction to stop the

4.3.5 Porosity of PPDVB55 Microspheres

The pore size and pore size distribution of some PPDVB55 microspheres were measured at the Department of Chemistry, Cornell University. Pore size distributions for micropores and smaller mesopores and specific surface areas were measured with a Quantachrome Autosorb-1 automated gas adsorption system using nitrogen at 77K. The porosity due to the larger mesopores and macropores were measured with a PMI 60K-A-1 automated mercury porosimeter.

Pore volumes were also examined by a solvent regain method based on the procedure described by Rolls *et al.*⁸ In this experiment, Centrex disposable centrifugal microfilters were employed, which consist of three pieces: a plastic cap, a receiver and a filter tube which was fitted with a 0.2 μm pore size Nylon membrane. The plastic receiver was used to collect centrifuged solvent. In a typical experiment, the weight of the empty filter tube was recorded, 200 mg of PPDVB55 microspheres were added, and the filter tube was then reweighed. Four milliliter of cyclohexane were added and the tube was sealed with the cap. In order to prevent the cyclohexane from draining through the membrane overnight, the filter tube was placed into cyclohexane in a 250 ml beaker with a cover for 24 h. The receiver tube was then connected to the filter tube (without the cap), and the excess cyclohexane was removed by centrifugation at high speeds for 5 min. The filter tube was weighed quickly, and the amount of cyclohexane absorbed by the sample, a , was calculated from the increase in weight of the filter tube. The solvent regain of the PPDVB microspheres was then calculated using the following equation:

$$R_s = \frac{d(a-b)}{w} \quad (4.1)$$

where d = density of cyclohexane = 0.78 (ml/g), w = weight of microspheres used in the experiment, b is the weight of cyclohexane retained by the membrane, which was obtained

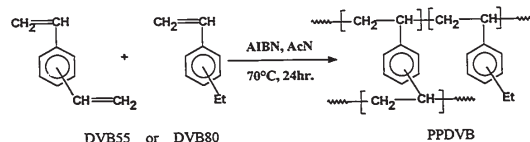


Figure 4.2 Precipitation polymerization of DVB55 or DVB80.

polymerization. These bottles were then stored in a freezer until work-up. This treatment had no effect on particle morphologies.

4.3.4 Determination of Size, Size Distribution and Yield of PPDVB Microspheres

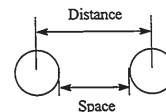
The size and size distribution of the microspheres were determined by a Coulter Multisizer II. Morphologies of microspheres were examined by ISI DC-130 scanning electron microscopy. The principles and operations of these techniques have been described in Chapter 2 and Chapter 3, respectively.

Monomer conversions were initially determined by the procedure described in Chapter 3. They were determined later by using the yield of microspheres instead. Briefly, the yield of the microspheres was obtained as the weight of clean and dry microspheres divided by the theoretical weight of polymer. Extraction of the raw polymer particles with tetrahydrofuran showed no noticeable fraction (less than 1%) of soluble polymer. In addition, the polymer microspheres were not accompanied by any coagulum fraction, and the microsphere yields are therefore identical to the monomer conversions. This method proved to be efficient compared with the former one.

from the difference between the filter tube filled with cyclohexane followed by centrifuged and the empty tube.

4.3.6 Calculations of Distance Between Microspheres and of Solubility Parameter of the Solvent Mixture

The distance between forming microspheres during polymerization is defined as below.



The calculation of this distance was conducted using the procedure described by Naka *et al.*⁹ It assumes that all microspheres have the same distance to the neighboring particles. The centre to centre distance is calculated using the equation for the hexagonal closest packing:

$$\text{Distance} = \sqrt{\frac{4V}{n} \times \frac{1}{\sqrt{2}}} \quad (4.2)$$

where V is the volume of the solution and n is the number of microspheres.

The solubility parameter of the solvent mixture was calculated using the following equation:¹⁰

$$\delta_{\text{mix}} = \left(\sum \Phi_i \delta_i^2 \right)^{1/2} \quad (4.3)$$

where Φ_i and δ_i are the volume fraction and solubility parameter of component i , respectively. Initiator was not considered in the calculation because it was present in only small quantities. The polymer produced from the monomer was not included in the calculation neither since it was located in a separate phase.

4.5 RESULTS AND DISCUSSION

4.5.1 Basic Parameters Influencing the Formation of PPDVB55 Microspheres

In this set of experiments, the effects of basic parameters, such as method of agitation, temperature, monomer concentration, initiator concentration and effective crosslinker concentration, on the formation and growth of PPDVB microspheres were examined. All polymerizations were performed in HPLC grade acetonitrile solvent.

4.5.1.1 Reactor Setup and Operation Conditions

As expected, the particle formation in the absence of stabilizer was even more sensitive to the method of agitation. Experiments were performed with 2 vol% of DVB55 (relative to total reaction mixture), and 2 wt% of AIBN (based on monomers). Magnetic stir bar and mechanical overhead paddle stirring gave only coagulum of polyDVB55. Particles were obtained in an ultrasonic water bath, but with poor reproducibility. Apparently, the enforced contact between the forming microspheres led to coagulation. Similar to the dispersion polymerization of DVB55, spherical polyDVB55 particles with broad size distribution were given in the absence of agitation, presumably due to the sedimentation of microspheres during the polymerization. Compared with DPDVB55 in which forming particles are partially stabilized by PVP, even more mild agitation is necessary for the synthesis of PPDVB55 particles. The major role of the agitation is to prevent sedimentation. Perhaps the best place for synthesizing monodisperse PPDVB55 microspheres would be a zero gravity lab in earth orbit.¹¹

Efforts were made to design a reactor which would be suitable for the precipitation polymerization of DVB55 system. The reactor setup is shown in Figure 4.3. It consists of a rotor plate holding a set of reaction vessels which were slowly rotated

around their long axes. It was found that PPDVB55 was quite sensitive to impurities such as water. Any leaking of the bottle during the polymerization will lead to coagulation of the microspheres. 30 ml polypropylene screw-cap bottles proved to be superior to several types of glass bottles in the capability to prevent leaking. The optimized conditions for obtaining monodisperse PPDVB55 microspheres are listed in Table 4.2.

Table 4.2 Conditions for Monodisperse PPDVB55 Microspheres

bottle reactor	polypropylene (30 ml)
rotating speed of rotor plate	30 rpm
starting temp. of polymerization	ambient
reaction temp. of polymerization	70°C
time needed from starting temp. to reaction temp.	70 min.

Figure 4.4 shows the SEM of the PPDVB55 microspheres, and reveals them to be spherical, highly uniform in size with relatively smooth surfaces. Consequently, 30 rpm rotating rate and increasing temperature profile were used as standard throughout this research.



Figure 4.3 Photograph of the reactor used for precipitation polymerization of commercial divinylbenzene.

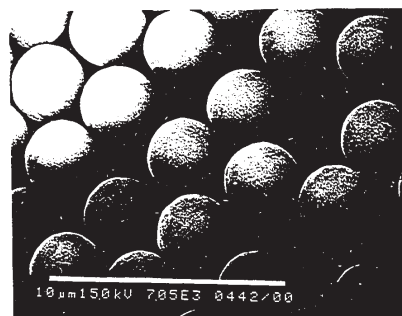


Figure 4.4 SEM of PPDVB55 microspheres. Conditions: 2 vol % DVB55; 2 wt % AIBN; 30 rpm; temperature: 20 to 70°C within 70 min., then at 70°C for 23 h.

4.5.1.2 Effect of initial monomer concentration

Since the monomer (DVB55) acts as cosolvent and as reagent, the initial monomer concentration may have a strong effect on the size of the resulting particles. Table 4.3 shows the effect of initial monomer concentration on the particle size. These PPDVB55 microspheres were prepared from 2-20 vol% DVB55 in acetonitrile. The relative amount of AIBN was held constant at 2 wt% relative to DVB55. Monodisperse microspheres were obtained from the reactions containing 2 and 5 vol% DVB55. The diameters and yield of microspheres increased with increasing monomer concentration. Figure 4.5 shows a typical size-histogram of PPDVB55 microspheres as measured by a Coulter Multisizer II using a narrow window (256-channel). These microspheres are essentially monodisperse as seen from the coefficient of variation of ca. 3%.

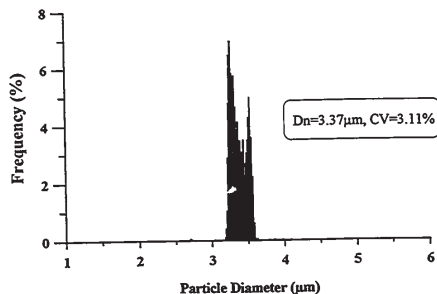


Figure 4.5 Size histogram of PPDVB55 microspheres (Run 38(1))

Table 4.3 Effects of DVB55 Concentration on PPDVB55 Microspheres^a

Run	DVB55 (Vol%)	D_n (μm)	δ_{mix}^b (cal/ml) ^{1/2}	σ^c (μm)	CV (%)	Yield (%)	Particle shape
1	2	3.37	11.85	0.11	3.1	31	monodisperse
2	5	3.63	11.77	0.11	3.0	51	monodisperse
3	10	—	11.64	—	—	—	coagulum
4	15	—	11.51	—	—	—	coagulum
5	20	—	11.38	—	—	—	coagulum

^a Reaction conditions: acetonitrile solvent; [AIBN] = 2 wt% relative to DVB55; 70°C; 24 hours;
^b Solubility parameter of the reaction mixture calculated by $\delta_{mix} = (\Phi_1 \delta_1^2 + \Phi_2 \delta_2^2)^{1/2}$, where δ and Φ are the solubility parameter and volume fraction of DVB55 and acetonitrile, respectively.
^c σ = standard deviation



Figure 4.6 SEM micrograph of PPDVB microspheres (Run 38(1)).

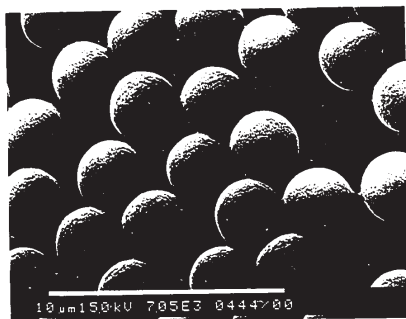


Figure 4.7 SEM micrograph of PPDVB55 microspheres (Run 38(1)) with higher magnification.

The SEM image of these PPDVB55 microspheres is shown in Figure 4.6. As can be seen, the PPDVB55 microspheres obtained have a perfectly spherical shape and are highly uniform in size. However, an SEM with higher magnification reveals that the surface of these microspheres is somewhat rough (Figure 4.7). This unique surface morphology was derived from the process of particle formation, which will be described later.

As discussed in Chapter 3, an increase in monomer concentration affects the nucleation process in many ways. The calculated solubility parameter changes from 11.85 to 11.77 when the initial concentration of DVB55 increases from 2 to 5 vol% (Table 4.3). Although the change of solubility parameter of the medium is small ($\Delta\delta_{mix} = 0.08$ (cal/ml)^{1/2}), an increase in the size of PPDVB55 microspheres was observed. The solvency of the continuous phase increased so that the oligomeric network could grow to a larger size before precipitation. Meanwhile, the propagation rate of the oligomer chains was also increased. At the higher level of monomer concentration, the forming particle nuclei which have relative low crosslinking density would be swollen by the monomer to a larger extent, and the surface would be more sticky. The sticky surface promotes same-size particle coalescence. Finally, unstabilized small particles are captured by those microspheres that have passed their sticky state due to the crosslinking. All of these effects contribute to an increase in the final size of PPDVB55 microspheres with increasing DVB concentration.

Here, again, the origin of the particle stability is thought to be the high crosslinking density. A further increase in the concentration of monomer above 10 vol% led to only coagulum. At higher DVB55 concentrations, stabilization fails, probably because the increased solvency of the continuous phase swells the particle surfaces, and makes them more prone to coalescence not only of larger particles with forming nuclei but

Table 4.4 Effects of DVB80 Concentration on PPDVB80 Microspheres^a

Run No	DVB80 (Vol.%)	D_n (μm)	δ_{mix} (cal/m ³) ^{1/2}	σ (μm)	CV (%)	Yield (%)	Particle shape
1	0.5	2.74	11.89	0.13	4.6	14	monodisperse
2	1.0	2.81	11.87	0.10	3.6	32	monodisperse
3	2.0	3.74	11.85	0.13	3.5	46	monodisperse
4	3.0	4.19	11.82	0.14	3.3	54	monodisperse
5	4.0	4.65	11.80	0.16	3.4	57	bimodal
6	5.0	5.28	11.77	0.21	4.0	66	bimodal
7	6.0	6.73	11.74	0.70	10.3	68	partial coagulum
8	7.0	—	11.72	—	—	71	coagulum
9	8.0	—	11.69	—	—	75	coagulum
10	9.0	—	—	—	—	78	coagulum

^a explanations of D_n , δ_{mix} , σ , and CV refer to earlier tables.

also between like-size larger particles. In addition, the higher solid loading reduces the free space between the microspheres, and increases the collision frequencies of the particles. It was found that samples taken early (less than 4 hour, e.g. Run 63) in the polymerization from a reaction mixture containing 10, 15 and 20 vol% DVB55 showed nearly monodisperse microspheres, while coagulation happened afterwards for all of three samples.

Precipitation polymerization of DVB80 gave results similar to those involving DVB55 (Table 4.4). In this set of experiments, the concentration of DVB80 was varied from 0.5 to 10 vol%. By increasing the amount of monomer, the final diameter and yield of microspheres formed increased. Polymerization after 10 hours showed no coagulation for all runs. After 24 hour reaction, monodisperse PPDVB80 microspheres were obtained in the range of DVB80 concentration from 0.5 to 3.0%. Samples with 4% and 5% DVB80 gave bimodal distribution patterns of the microspheres, and further increases in the concentration of DVB80 led to partial or complete coagulation of the particles.

In general, the conversion of monomer increased with increasing monomer concentration, however, the microsphere surface changed from smooth to rough. The optimum concentration for both DVB55 and DVB80 monomer for the preparation of monodisperse microspheres appears to be 2 vol%. Higher loading of monomer is not favorable for the preparation of monodisperse microspheres, but it is suitable for the preparation of large particles with larger surface area.

It was noted that, for the same level of DVB55 loading, the size of microspheres obtained in the present precipitation system was much larger than that in DPDVB55 (dispersion polymerization of DVB55). Because DPDVB55 particles were synthesized using an ultrasonic stirring system, actually, there is no direct comparison between the two. Accordingly, DPDVB55 was carried out in the present rotor system

under the exact conditions as that of PPDVB55. The results indicated that the size of the DPDVB55 particles was indeed much smaller due to the stabilizer effect, and that the size distribution was also much broader. Figure 4.8 shows the size distribution pattern of DPDVB55 particles produced in the present reaction system. The diameter of DPDVB55 particles with 5 vol% monomer was 1.69 μm compared to 3.63 μm for PPDVB55 microspheres (Table 4.3). As well, the size distribution for the dispersion polymerization was much broader (24%) than that for the precipitation polymerization system (3.1%).

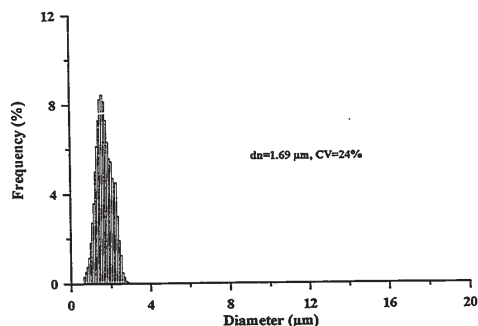


Figure 4.8 Size distribution pattern of DPDVB55 obtained under PPDVB55 conditions. Conditions: DVB55: 5 vol%; PVP: 16 g/L; acetonitrile; 70°C for 24 h. (Run dpdvb01).

4.5.1.3 Effective crosslinker concentration

In general, in order to obtain spherical microspheres, some types of additives must be used to give stability to the microspheres in the solution. The stabilization of the interface between monomer/polymer phases and liquid phase is the key for the preparation of spherical particles. In Chapter 3, we have discussed that the stability of the narrow disperse DPDVB55 particles stemmed jointly from the contributions of crosslinking and PVP stabilizer. As we have seen here, monodisperse polymer microspheres can be synthesized by precipitation polymerization of DVB55 in acetonitrile without using PVP. It was thought that the highly crosslinked structure of the microspheres together with their roughness were the source of their stability.

To test the effect of the effective concentration of crosslinker, DVB55 was diluted with 4-methylstyrene (4MSt) to give a series of comonomer mixtures labeled DVB50 to DVB5, with corresponding effective divinylbenzene fractions. The total monomer (DVB55 + 4MSt) concentration was kept as 2 vol% (based on total volume) to prevent any change of initial solvency. The radical reactivities of 4-methylstyrene and ethylvinylbenzene (ethylstyrene) are considered comparable in this experiment.¹² Table 4.5 shows that microspheres were obtained for effective divinylbenzene percentages between 55 and 35%. The diameters and particle size distributions increased with decreasing crosslinker percentages. Below 35% divinylbenzene, only coagulum was obtained.

The same dilution procedure was also applied to DVB80 to cover the effective crosslinker concentration from 50% up to 80%. Monodisperse microspheres were produced from the runs with effective crosslinker concentration above 55% (Run FM8d).

These results indicate that a high effective percentage of crosslinker molecules in the comonomer mixture is crucial to the formation of stable, monodisperse particles.

Table 4.5 Effect of Crosslinker Percentage in Comonomer Mixture on Diameter^a

Comonomer Mixture	(<i>m+p</i>)-Divinylbenzene (%)	D _n (μm)	CV (%)	Particle Size Distribution
DVB55 ^b	55	3.6	3.0	mono
DVB50 ^c	50	4.3	—	bimodal
DVB45 ^c	45	4.0	—	bimodal
DVB40 ^c	40	5.2	—	bimodal
DVB35 ^c	35	5.4	22	broad
DVB5-	5 - 30	—	—	coagulum
DVB30 ^c				

^a Data from run 40; reactions done at 5 vol% of combined monomers (DVB55 + 4MS) in acetonitrile as described in Table 4.1.

^b commercial DVB55 (55% *m+p*-divinylbenzene)

^c mixtures of DVB55 with 4-methylstyrene

The high crosslink density prevents particle coagulation. As previously discussed, at lower crosslinker/monomer ratios the microspheres will be more easily swollen by the monomer and solvent, making the particles more sticky and facilitating coagulation.

4.5.1.4 Initiator concentration

The size of the PPDVB55 microspheres as well as the overall conversion were influenced by the amount of initiator present at the start of the reaction. Figure 4.9 shows the effect of initiator concentration on DVB55 conversion and microsphere diameter. Both PPDVB55 microsphere diameter and DVB55 conversion increase with increasing AIBN concentration. However, the conversion of DVB55 was not complete even in the presence of 6 wt% of initiator. This, perhaps, is due to the low initiator efficiency caused by the low monomer concentration.

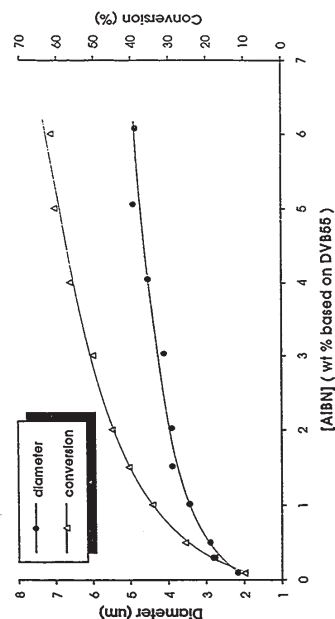


Figure 4.9 Effect of initiator concentration on the size of PPDVB55 microspheres and DVB55 conversion. (Run 42).

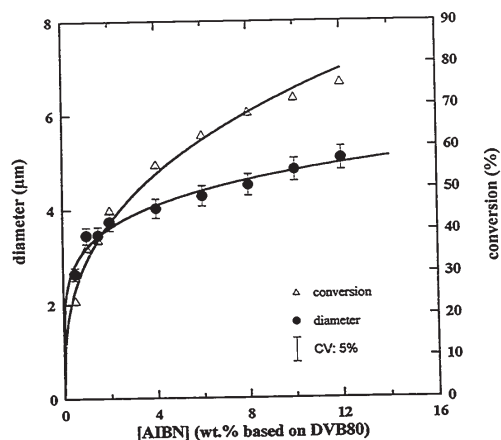


Figure 4.10 Effect of initiator concentration on the size of PPDVB80 microspheres and DVB80 conversion. (Run 56c).

Similar results were obtained in the precipitation polymerization of DVB80. Figure 4.10 shows the influence of AIBN concentration on PPDVB80 microspheres. The size of the microspheres increased with increasing amount of initiator. By 12 wt% of AIBN, the diameter of PPDVB80 was 5.07 μm (CV=3.1%). All runs gave monodisperse microspheres.

In the common dispersion polymerization of styrene, increasing the amount of initiator usually gives larger particles, with broader distribution.^{13,14} In our case, the monodispersity of PPDVB55 (or 80) was kept for a quite wide range of AIBN, from 0.5% to 15%. Increasing the initiator concentration will certainly increase the initial number of free radicals, which will lead to a higher number of nuclei. These nuclei are highly unstable and prone to coagulate to afford larger primary particles. The primary particles will soon become stable due to the internal and surface crosslinking reactions. The coagulation between such primary particles will be minimized. These stabilized primary particles will efficiently scavenge any newly formed nuclei onto their surface and grow. Clearly, the more initiator is used, the more nuclei (or small unstable particles formed by fast aggregation of the nuclei) will be produced. They serve as a source of growing for early formed stable particles. Therefore, the monodispersity is preserved even at high initiator concentrations.

Further insight into the polymerization can be obtained by examining Figure 4.11, which shows how the particle concentration varies with the concentration of initiator. It is interesting to note that the final number of microspheres decreases with increasing amounts of initiator. Because of this effect, the free space (distance) between PPDVB microspheres increased although their sizes were larger. This is one of the factors that help to preserve monodispersity.

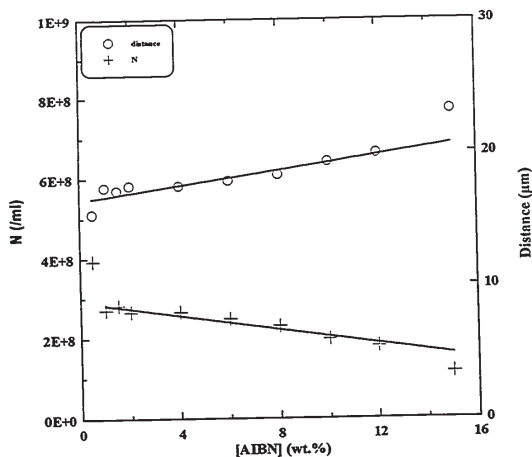


Figure 4.11 Number of PPDVB80 microspheres (+) and distance (o) among them vs. initial initiator concentration. (Run 56c).

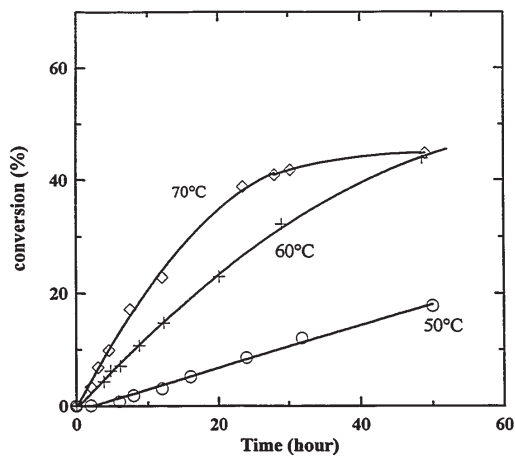


Figure 4.12 Conversion of DVB55 at various temperatures in precipitation polymerization. (Run 47a, 47b).

4.5.1.5 Polymerization Temperature

The reaction temperature may affect polymerization systems in many ways. The rate of free radical generation from azo initiators increases with increasing temperature. The thermodynamic properties of the polymerization medium also change with temperature. For example, the theta temperature, the temperature at which a polymer will precipitate, is related to the Flory-Huggins interaction parameter (χ). The theta temperature is highly dependent on the chain length (or molecular weight) of a polymer. The polymer chain conformation and even solubility (low molecular weight) can be affected by such a change of temperature. In the case of linear polymer, a soluble polymer of 10,000 molecular weight at a higher temperature can easily become insoluble at a lower temperature or *vice versa*. Since the nucleation process at early stages will be affected by these factors, changing temperature is then expected to influence the polymerization results.

A severe temperature effect was observed during the optimization of PPDVB55. A starting temperature of 70°C usually led to polydisperse particles. However, if the temperature was increased from ambient temperature (ca. 20°C) to 70°C during 70 minute period, monodisperse PPDVB55 microspheres were produced. This indicates that the temperature was critical to the particle formation stage, but not so crucial to the growth stage.

Polymerizations of DVB55 in acetonitrile conducted in the temperature range of 50 to 70°C indicated that yield and size of microspheres tended to increase with increasing temperature. Figure 4.12 shows a plot of percent conversion *versus* time at three of the temperatures examined (50, 60 and 70°C). As expected the initial rate of polymerization increased with reaction temperature because of the greater rate of free radical formation.

At higher conversion, however, the rate of polymerization at the higher temperature slowed down to such an extent that crossover occurred. After 50 hours, the polymerization at 60°C reached a higher degree of conversion than the reaction at 70°C. This result can be explained by differences in the initiator efficiency and kinetic chain lengths that occur in the three cases. At lower temperatures more monomer is converted to polymer per initiator fragment than at higher temperatures, where the higher rate of free radical formation will actually enhance the probability of chain termination by initiator. The initiator becomes exhausted more quickly at the higher temperatures and the polymerization slowed down and would be overtaken by those polymerizations run at a lower temperature.

In general, a strong auto-acceleration or Tromsdorf effect should be seen in a precipitation polymerization.¹⁵ Under our conditions, however, the precipitation polymerization of commercial divinylbenzene in acetonitrile is a slow process with no sign of such effect. During the polymerization, the viscosity of the particle interior increases, therefore, the rate of the termination reaction between the growing radicals decreases. In other words, polymerization should proceed under gel effect conditions if the main locus of polymerization is inside the growing particles. The plot of conversion *versus* time (Figure 4.12) indicates that the reverse is true, *i.e.*, the rate of polymerization decreases with conversion. Gel effect is almost entirely absent. In fact, slow polymerization rates of this system make it resemble a solution polymerization. This is probably because the solvent, acetonitrile, is a rather good solvent for both monomer and initiator. Both monomer and initiator (AIBN) are probably partitioned largely into the solution where most of the polymerization takes place instead of inside the particles. In addition, with DVB55 as monomer, the crosslinking density of the forming particles is quickly built up, which dramatically slows down the diffusion of monomer from the continuous phase, and

depresses the gel effect. A lack of gel effect in dispersion polymerization of styrene has been observed by Ober and Hair,¹⁶ which has been attributed to that most of the monomer remains in the continuous phase during the polymerization.

4.5.2 Effect of Initiator Type on PPDVB55 Microspheres

The conversion of the monomer in precipitation polymerization of DVB55 or DVB80 was rather low even with high levels of AIBN initiator (Figure 4.9, 4.10). We have assumed that the initiation and polymerization mainly happen in the liquid phase. If a initiator with a longer half life time than AIBN was used, the growth of microspheres might be prolonged. Accordingly, the conversion of monomer could be increased.

We used different initiators in the precipitation polymerization of DVB55. Here we define the oil soluble initiators as initiators that are soluble in both monomer and solvent (acetonitrile) phase and solvent soluble initiator as initiator that is only soluble in the solvent (acetonitrile). It was expected that by using two different types of initiators, the locus of precipitation polymerization of DVB55 could be changed, yielding some useful information about this system.

4.5.2.1 Oil soluble initiator

The oil soluble initiators we chose were 2,2'-azobis(2,4-dimethylvaleronitrile) (ADV N), 2,2'-azobis(isobutyronitrile) (AIBN) and benzoyl peroxide (BPO). Table 4.6 shows some physical parameters of these initiators and the size and size distribution of PPDVB55 microspheres prepared in acetonitrile using them. As can be seen, monodisperse particles were obtained with initiators having moderate decomposition rates

As expected, the more active initiator led to a low yield of PPDVB55 microspheres. The conversion curve with ADVN is nearly linear up to ca. 20% conversion and then slowly levels off within 25 h (Figure 4.13). The final conversion of DVB55 with either AIBN or BPO initiator was twice that with ADVN, and the polymerization process lasted a rather long period (more than 40 h). Apparently, the fast depletion of ADVN due to the high rate of termination caused by the high concentration of free radicals in the continuous phase led to the low conversion of the polymerization. The conversion with BPO was expected to be higher compared with AIBN due to BPO's longer half life time. Figure 4.12, however, indicates that the conversions of monomer were nearly the same in both systems. Apparently, BPO's high tendency toward cage-effect compared with AIBN led to its lower initiation efficiency,³⁶ and therefore, the lower conversion than it was expected. In addition, gel effect was absent for all initiator systems due to the reasons discussed in section 4.5.1.5.

4.5.2.2 Solvent soluble initiator

A polar azo-type initiator, 2,2'-azobis[2-(2-imidazolin-2-yl)] propane (AIYP), was used in this study. The structure of this initiator is shown in Table 4.1. AIYP has a 10 hour half life temperature of 61°C (the 10 hour half life temperature for AIBN is 65°C).¹⁸ The solubility of this initiator in several solvents was tested, and the results are shown in Table 4.7. As one can see, AIYP is soluble in methanol, but insoluble in toluene and water. In acetonitrile, it is partly soluble, but it becomes soluble when n-butanol is added (at the level of [butanol] > 2 vol%).

A mixture of acetonitrile with n-butanol was then employed as solvent. As we have seen earlier, precipitation polymerization of DVB55 in acetonitrile is sensitive to

at 70°C (AIBN and BPO). PPDVB55 particles with broad PSD were obtained in the system initiated by ADVN. That a high decomposition rate of initiator tends to produce particles with larger PSD has been observed in other systems.¹⁷ It was noted that the final size of microspheres did not change much with these initiators. Usually, in dispersion polymerization, a higher rate of initiation would lead to a higher degree of aggregation early in the polymerization, resulting in fewer but larger microspheres. Indeed fewer particles were produced by ADVN, however, the low conversion of this polymerization (ca. 20%, see Figure 4.13) made the size of microspheres smaller than what they should have been. As we have discussed earlier, the size of PPDVB55 microspheres increases monotonically with increasing conversion of DVB55 (Figure 4.9). If the conversion had reached 40% (which is the equivalent conversion of DVB55 initiated by AIBN under the same conditions), the average diameter would have been 4.5 μm instead of 3.6 μm.

Table 4.6 Effect of Initiator Decomposition Rate on Microspheres^a

Initiators	k_d (AN) ^b (s ⁻¹)	k_d (Tol) ^b (s ⁻¹)	$t_{1/2}$ (Tol) ^b (min)	D_n (μm)	CV (%)
ADV N		2.0×10^{-4}	58	3.6	19
AIBN		4.0×10^{-5}	289	3.8	3.2
BPO	1.76×10^{-5}	1.1×10^{-5}	1049	3.2	3.9

^a polymerization in acetonitrile at 70°C for 30 hours, other conditions as in Table 1.

^b k_d = dissociation rate at 70°C, $t_{1/2}$ = half-life time at 70°C in toluene.

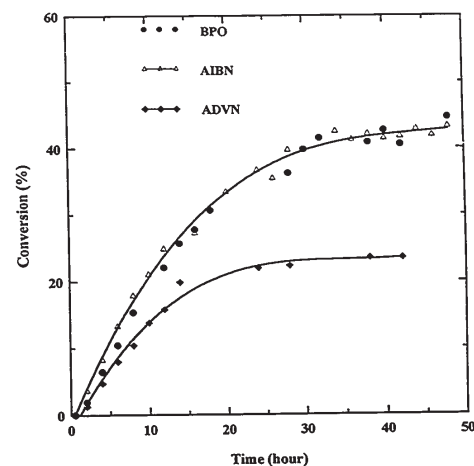


Figure 4.13 Conversion - time curve. conditions: 70°C, 2 vol% of DVB55, 2 wt% of initiator (relative to DVB55).

Table 4.7 Solubility of AIYP in Some Solvents

Solvent	Comment
Acetonitrile	partly soluble
Acetonitrile/n-Butanol	soluble
Methanol	soluble
Toluene	insoluble
Water	insoluble

* ca. 0.01g AIYP in 5 ml solvent.

many factors. Changing the solvent of the system will have an impact on the particle formation. Therefore, the effect of variable amounts of cosolvent, n-butanol, was examined. Table 4.8 shows the results.

The concentration of butanol was varied from 2% to ca. 72% (v/v, based on total), which led to the change in solubility parameter of the system from 11.84 to 11.42. Monodisperse PPDVB55 microspheres were produced in runs containing butanol from 2% to ca. 30%. Figure 4.14 is a typical size distribution pattern of PPDVB55 microspheres obtained in this system. Further increase in amount of butanol resulted in spherical but broad distributed microspheres. With above ca. 60% of butanol, coagulum resulted. The sizes of the microspheres obtained in this system decreased when the amount of n-butanol was increased as seen from Table 4.8. This may be due to viscosity change. With increasing level of butanol, the viscosity of the medium increased as well. Once the polymerization started, the coagulation of the nuclei or primary particles was slowed down while their crosslinking continued, leading to the final smaller microspheres.

Let us consider the properties of PPDVB55 microspheres produced with this solvent soluble initiator. The solubility of AIYP in polar solvents is due to the -NH-

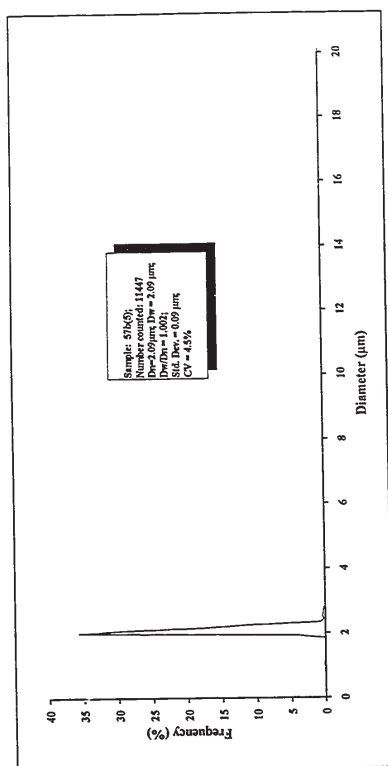


Figure 4.14 Typical size distribution pattern of PPDVB55 microspheres obtained by using AIYP initiator in solvent mixture of AcN/n-butanol (80/20, v/v). (Run 576(5)).

groups. Upon heating, free-radicals are formed to start polymerization. The forming oligomeric network radicals grow up and precipitate out to form nuclei which aggregate quickly to afford the primary particles. During this process, the polymer chain ends with these -NH- groups produced from the fragments of initiator will tend to be oriented on the surface. It was observed that the microspheres obtained by using AIYP tended to adhere to the glass wall, while microspheres obtained with AIBN settled down to the bottom. With using AIYP, the situation may be comparable to that in an emulsifier-free emulsion polymerization, where the forming particles are stabilized by surface charges introduced by the fragments of initiator such as sodium persulfate. The surface -NH- groups will help to stabilize the forming PPDVB55 particles in a polar medium. The combination of increasing crosslinking density and surface -NH- groups will make particles become stable at an earlier stage compared with the AIBN initiation system. Therefore, smaller size and high number of PPDVB55 microspheres will be expected for the AIYP initiator.

On the other hand, the increasing concentration of butanol increased the solvency of the medium as shown in Table 4.8. The initial solubility parameters of the medium are reduced from 11.84 to 11.68 when the butanol concentration was changed from 2% to ca. 30%. This increase in solvent power did not increase the size of the microspheres, and broaden the size distribution. As indicated in Table 4.8, with increasing concentration of n-butanol, the diameter of PPDVB55 microspheres was reduced from 2.48 μm to 1.39 μm , while the number of microspheres increased from 4.8×10^8 to 1.91×10^9 (per milliliter). No microspheres were observed when n-butanol fraction was above 50%. For this system, 50 vol.% of n-butanol seems the upper limit to have microspheres.

The size of the PPDVB55 microspheres was decreased and their monodispersity preserved when the amounts of n-butanol increased. It seemed that the forming particles were more stable at increasing solvenicities. To explain this, perhaps,

Table 4.8 Effect of n-Butanol on PPDVB55 Microspheres in the System Using AIYP as Initiator

Run	BuOH (Vol%)	D _n (μm)	σ (μm)	CV (%)	δ_{mix} (cal/ml) ^{1/2}	N ($\times 10^8/\text{ml}$)	Yield (%)	Particle
1	2.0	2.48	0.10	4.0	11.84	4.8	24	monodisperse
2	4.9	2.53	0.10	4.0	11.83	4.6	24	monodisperse
3	9.8	2.38	0.10	4.3	11.80	5.1	22	monodisperse
4	14.7	2.19	0.10	4.4	11.77	5.4	18	monodisperse
5	19.6	2.09	0.09	4.5	11.74	6.2	18	monodisperse
6	29.4	1.83	0.10	5.3	11.68	7.4	15	monodisperse
7	39.2	1.61	0.14	8.6	11.62	10.8	15	broader
8	49.0	1.39	0.24	17.0	11.56	19.1	16	broad
9	58.8	—	—	—	11.50	—	—	coagulum
10	71.9	—	—	—	11.42	—	18	coagulum

Conditions: [PPDVB55]=2 wt%, [AIYP]=2 wt% (based on DVB55); 70°C; 24h.

Hansen solubility parameters may be used instead of using a single solubility parameter alone (see Chapter 2). Hansen broke the solubility parameter (δ) into three components, δ_d (dispersion term), δ_p (polarity term), and δ_h (hydrogen bonding term).^{19,20} Table 4.9 lists these Hansen parameters for acetonitrile, n-butanol and styrene.

Table 4.9 Hansen solubility parameters³⁴

Compound	δ_t (cal/ml) ^{1/2}	δ_d (cal/ml) ^{1/2}	δ_p (cal/ml) ^{1/2}	δ_h (cal/ml) ^{1/2}
Acetonitrile	11.9	7.5	8.8	3.0
n-Butanol	11.3	7.8	2.8	7.7
Styrene	9.3	9.1	0.5	2.0

Even though acetonitrile and n-butanol have almost the same solubility parameter, their Hansen parameters are quite different. The δ_d is about equal for both of them, however, acetonitrile has higher δ_p and lower δ_h compared with n-butanol. When the composition of the mixture of acetonitrile with n-butanol is altered, δ_p and δ_h of the medium will be changed as well. It is likely that the hydrogen bonding term of the medium (δ_h^{mix}) would be increased with increasing the content of n-butanol although a simple calculation of δ_h^{mix} based on the δ_h of each individual component is not available at present time. This enhancement of δ_h^{mix} would make the -NH- groups on the forming particle surface become even more efficient. This phenomenon deserves further investigation.

The effect of initial loading of AIYP initiator in this system was studied using a mixture of acetonitrile with n-butanol (7.5 vol%). The amounts of AIYP initiator were varied from 1 to 10 wt% based on total monomer. It was observed that a solution with 10 wt% AIYP appeared milky due to the insoluble AIYP initiator at room temperature. In the

range of 1 to 6 wt% of AIYP, the polymerization followed the general trend as in the AIBN system, *i.e.*, the size of microspheres and the conversion of monomer increased with increasing amounts of AIYP initiator. The monodispersity was preserved up to 10 wt% of initiator (Figure 4.15). Conversions at the same level of initiator were lower with AIYP than with AIBN. The low conversion in this system may be due to the low efficiency of initiator. Because all AIYP molecules and all free-radicals generated from it were absolutely dissolved in the continuous phase, a high degree of termination due to the cage-effect was expected.

With initiation by AIYP, PPDVB55 microspheres were also produced in the mixture of acetonitrile/ethylene glycol. The diameter of PPDVB55 was 1.86 μm (CV=4.4%) in acetonitrile/ethylene glycol (80/20, v/v; run 57b-9) compared with 2.09 μm (CV=4.5%) in acetonitrile/n-butanol (80/20, v/v; run 57b-5). PPDVB55 microspheres obtained with using this initiator contained functional -NH- groups on the surface.

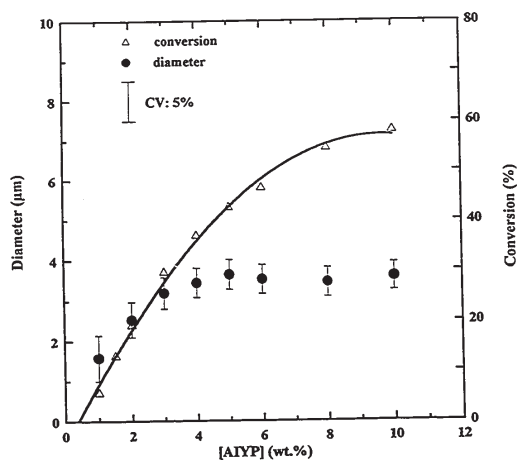


Figure 4.15 Effect of AIYP initial loading on PPDVB55 microspheres. (Run 57c).

4.5.3 Effect of Solvent

Acetonitrile meets the general requirement for a styrene precipitation polymerization solvent as it is miscible with monomers and initiator, but is a nonsolvent for the polymer formed. For dispersion polymerization of styrene in ethanol and related aliphatic alcohols, the polarity of the solvent had a notable effect on the ultimate particle size, and a correlation exists between particle size and the solubility parameter of the dispersion medium.²¹ Usually, smaller polystyrene particles are obtained in more hydrophilic solvents. Other studies have included the use of mixed solvents to finely tune the polarity of the reaction medium.^{15,18,22} We performed PPDVB experiments in several solvents in order to study the effect of the solvent on the particle formation.

4.5.3.1 Single solvent system

Precipitation polymerization of DVB55 was carried out using the standard recipe (2 vol% monomer, 2 wt% AIBN) in different solvents listed in Table 4.10. The solvents chosen have a wide range of polarity with the solubility parameter changing from 16.3 to 8.18 (cal/ml)^{1/2}. The polymerization results were surprising because spherical microspheres were only produced in the presence of acetonitrile. Even in solvents such as n- (or iso-) propanol, n-butanol, which have very similar solubility parameters, only irregular shaped particles (sometimes aggregated) were obtained. Since PPDVB55 microspheres were not produced in propionitrile or butyronitrile which have a chemical structure very similar to acetonitrile, the chemical properties of the solvent were not the only reason for the formation of microspheres in acetonitrile. It has been noted by Paine²³

Table 4.10 Solvent Effect on the Formation of PPDVB55 Microspheres (cont. on the next page)*.

Solvent	δ (cal/ml) ^{1/2}	δ_d (cal/ml) ^{1/2}	δ_p (cal/ml) ^{1/2}	δ_h (cal/ml) ^{1/2}	η (cP)	Particle Shape
Water	23.5	6	15.3	16.7	0.89	-
Ethylene Glycol	16.30	8.25	5.4	12.7	13.76(30°C)	Gel
Methanol	14.28	7.42	6.0	10.9	0.551	Coagulum
Dimethylsulfoxide	12.93	9.00	8.0	5.0	1.991	Gel
Ethanol	12.92	7.73	4.3	9.5	1.080	Coagulum
N,N-Dimethylformamide	12.14	8.52	6.7	5.5	0.802	Gel
n-Propanol	11.97	7.75	3.3	8.5	1.943	Deformed
Acetonitrile	11.90	7.50	8.8	3.0	0.341	Spherical
i-Propanol	11.50	-	-	-	2.044	Deformed
n-Butanol	11.30	7.81	2.8	7.7	2.998	Deformed
Nitroethane	11.09	7.80	7.6	2.2	0.638	Coagulum

and others²⁴ that the simple solubility parameter alone is not sufficient to account for the solvent behavior in dispersion polymerization of styrene. They instead used the Hansen parameters and found good correlations. We accordingly tried to use the Hansen parameters in this system. For instance, nitroethane has all three Hansen parameters which are close to that of acetonitrile, however, the polymer produced in this solvent was completely coagulated. No clear conclusion could be drawn. Perhaps, the viscosity of the medium may also have some effects on the polymerization, as we can see that acetonitrile has the lowest viscosity among these solvents (except for n-hexane).

It would appear from these data that acetonitrile is crucial for the precipitation polymerization of divinylbenzene, though the reason for this is not clear at this point.

4.5.3.2 Binary solvent systems-(acetonitrile/propionitrile)

PPDVB55 microspheres were not obtained in neat solvents other than acetonitrile, but were produced in some solvent mixture containing acetonitrile and other solvents as we have seen in section 4.5.2.2. The syntheses of PPDVB55 microspheres in these binary solvents were examined in this study.

Figure 4.16 shows the effect of propionitrile concentration on PPDVB55 microspheres. Clearly, PPDVB55 in pure acetonitrile was severely disturbed upon adding even small amounts of propionitrile. The size of microspheres decreased from 3.33 μm to 1.64 μm with CV increasing from 3.6% to 23.0% upon addition of only 2 vol% of propionitrile. When more propionitrile was added, the particle size slowly increased again. In the range of 2 to ca. 40 vol% of propionitrile, size-distribution patterns were unimodal, however, distributions were rather broad (CVs between 17 and 23%). With ca. 60 vol% of propionitrile, bimodal and multimodal particle distributions were obtained. Propionitrile is a less polar solvent than acetonitrile. Therefore, both size and size distribution

Table 4.10 (cont.) Solvent Effect on the Formation of PPDVB55 Microspheres.*

Solvent	δ (cal/ml) ^{1/2}	δ_d (cal/ml) ^{1/2}	δ_p (cal/ml) ^{1/2}	δ_h (cal/ml) ^{1/2}	η (cP)	Particle Shape
2-Methoxyethanol	10.80	-	-	-	1.60	Coagulum
Propionitrile	10.80	-	-	-	0.389(30°C)	Coagulum
Acetic Anhydride	10.30	7.50	5.4	4.7	0.783(30°C)	Coagulum
Butyronitrile	9.96	7.50	6.1	2.5	0.515(30°C)	Coagulum
Tetrahydrofuran	9.52	8.22	2.8	3.9	0.46	Coagulum
2-Butanone	9.27	7.77	4.4	2.5	0.378	Coagulum
Ethyl acetate	9.10	7.44	2.6	4.5	0.43	Gel
EGDE	8.60	-	-	-	0.98	Gel
Cyclohexane	8.18	8.18	0	0	0.898	Coagulum
n-Hexane	7.23	7.23	0	0	0.294	Coagulum

* solubility parameter (δ), Hansen parameters (δ_d , δ_p , δ_h) and solvent viscosity were adopted from ref. 34, 35.

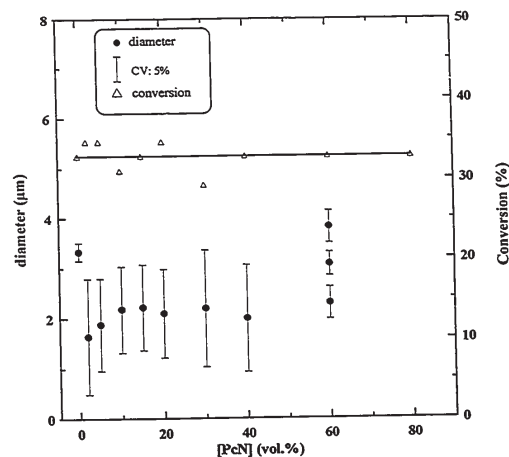


Figure 4.16 Effect of propionitrile concentration on the precipitation polymerization of PPDVB55 in acetonitrile/propionitrile binary solvent system. (Run 54b).

of particles will increase with increasing propionitrile fraction in the mixture due to the solvency effect which we have discussed earlier. However, the reason why the size of particles decreased in the presence of 2 vol% of propionitrile is not clear at this time. Under an optical microscope, these particles had rough surfaces compared with the particles obtained in pure acetonitrile, and the roughness of the surface increased with increasing amounts of propionitrile. The monomer conversions were almost the same for all runs.

4.5.3.3 Binary solvent systems-(acetonitrile/n-butanol)

n-Butanol is a less polar solvent than acetonitrile. The solvency of the medium was increased when the concentration of n-butanol was increased (see Table 4.11). As expected, the size distribution widened in the presence of n-butanol, and the monomer conversion increased with increasing n-butanol concentration. However, the size of the particles decreased slightly when n-butanol was added. This inconsistency is perhaps due to the higher viscosity of the medium. n-Butanol is a rather viscous solvent ($\eta = 2.998$). As we have mentioned earlier (section 4.5.2.2), the increasing viscosity of the medium may reduce the rate of coalescence, and lead to small final particles.

It is interesting to see that precipitation polymerization of DVB55 initiated by BPO in a 30 n-butanol/70 acetonitrile mixture resulted in monodisperse microspheres. Figure 4.17 is the SEM photograph of these PPDVB55 microspheres. Presumably, the slower initiation by BPO is responsible for this effect.

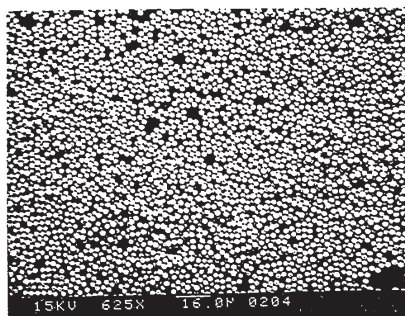


Figure 4.17 SEM micrograph of PPDVB55 microspheres. ($d_n=3.12 \mu\text{m}$; $CV=3.4\%$). Conditions: 2 vol % DVB55; 2 wt % BPO; acetonitrile/n-butanol=7/3 (v/v); 70°C for 24 hours. (run PPP6-6).

Table 4.11 Effect of n-Butanol on PPDVB55 Microspheres in Binary Solvent System.

Run 57a	BuOH (vol%)	d_n (μm)	CV (%)	δ_{mix} (cal/ml) ^{1/2}	Conversion (%)	Comment
1	0	3.53	3.9	11.85	36	Spherical
2	2	3.20	6.7	11.84	36	Spherical
3	5	3.37	15.1	11.83	38	Spherical
4	10	3.11	20.1	11.80	36	Spherical
5	15	3.46	19.4	11.77	38	Spherical
6	20	—	—	11.74	46	Spherical
7	29	—	—	11.68	40	Spherical
8	39	—	—	11.62	44	Deformed
9	59	—	—	11.50	46	Deformed
10	72	—	—	11.42	51	Coagulum

4.5.3.4 Binary solvent systems-(acetonitrile/water)

Water has the highest solubility parameter of all solvents tested, 23.5 (cal/ml)^{1/2}. PPDVB55 in acetonitrile changes substantially upon addition of water. The miscibility of DVB55 in acetonitrile/water was tested (Table 4.12) prior to polymerization simply by observing the turbidity of the solution with the unaided eye.

Table 4.12 Miscibility of 2 vol.% DVB55 in Mixture of Acetonitrile and Water

AcN/E ₂ O (v/v)	95/5	90/10	85/15	80/20	75/25	70/30	65/35	60/40	55/45
DVB55 (2 vol.%)	<i>m</i>	<i>m</i>	<i>m</i>	<i>m</i>	<i>m</i>	<i>m</i>	<i>m</i>	<i>i</i>	<i>i</i>

* *m* = miscible; *i* = immiscible.

Polymerizations were then performed in mixtures containing water between 0 to 9 vol.%. The solubility parameter of the medium increased from 11.85 to 13.30 (cal/ml)^{1/2} in this range, as indicated in Table 4.13.

Table 4.13 Calculated Solubility Parameters for Mixture of Acetonitrile/Water

Run 53d	1	2	3	4	5	6	7	8	9	10
[H ₂ O] (vol%)	0	1.0	2.0	2.9	3.9	4.9	5.9	6.9	7.8	8.8
δ_{mix} (cal/ml) ^{1/2}	11.85	12.02	12.19	12.35	12.52	12.68	12.83	12.99	13.14	13.30

As can be observed readily (Figure 4.19), a small amount of water (1 vol%) caused sharp reductions in the particle size. Upon adding 1 vol% of water to the medium, size of PPDVB55 microspheres changed from 3.57 μm to 1.42 μm . The particle size continued to decrease until ca. 3 vol% of water. Further increases in water content led to small increases in particle sizes. However, the size of the particles was never bigger than 3 μm even when 9 vol% of water was used. The size distributions were broad for these polymerization. The conversions stayed at about the same level of 37%.

The change in the concentration of water would be expected to alter not only the polarity of the reaction mixture but also the partitioning properties of the reaction mixture. Water is a much worse solvent for polydivinylbenzene than acetonitrile is. With increasing water content, the rate of nuclei formation should increase, resulting in more smaller particles. Also, the high rate of generation of nuclei would make it more difficult for existing particles to capture all oligomers from the continuous phase before they become stable particles. Therefore, the particle formation stage would be extended, resulting in broad distributions. As well, the surface of forming particles would be less sticky due to the poor solvency, again reducing the efficiency for these particles to capture oligomers. However, it is conceivable that with even more water in the solution, the loci of monomer and initiator would change. More and more monomer and initiator would partition into the particles. Because of the highly crosslinked structure, the penetration of these monomers and initiator into particles would be limited; so they would stay on the surface of the particles, making these surfaces more sticky and surface active. The forming nuclei or even some particles would be easily caught by the existing larger particles. In addition, the reaction medium becomes so polar that the hydrophobic

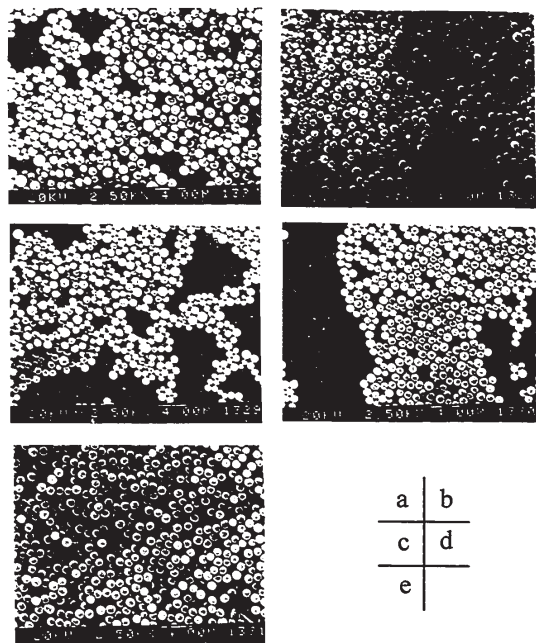


Figure 4.20 Effect of water on PPDVB55 particles. Water content (vol %): a) 1%; b) 2%; c) 3%; d) 4%; e) 5%. (cont. on the next page).

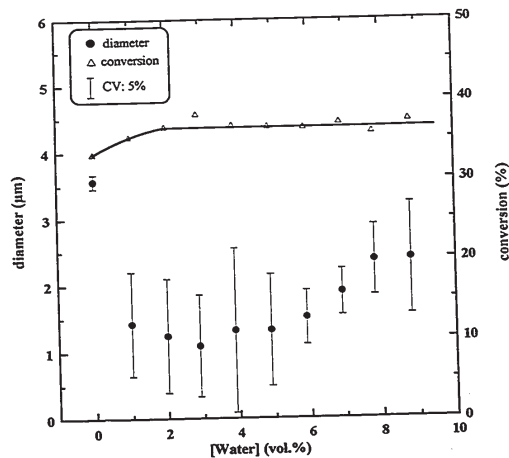


Figure 4.19 Effect of water content on PPDVB55 microspheres in the mixture of acetonitrile and water. (Run 53d, ref. 53c).

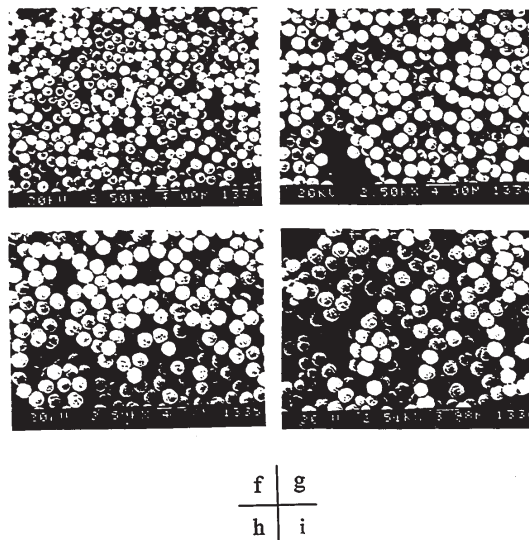


Figure 4.20 Effect of water on PPDVB55 particles. Water content (vol %): f) 6%; g) 7%; h) 8%; i) 9%.

particles would be forced together, leading to larger particles with broad distribution and surface roughness. Figure 4.20 clearly shows that these particles have popcorn-like surfaces. The competition between these opposing factors just mentioned above may explain the nonlinear change in particle size, in particular, the minimum in the particle diameter around 3% water.

4.5.4 Cause of Low Conversion in PPDVB

The conversion for precipitation polymerization of commercial divinylbenzene in acetonitrile is usually only around 40% under the conditions used (2 vol.% monomer, and 2 wt% AIBN). Polymerizations done in different solvent mixtures or with different types of initiators also gave low conversions. Several factors are thought to contribute to this effect.

First, the concentrations for both monomer and initiator were rather low. Under these conditions, cage-effect may operate. This means that a substantial portion of the initiator radicals may self-terminate before escaping from their solvent cage, and the efficiency of the initiator may become very low. Bevington²⁵ demonstrated that the efficiency of AIBN could be below 0.2 for the system of ca. 0.1M styrene and 0.50g/l AIBN. In our system, the monomer concentration was about 0.12M, and initiator concentration was 0.37g/l. As we have seen the conversion of DVB55 increased with increasing the amount of initiator (Figure 4.9, 4.10), indicating that low initiator efficiency existed in this system.

Second, the highly crosslinking structure is also a factor which may cause limiting conversion. Since polyDVB55 is totally insoluble in the medium, the growing

radicals soon precipitate from the liquid phase and becomes tightly coiled. If polymer particles are already present in the medium, the growing radical may be captured by the existing particles instead. Many radical chain ends become more or less buried inside the particles. The polymerization initially happens in both the oligomer and liquid phases, and the rate of polymerization is fast at the beginning. The monomer consumed inside the oligomers and late particles was supplied through diffusion of monomers. Upon depletion of the initiator in the liquid phase, the locus of polymerization shifted completely to the polymer phase. At this stage, the highly crosslinked structure of the particles resists monomer diffusion inside the particle. Eventually, the polymerization becomes monomer-diffusion-controlled. The conversion-time curve at 70°C (Figure 4.12) clearly shows this effect. The rate of polymerization became slow after 23 hour reaction. The concentration of initiator or free-radicals in the liquid phase, calculated by using $t_{1/2}$ of AIBN is near zero at this time. So the slow increase in conversion after that time was largely due to polymerization inside the particles using long buried immobile radical ends. It is possible that if the polymerization could be run near the glass transition temperature, T_g , of the polymer, the conversion might be increased due to the enhancement of monomer diffusion toward trapped radicals as pointed out by Hamielec.²⁶ In the present system, reducing the difference between polymerization temperature and T_g , however, is limited by the boiling point of acetonitrile (80°C) and the high T_g of the polymer (above 220°C).

A third reason for the low limiting conversion may lie in the unique particle formation process. As we will discuss later, the PPDVB55 microsphere formation involves a continuing coalescence process. The forming particles grow by absorbing polymeric radicals, nuclei (may contain free-radicals), and other small entities onto their surfaces. Most of the active radicals on these small entities will be deactivated quickly due to this aggregation process, either by termination or because they become buried inside the

polymer matrix and become inaccessible. On the other hand, the extensive aggregation leads to a low concentration of relatively large polymer microspheres in this system. In general, PPDVB55 initiated with AIBN gave particle concentration in the range of 10^8 /ml, compared with ca. 10^{10} /ml in dispersion polymerization and ca. 10^{14} /ml in emulsion polymerization. The low particle concentration, *i.e.* low specific surface area, may also contribute to the low rate of polymerization, and therefore, the low conversion.

In addition to the three factors mentioned above, there may be others such as chain transfer reaction, that may contribute to the low conversion as well. These deserve further investigation in future work.

4.5.5 Kinetic Considerations

4.5.5.1 Overall rate of polymerization at different temperatures

The kinetic curve (conversion-time curve, Figure 4.2) indicates that the precipitation polymerization of DVB55 is a slow reaction. Figure 4.21 demonstrates that the reaction is first order with regard to the monomer at three different temperatures. Table 4.14 shows the half-life time ($t_{1/2}$) of DVB55 and the pseudo first-order rate constant (K_a) for the polymerization of DVB55 at 50, 60 and 70°C.

4.5.5.2 Apparent rate constants of individual monomers

Commercial divinylbenzene consists of four components, *m*- and *p*-divinylbenzene (ca. 55%), the rest being mainly *m*- and *p*-ethylstyrene. In this study, the behavior of each individual component during the polymerization was investigated.

Samples (30 ml reactor) were picked at different times, quenched with a trace of benzoquinone and left in the refrigerator for 15 min. After the sample was centrifuged, 1.00 ml of the supernatant was withdrawn and diluted with 99 ml of

Table 4.14 First-Order Kinetics of PPDVB55

Temperature (°C)	K_a (h ⁻¹)	$t_{1/2}$ (h)
50	3.4×10^{-3}	193
60	1.3×10^{-2}	53
70	2.1×10^{-2}	33

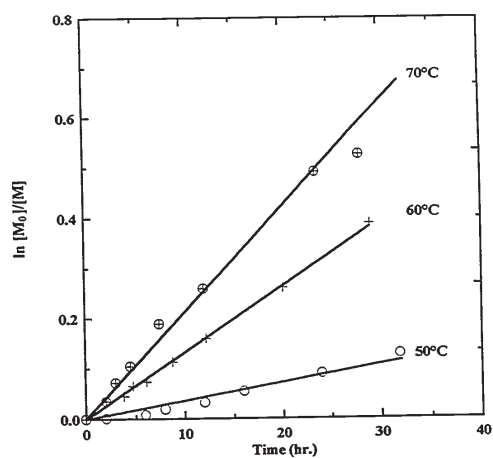


Figure 4.21 Kinetic curves for the polymerization of DVB55. Polymerization conditions: 2 vol% monomer; 2 wt% AIBN; acetonitrile as solvent.

methanol/water (70/30, v/v) solution. The content of DVB and EVB isomers in the reaction mixtures was determined by reverse-phase HPLC chromatography using a Waters 590 pump with 441 UV detector. A SEPARON column was used. The operations conditions were: eluent: methanol/water (v/v): 70/30; flow rate: 1 ml/min.; UV detector: 254 nm; temperature: ambient.

Under these conditions the retention times were 29, 31, 38 and 42 minutes for *m*-DVB, *p*-DVB, *m*-EVB and *p*-EVB, respectively. Figure 4.22 is an example of the reverse-phase HPLC chromatogram of DVB55. A calibration curve is shown in Figure 4.23. Detector response is linear at least up to a DVB55 concentration of 0.25 mg/ml.

The change in each individual peak during the polymerization process was monitored. The conversion of each monomer was calculated according to the following equation:

$$x_{it}\% = \frac{C_{i0} - C_{it}}{C_{i0}} = \frac{A_{i0} - A_{it}}{A_{i0}} \quad (4.2)$$

x_{it} — conversion of *i* component at *t* h;

C_{i0}, A_{i0} — concentration and peak area of *i* component at 0 h;

C_{it}, A_{it} — concentration and peak area of *i* component at *t* h.

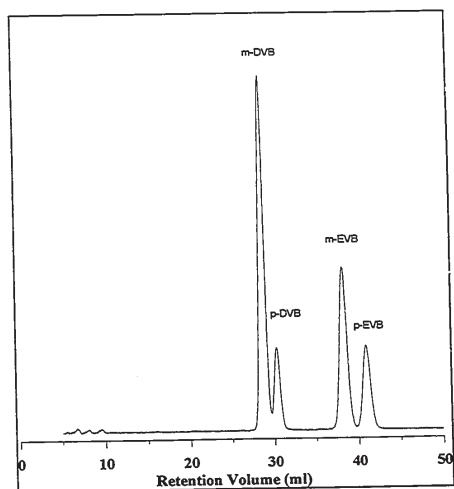


Figure 4.22 Reverse-phase HPLC profile of DVB55. Conditions: methanol/water = 70/30 (v/v); 1.0 ml/min, room temperature.

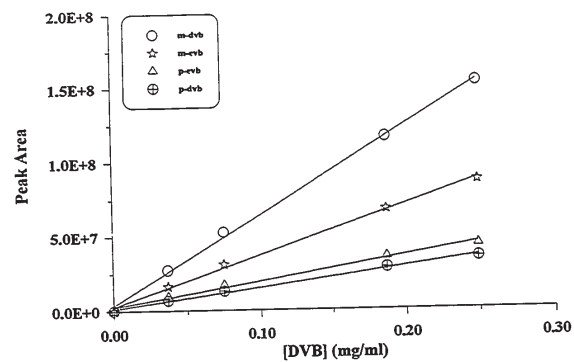


Figure 4.23 Reverse-phase HPLC calibration curve for DVB55.

A conversion curve is shown in Figure 4.24. As can be seen, the most reactive monomer is *p*-divinylbenzene, followed by *m*-divinylbenzene. The conversion rates for *para*- and *meta*-ethylvinylbenzenes are very similar. This result agrees quite well with the conversion curves for suspension polymerization of commercial divinylbenzene reported by Gayot *et al.*²⁷

The changes in concentration of individual monomers indicate that the rates at which they are incorporated into the polymer are not equal. Figure 4.25 shows that for each monomer, the polymerization reaction is of the first order with respect to its concentration. The relationships $\ln [M_0]/[M]$ vs. time where $[M]$ and $[M_0]$ are the actual and initial concentration of monomer, respectively, seem to remain linear through the whole process. The apparent rate constants of polymerization include the propagation, initiation and termination constants as well as various cross-terms of these values for different monomers. They are listed in Table 4.15. The values characterize numerically the reactivities of each component in DVB55. It can be seen that *p*-DVB is the most reactive component, which is about 1.5 times more reactive than *m*-isomer and about three times more reactive than EVB isomers.

Table 4.15 Apparent rate constant of individual monomer in PPDVB55.

Monomer	k_a (hr ⁻¹)
<i>p</i> -DVB	7.25×10^{-2}
<i>m</i> -DVB	5.35×10^{-2}
<i>m</i> -EVB	2.34×10^{-2}
<i>p</i> -EVB	2.26×10^{-2}

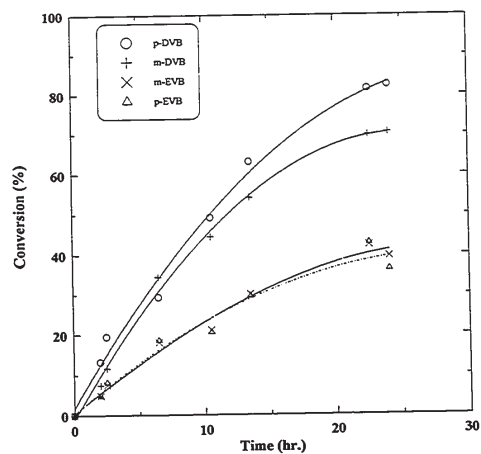


Figure 4.24 Conversion curves of individual monomer in precipitation polymerization of commercial divinylbenzene (DVB55), conditions: 2 vol% monomer, 8 wt% AIBN; acetonitrile as solvent; 70°C.

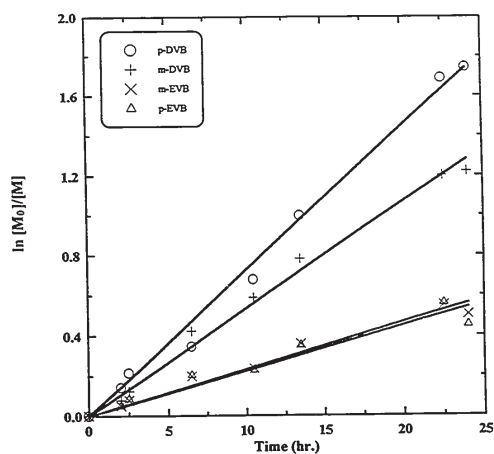


Figure 4.25 First order plots of the monomer consumption with the time of DVB55 in precipitation polymerization. conditions: 2 vol% monomer; 8 wt% AIBN; acetonitrile as solvent; 70°C.

m-EVB is only slightly more reactive than its *p*-isomer. Apparently, the reactivity of individual monomer of DVB55 in this system has the following order:

$$p\text{-DVB} > m\text{-DVB} > m\text{-EVB} > p\text{-EVB}$$

This order is the same as that given by Walczynski *et al.* (see chapter 3, Table 3.7).

4.5.6 Composition of PPDVB55 Microspheres

Due to the high reactivities of *p*- and *m*-DVB, they will be incorporated into the polymer matrix much faster than *m*- and *p*-EVB. PPDVB55 microspheres obtained in this system have a heterogeneous structure due to the differences among these individual monomers. During the polymerization, the oligomers formed at an early stage contain relatively more divinylmonomers, *p*- and *m*-DVB, while those formed at later stages contain more monovinylmonomers, *m*- and *p*-EVB. As discussed in Chapter 3, the final PPDVB55 microspheres, therefore, have core-shell type structures, *i.e.*, cores with high crosslinking densities and surfaces with somewhat lower crosslinking densities.

The residual monomer left after 24 hours still contains substantial levels of crosslinker because of the low final conversion. This ensures that the surface of the microspheres is rigid enough to maintain microsphere stability.

4.5.7 Growth of PPDVB55 microspheres

The increase in particle size during the course of the polymerization would be expected to be proportional to conversion provided that (a) all or a constant fraction of polymer was incorporated into the particles and (b) little or no coalescence occurred between particles of the same size.

In order to investigate the mechanism of the formation of monodisperse polymer particles in the present system, conversion and size of the microspheres were followed through a reaction. The volume growth of these microspheres as a function of conversion is shown in Figure 4.26. The linear relationship means that the number of particles present throughout the polymerization is essentially constant, and therefore the nucleation takes place only at an early stage of the polymerization.

4.5.8 Porosity of PPDVB55 Microspheres

The porosity of PPDVB55 particles was studied by applying solvent regain method as well as BET method. Figure 4.27 shows the solvent regains of PPDVB55 microspheres and other samples. PolyDVB55 particles (sample e) synthesized by suspension polymerization was also measured for comparison. Sample e was synthesized under the condition described in the literature.²⁸ Sample identifications are listed under the figure. The solvent regain (R_s) for PPDVB55 microspheres obtained in acetonitrile (sample a) was 0.51 ml/g. The solvent regain did not change very much when the polymerization was carried out in binary solvents (sample b and c). Sample d was

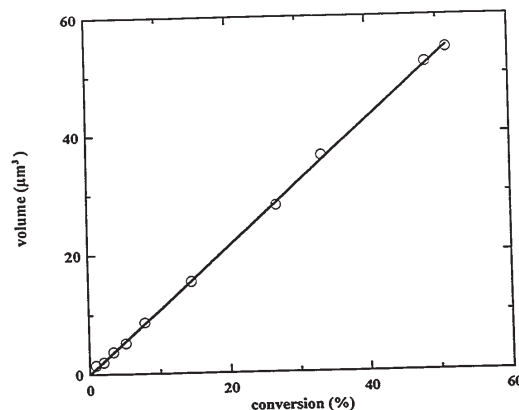


Figure 4.26 Particle volume versus conversion during growth of PPDVB55 microspheres. (Run 60a).

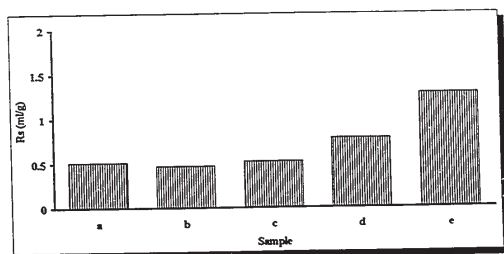


Figure 4.27 Solvent regains of different samples: PPDVB55 synthesized in (a) acetonitrile; (b) acetonitrile/1-propanol (70/30); (c) acetonitrile/n-butanol (70/30); (d) n-butanol; (e) polyDVB55 particles obtained by suspension polymerization.

synthesized in n-butanol alone and had relatively high porosity ($R_s=0.78$ ml/g). Compared with particles synthesized by suspension polymerization (sample e), the porosity of PPDVB55 particles were much lower.

The porosity data obtained from the automated nitrogen adsorption and mercury intrusion analyses are listed in Table 4.16 and 4.17, respectively. The sample (Run 39) was synthesized with 5 vol% of DVB55 in acetonitrile. The surface area was 46.8 m²/g, and the low total pore volume given by both methods imply a low porosity. From the total pore volume of 0.27 ml/g, the porosity can be calculated to be ca. 23%, which is even lower than that of particles obtained by dispersion polymerization of DVB55 (29% porosity of DPDVB55, see Chapter 3). The differential mercury porosimetry curves for this polymer shows only a few small pores (<1000 Å) (Figure 4.28).

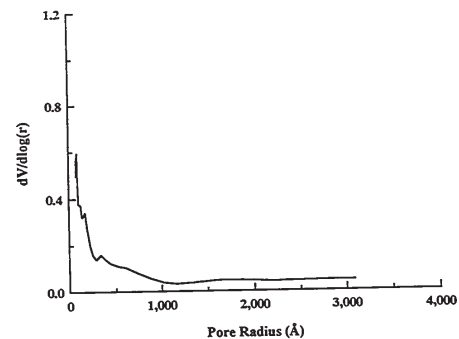


Figure 4.28 Porosity of PPDVB55 determined by Mercury porosimetry measurement.

Table 4.16 Porosity Data from Nitrogen Adsorption Analyses

Sample	Pore volume (ml/g)			Total	Surface Area (m ² /g)	Average pore diameter (Å)
	<20Å	<100Å	100-200Å			
#39	0.008	0.041	0.004	0.0594(<1453Å)	46.8	51Å

Table 4.17 Porosity Data from Mercury Intrusion Analyses

Sample	Pore Volume (ml/g)			
	<100Å	100-200Å	200-500Å	500-1000Å
#39	0.058	0.100	0.067	0.022
	1000-3000Å			Total (<3000Å)
				0.267

The lack of porosity, especially of larger pores, is evident by SEM and optical microscopy of these microspheres. The absence of a system of pores within PPDVB55 particles may be assessed by their visual appearance. Figure 4.29 is an optical photomicrograph of PPDVB55 microspheres. The translucent appearance implies the lack of macropores.²⁹ Details of the surface structure of the microspheres are shown in Figure 4.30. Clearly, there are no apparent macropores.

The theory of pore formation in macroporous resins has been well documented.³⁰ Briefly, the process contains two steps: a) the production and agglomeration of gel microspheres to form a bead of polymer; b) the binding together of microspheres while polymerization proceeds lead to porosity of the polymer.³¹ Suspension polymerization of commercial divinylbenzene in presence of a porogen such as dodecanol or toluene typically give a polymer containing a large number of pores. Porosity might be promoted in PPDVB55 if a suitable porogen could be used that would lead to phase separation within the microsphere. Such porogen might even be linear polymers.

In the present system, phase separation occurs at a very early stage because of the large amount of non-solvent present (> 95 vol%). As we have discussed earlier, the aggregation of nuclei affords primary particles which will grow up by absorbing other small entities from the solution. Interstitial pores may be created during the aggregation process. However, the subsequent polymerization on the surfaces of these pores and continued adsorption of small newly formed nuclei and other entities into the pores will tend to eliminate the pores.³² The overall process resembles that of dispersion polymerization of DVB55, and reference is made to the discussion in section 3.4.5 in Chapter 3.

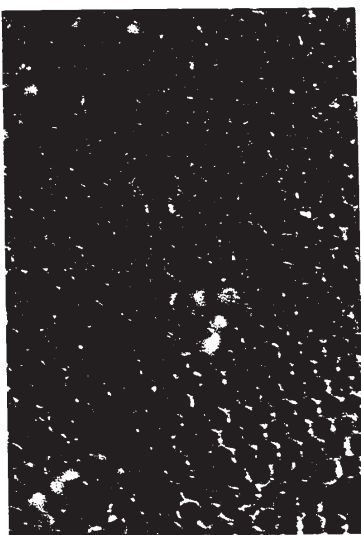


Figure 4.29 Optical photograph of PPDVB55 microspheres.

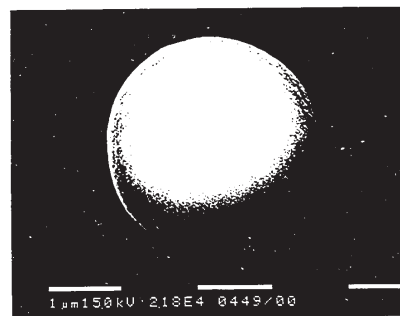


Figure 4.30 SEM micrograph of PPDVB55 microspheres.

4.5.9 Morphology of PPDVB55 Microspheres

With low monomer loading, PPDVB55 microspheres obtained in acetonitrile have a spherical shape. The surface texture appeared to be not as smooth as linear polymer microspheres obtained in either dispersion or emulsion polymerization. High magnification SEM micrographs reveal the rough structure of the microspheres. As can be seen from Figure 4.31, in addition to the bumpy structure, there are some small particles of different sizes (<200 nm) on or submerged in the surface of the microsphere. This agrees with our assumption that PPDVB55 microspheres grow up by adsorbing small entities from the medium.

In a dispersion polymerization of styrene in absence of crosslinker, nearly all the polymerization takes place within the particles due to the diffusion of monomer from solution. The appearance of the particles is smooth and spherical, the electron microscope revealing only a fine surface texture. In precipitation polymerization of DVB55, however, there is little diffusion of monomer into the particles from solution because of the high crosslink density. The microspheres grow up by absorbing oligomeric radicals, nuclei, *etc.* which are formed continuously in the liquid phase, and therefore the final particles of PPDVB55 had such rough appearance.

As discussed earlier, the surface morphology indicated no apparent macropores. The internal structure of PPDVB55 microspheres was also examined with SEM, and the results showed no apparent macropores either (Figure 4.32).

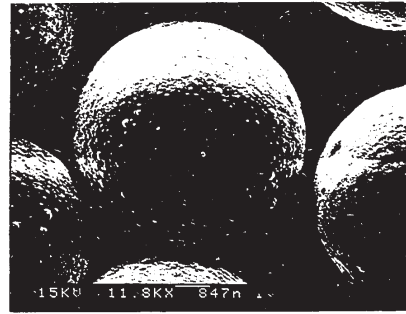


Figure 4.31 Surface morphology of PPDVB55

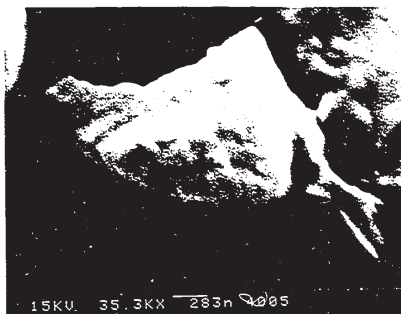
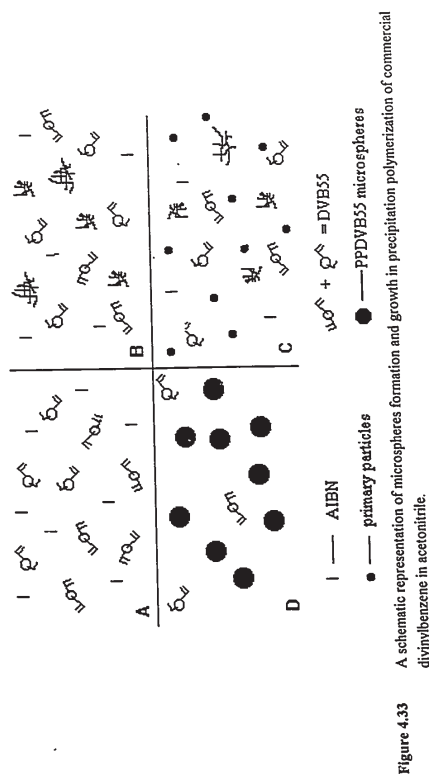


Figure 4.32 Internal structure of PPDVB55 microspheres.

4.5.10 Proposed Mechanism of Microsphere Formation and Growth in PPDVB55

Figure 4.33 gives a schematic representation of the proposed mechanism for PPDVB55 microsphere formation and growth. The starting system contains monomer (DVB55), initiator and acetonitrile (A). At the reacting temperature, initiator (AIBN) decomposes and the free radicals react with solute monomer to form oligomeric radical networks (B). Due to the crosslinking, these oligomeric radicals will precipitate out quickly to form nuclei particles. These aggregate to produce primary particles (C). The forming primary particles quickly become stable due to their highly crosslinking densities. Initially, on the surface of forming primary particles, there are some polymer chains containing free radicals expanding into the medium. If these polymer chains continue to grow without any kind of control, they would reach polymer chains on another primary particle, and coagulation among primary particles would happen. In the present system, the tendency of these surface polymer chains to expand is restrained by the crosslinking density and by the poor solvent medium. At this stage, the number of particles is fixed. The particles then grow up by absorbing monomers, or capturing oligomers, or new nuclei to afford final monodisperse particles (D).

During the growing process, the coagulation between the mature (or stable) particles is negligible because of their hard, non-sticky surfaces. In addition, the concentration of particles is rather low (10^8 /ml) compared with other heterogeneous polymerization processes; it is even lower than in Naka and Yamamoto's precipitation polymerization of diethylene glycol dimethacrylate system (ca. 10^{10} /ml).³³ Therefore, the low probability of collision reduce the coagulation among the like-size particles.



This picture of PPDVB55 microsphere formation (Figure 4.33) is somewhat similar to that of DPDVB55 particles. However, there is a difference between them at stage (C). In PPDVB55, the forming oligomeric radicals are efficiently captured by existing particles because there is no stabilizer or other substances to stabilize them. Even though some of the oligomeric radicals may escape from being captured to form nuclei particles, these will be also highly unstable due to the same reason, and will be scavenged by the existing particles as well. The oligomeric radicals or new nuclei will not be able to grow up independently. Therefore, monodisperse particles are produced. In contrast, in DPDVB55, the newly formed nuclei can be stabilized by absorbing PVP stabilizer before the depletion of PVP in the solution. Some of them may be captured by existing particles or aggregate to bigger particles; and some of them will be stable enough to grow up and become mature particles. As discussed in section 3.4.6, the presence of PVP stabilizer leads to particles that have small dispersity, but not monodisperse.

As we have seen earlier, the process of PPDVB55 appeared to be one of solution polymerization followed by precipitation or aggregation with existing particles. The monomer dissolves little in the polymer. Polymerization in the precipitated polymer phase plays a little role in the growth of primary particles.

REFERENCES

- 1 G. Vidotto, A. Crosato-Arnaldi, and G. Talamini, *Makromol. Chem.*, **122**, 91 (1969).
- 2 B.F. Törnell, and J.M. Uustalu, *Polymer*, **27**, 250 (1986).
- 3 M.W. Allsopp, *Pure Appl. Chem.*, **53**, 449 (1981).
- 4 R.H. Pelton, and P. Chibante, *Colloids Surfaces*, **20**, 247 (1986).
- 5 H. Kawaguchi, M. Kawahara, N. Yaguchi, F. Hoshino, and Y. Ohtsuka, *Polym. J.*, **20**, 903 (1988).
- 6 H. Kawaguchi, Y. Yamada, S. Kataoka, Y. Morita, and Y. Ohtsuka, *Polym. J.*, **23**, 955 (1991).
- 7 Y. Naka, I. Kaetsu, Y. Yamamoto, and K. Hayashi, *J. Polym. Sci. Polym. Chem.*, **29**, 1197 (1991).
- 8 W. Rolls, F. Svec, and J.M.J. Fréchet, *Polymer*, **31**, 165 (1990).
- 9 Y. Naka, and Y. Yamamoto, *J. Polym. Sci. Polym. Chem.*, **30**, 1287 (1992).
- 10 C. K. Ober, and K. P. Lok, *Macromolecules*, **20**, 268 (1987).
- 11 A.M. Lovelace, J. W. Vanderhoff, F.J. Micala, M.S. El-Aasser, and D.M. Kornfeld, *J. Coat. Technol.*, **54**, 691 (1982).
- 12 D.Y.D. Chung, M. Bartholin, and A. Guyot, *Angew. Makromol. Chem.*, **103**, 109 (1982).
- 13 S. Shen, E.D. Sudol, and M.S. El-Aasser, *J. Polym. Sci. Polym. Chem.*, **31**, 1393 (1993).
- 14 C.M. Tseng, Y.Y. Lu, M.S. El-Aasser, and J.W. Vanderhoff, *J. Polym. Sci. Polym. Chem.*, **24**, 2995 (1986).
- 15 K.E.J. Barrett, *Dispersion Polymerization in Organic Media*, Wiley, London, 1975.
- 16 C.K. Ober, and M.L. Hair, *J. Polym. Sci. Polym. Chem.*, **25**, 1395 (1987).
- 17 D. Zou, V. Derlich, K. Gandhi, M. Park, L. Sun, D. Kriz, Y.D. Lee, G. Kim, J.J. Aklonis, and R. Salovey, *J. Polym. Sci. Polym. Chem.*, **28**, 1909 (1990).
- 18 Polysciences, Inc. material data sheet.
- 19 C.M. Hansen, *Ind. Eng. Chem., Prod. Res. Develop.*, **8**, 2 (1969).
- 20 C.M. Hansen, *J. Paint Technol.*, **39**, 104 (1967).
- 21 Y. Almog, S. Reich, and M. Levy, *Br. Polym. J.*, **15**, 131 (1981).
- 22 C.K. Ober, K.P. Lok, and M.L. Hair, *J. Polym. Sci. Polym. Letters Ed.*, **23**, 103 (1986).
- 23 A. J. Paine, *J. Polym. Sci. Polym. Chem.*, **28**, 2485 (1990).
- 24 K.P. Lok, and C.K. Ober, *Can. J. Chem.*, **63**, 209 (1985).
- 25 J.C. Bevington, *Trans. Faraday Soc.*, **51**, 1392 (1952).
- 26 A.E. Hamielec, R. Gomez-Vaillard, and F.L. Marten, *J. Macromol. Sci., Chem.*, **A17**, 1005 (1982).
- 27 D-Y.D. Chung, M. Bartholin, and A. Guyot, *Angew. Makromol. Chem.*, **103**, 109 (1982).
- 28 W.H. Li, H.D.H. Stöver, and A.E. Hamielec, *J. Polym. Sci. Polym. Chem.*, **32**, 2029 (1994).
- 29 A.B. Stiles, *Catalyst Supports and Supported Catalysts*, Butterworth, p165, 1987.
- 30 A. Guyot, *Synthesis and Structure of Polymer Supports*, in *Syntheses and Separations using Functional Polymers*, D.C. Sherrington and P. Hodge ed., John Wiley & Sons, 1988, and paper therein.
- 31 K.A. Kun, R. Kunin, *J. Polym. Sci., Part A-1*, **6**, 2689 (1968).
- 32 W. Rolls, F. Svec, and J.M.J. Fréchet, *Polymer*, **21**, 165 (1990).
- 33 Y. Naka, I. Kaetsu, Y. Yamamoto, and K. Hayashi, *J. Polym. Sci. Polym. Chem.*, **29**, 1197 (1991).
- 34 J. Brandrup, and E.H. Immergut, *Polymer Handbook*, 2nd ed. Wiley, New York, 1975.
- 35 J.A. Riddick, W.B. Bunger, and T.K. Sakano, *Organic Solvents-Physical Properties and Methods of Purification*, 4th ed., Wiley, New York, 1986.
- 36 Z.R. Pen, and Z.Z. Yu, *Radical Polymerization*, Chemical Industry, Beijing, 1983.

CHAPTER 5

INTRODUCING POROSITY INTO POLYMER MICROSPHERES

5.1 AIM OF THE RESEARCH

PolyDVB55 particles synthesized by either dispersion or precipitation polymerization as described in Chapters 3 and 4, have spherical shapes with narrow or monodispersity. Their size can be controlled in the range of 1 to 9 μm . The porosity of these particles, in general, is below 30%. In terms of template polymer applications, it is desirable to increase the particle porosity further.

The purpose of this research is to explore possible ways for introducing porosity into PPDVB55 microspheres, and to provide a basis for the preparation of porous monodisperse PPDVB55 microspheres in the future. Porous PPDVB55 microspheres will be useful not only in the field of template polymer application, but also as chromatographic supports in size-exclusion chromatography, biological separation and as catalytic supports.

199

201

Hosoya and Fréchet published a full procedure on the syntheses of monodisperse porous polystyrene/divinylbenzene particles using a similar approach. Monodisperse polystyrene latex of 1.5 μm diameter obtained by emulsion polymerization was used as seed. This seed latex was first swollen with a solution of benzoyl peroxide and dibutyl phthalate, then with emulsified monomers (a mixture of styrene and commercial divinylbenzene). The swollen seed particles showed a 64 fold increase in volume and ended with final size of 6 μm . The final particles had monodisperse size distribution and high porosity with broad pore size distributions. The evaluation of these porous particles with HPLC showed excellent performance.^{9,10}

Independently, Cheng *et al.*^{11,12} also reported their work on the syntheses of monodisperse porous polystyrene/divinylbenzene particles by a similar process. Monodisperse polystyrene latexes with particle diameter of 0.17 μm obtained by emulsion polymerization, and of 3 μm obtained by dispersion polymerization, were used as seeds. Monodisperse porous styrene/divinylbenzene copolymer particles in the size range of 10 μm in diameter were prepared via seeded emulsion polymerization. Linear polymer (polystyrene seed) or a mixture of linear polymer and solvent (toluene) or nonsolvent (n-hexane) were used as inert diluents (porogens). The porous particles obtained had pore diameters on the order of 1000 Å with pore volumes up to 0.9 ml/g and specific surface areas up to 200 m^2/g .

Seeded polymerization proved to be an excellent technique to produce monodisperse porous particles. Although the procedure is more tedious compared with suspension polymerization, the good performance of the obtained particles in chromatographic applications makes it very attractive.

5.2 A SURVEY: MONODISPERSE MACROPOROUS POLYMER MICROSPHERES

The conventional method of preparing polymeric separation media is by suspension polymerization processes. In this method, monomers, crosslinking agent, and polymerization initiator are dissolved in a suitable organic diluent or porogen, and stirred with water in the presence of suspension stabilizer.^{1,2,3} The organic diluent is responsible for the formation of the porous structure. After polymerization, the porogen is removed, leaving a porous structure within the polymer particles. Changes in the nature or amounts of the porogens that are used lead to different pore sizes and pore size distributions.⁴ The porogens used can be solvating or nonsolvating diluents (solvents or nonsolvents) for the polymer chains, or they can be inert linear polymer. The particle size distribution of the product is largely determined by stirring speed, stirrer shape, polymerization temperature and type and amount of particle stabilizer. A broad particle-size distribution is a typical result of this method, and size classification is often done to improve the column packing. Even after the tedious size classification process, the particles are not uniformly sized. To optimize both resolution and column back pressure, particles should be monodisperse. Columns packed with such particles provided excellent column efficiency with very low column pressure drops.^{5,6}

The syntheses of monodisperse porous polymer particles have been reported by a few groups recently. Ugelstad *et al.* developed the activated swelling process⁷ to synthesize monodisperse porous particles in a wide range of particle sizes (2-50 μm) and pore-size distributions.^{5,8} This type of particle showed excellent chromatographic performance due to the high porosity and lack of any fine particles among the monodisperse particles. The procedure of synthesis was, somehow, not given in detail.

202

5.3 EXPERIMENTAL

5.3.1 Materials

4-Methylstyrene (97% Aldrich) and technical-grade divinylbenzene (DVB55, Aldrich) were purified prior to use by passing them through a short column of alumina to eliminate the inhibitor. Poly(N-vinylpyrrolidone) (PVP, special grade, $M_w=40,000$; Aldrich) and poly(vinyl alcohol) (PVA, 80% hydrolyzed, $M_w=9000-10000$) were used as polymeric stabilizer. 2,2'-Azobis(isobutyronitrile) initiator (AIBN, Kodak) and benzoyl peroxide (BPO, Aldrich) were purified by standard method. HPLC grade water, absolute ethanol and hydroquinone were BDH products and utilized as received.

5.3.2 Synthesis of Monodisperse Seed Particles

In this study, both crosslinked polymer particles (PPDVB55) and linear poly(4-methylstyrene) particles were used as seed to synthesize porous polymer particles. The synthesis of crosslinked seed particles is described in the experimental part of Chapter 4.

Linear seed particles were synthesized by means of dispersion polymerization. All preparations were carried out by bottle polymerizations. The general procedure is as follows. AIBN initiator was added to a series of 30 ml polypropylene screw cap bottles which contained solution of 4-methylstyrene monomer and PVP stabilizer in ethanol. The bottles were attached to a rotor plate which has been described in Chapter 4. The reactor setup was similar to the one used in precipitation polymerization of DVB55, except that the rotor was submerged in a thermostated water bath. The rotor rotated around the long axis at 30 rpm. The temperature of the water bath was controlled at $70 \pm 0.1^\circ\text{C}$ for a predetermined reaction time. The reactions were stopped by cooling the bottles with a

mixture of dry ice and acetone. A trace amount of hydroquinone was added to prevent postpolymerization of residual monomer. The supernat of the reaction mixture was decanted, and the microspheres obtained were redispersed in 50 ml methanol and centrifuged three times. The polymer microspheres were predried in a dust free environment at room temperature and further dried in a vacuum oven at 40°C for two days if necessary.

5.3.3 Polymerizations

The synthesis of porous polymer particles was conducted by using a literature procedure¹¹ with some modifications. The recipes for this experiment is listed in Table 5.2 and 5.3 on page 211. In general, seed particles were mixed with a solution composed of commercial divinylbenzene monomer, porogen (n-hexane), initiator (AIBN), inhibitor (hydroquinone), stabilizer (PVP), and water. The swelling processes were carried out in capped glass bottles. Prior to polymerization, bottles containing the ingredients were rotated end-over-end (20 rpm) at ambient temperature for 24 h which was long enough to allow the seed particles to swell with the n-hexane/DVB55 mixture. The polymerizations were then performed in a thermostat water bath at 70°C for 24h with the same rotating speed. After the polymerization was completed, the polymerized dispersion was mixed with 45 ml of methanol and the supernatant was discarded after sedimentation of the particles. This procedure was repeated one more time in methanol, two times in THF and two times in acetone. The particles obtained were dried at room temperature.

In addition to the procedure mentioned above, we also used another approach to synthesize porous particles. The dynamic monomer swelling method was originally developed by Okubo *et al.* to prepare micron-size monodisperse polymer particles.¹³ This method does not require a swelling agent, and has only one step. In general, the seed

particles and the monomer were mixed in a solvent for the monomer. To this system was added a nonsolvent (e.g. water) for the monomer. By careful control of amount and speed of addition of the nonsolvent, the monomer did not precipitate as a separate phase but became absorbed by the polymer seed particles. It has been demonstrated that this method was able to produce monodisperse large particles.

In our work, the swelling of the poly(4-methylstyrene) seed particles with DVB55 monomer was carried out as follows. In a 20 ml glass bottle, DVB55 monomer (0.24 g), BPO (0.01 g), ethanol (3.9 g), PVA or PVP (10.0 mg), and water (2.0 g) were mixed together. 1 ml of ethanol/water (80/20, v/v) containing 0.02 g of poly(4-methylstyrene) seed particles was added to this solution. An additional 9 ml of water was added dropwise over a 4 h period under stirring with a magnetic stirrer in order to complete the swelling process. The polymerization was performed immediately at the end of swelling process. The reaction conditions and workup procedure were the same as described in the last section.

5.3.4 Characterization

Molecular weight and molecular weight distribution of poly(4-methylstyrene) seed particles were measured with a Waters GPC (pump model 590) using three Ultrastaygel columns in series. Tetrahydrofuran was used as eluent and the flow rate was 1.0 ml/min. The instrument was calibrated by using monodisperse polystyrene standard purchased from Polysciences. A refractive index detector was employed, and the calculation of molecular weights was carried out by using a standard curve based on these polystyrene standards.

All other characterization techniques used were the same as described earlier either in Chapter 3 or in Chapter 4.

5.4 RESULTS AND DISCUSSION

It was thought that starting from the microspheres prepared by dispersion polymerization would allow better control of the particle geometry, since the enlargement factor during the subsequent seeded polymerization are orders of magnitude smaller than those from emulsion polymerization.¹⁴ In addition, swelling of the microspheres obtained by dispersion polymerization can be carried out easily due to the relatively low degree of polymerization.¹⁵ In this work, monodisperse poly(4-methylstyrene) microspheres synthesized by dispersion polymerization were then used as seed particles.¹⁶

5.4.1 Dispersion Polymerization of 4-methylstyrene

Commonly, the syntheses of monodisperse polymer microspheres by dispersion polymerization were performed either in a shaker bath or in an end-over-end rotating reaction system. To assess the efficiency of our rotor plate stirring system, dispersion polymerization of styrene in ethanol was conducted first. Figure 5.1 shows an example of the monodisperse polystyrene microspheres obtained by this process. Our results confirm that the dispersion polymerization of styrene in this system follows general trends, i.e., the size and size distribution of PS microspheres increase with increasing concentration of styrene and/or AIBN; but decrease with increasing concentration of PVP.

Although no research on dispersion polymerization of 4-methylstyrene has been reported, it can be predicted that the results would be similar to those of styrene. Dispersion polymerization of 4-methylstyrene was briefly studied. We found that the size and size distribution of poly(4-methylstyrene) microspheres varied depending upon reaction parameters such as initial monomer and initiator loading; reaction

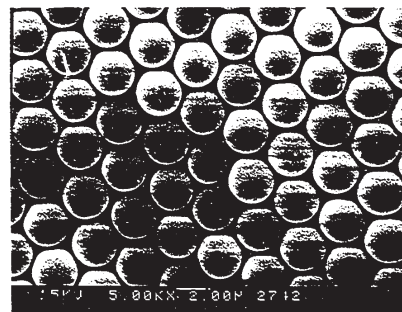


Figure 5.1 Monodisperse polystyrene particles synthesized in the present system.

temperature and the amount of PVP. For this experiment, AIBN concentration was fixed at 2 wt % (relative to monomer), and PVP concentration was kept at 16g/L. Only the initial loading of 4-methylstyrene was varied in order to regulate the size of microspheres. The results are listed in Table 5.1.

As seen from Table 5.1, monodisperse poly(4-methylstyrene) microspheres were obtained when monomer loading was in the range of 10 to 25 vol % under the conditions used. The number average molecular weight (M_n) of poly(4-methylstyrene) increases with increase of monomer concentration. Molecular weights are in the order of 10^4 . Figure 5.2 shows a SEM photomicrograph of poly(4-methylstyrene). Microspheres prepared from 10 vol % of monomer and Figure 5.3 shows the size distribution pattern of these microspheres as measured by a Coulter Multisizer II.

It is expected that poly(4-methylstyrene) microspheres will largely behave like polystyrene microspheres, chemically and physically. However, there are a lot of methyl groups on the surface of poly(4-methylstyrene) microspheres, which could be selectively oxidized to afford a hydrophilic surface of the microspheres. That will be the subject of Chapter 6.

5.4.2 Porous Particles by Seeded Polymerization

Monodisperse poly(4-methylstyrene) microspheres were used as seed particles. Because of the relative large diameters ($d_n = 3.4 \mu\text{m}$) of these seeds, the process was designed to reach larger final particles with a single swelling step instead of multiple swelling steps.¹⁴ Table 5.2 and 5.3 are typical polymerization recipes for preparation of porous polymer particles by using linear and crosslinked polymer seed, respectively. n-Hexane was used as solvent-type porogen. The weight ratio of monomer to the seeds was

Table 5.1 Dispersion Polymerization of 4-Methylstyrene^a

Sample	[4MSt] (vol %)	D_n (μm)	CV (%)	M_n	M_w	M_w/M_n
1	5	2.64*	11.1	9.67×10^3	2.76×10^4	2.86
2	10	2.79	6.3	1.52×10^4	5.44×10^4	3.59
3	15	2.98	7.0	1.68×10^4	5.22×10^4	3.11
4	20	3.40	9.5	1.79×10^4	5.07×10^4	2.84
5)	25	3.92	6.4	1.89×10^4	5.63×10^4	2.98

^a Reaction conditions: ethanol solvent; [AIBN] = 2.0 wt% (based on monomer); [PVP] = 16g/L; 70°C; 24 h.

CV = coefficient of variation = standard deviation/ D_n

* bimodal distribution, main peak at 2.64 μm with minor at about 1 μm .

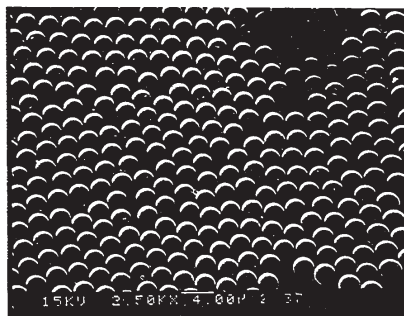


Figure 5.2 SEM micrograph of poly(4-methylstyrene) microspheres. (run 24 (2)).

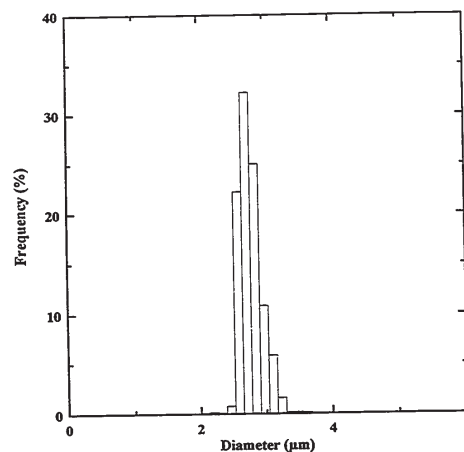


Figure 5.3 Typical poly(4-methylstyrene) microsphere histogram.

Table 5.2 Recipes for Preparation of Porous Particles with Linear Polymer Seed

Material	Weight (g)	Wt % (based on total)
PMSt seed (sample 24(4)) dn=3.40 μm	0.39	7.84
DVB55	0.56	11.16
n-Hexane	0.50	10.0
Water	3.50	70.0
PVP	0.04	0.8
AIBN	0.005	0.1
Hydroquinone	0.005	0.1

Table 5.3 Recipes for Preparation of Porous Particles with Crosslinked Polymer Seed

Material	Weight (g)	Wt % (based on total)
PPDVB55 seed (sample DVB9(4)), dn=1.38 μm	0.2	2.04
DVB55	0.42	4.29
n-Hexane	0.66	6.75
Water	8.00	81.76
PVP	0.40	4.09
AIBN	0.005	0.05
Hydroquinone	0.10	1.02

set to below 2 in order to prevent coagulation of the soft monomer-swollen polymer particles. The higher swelling ratio (weight ratio of the mixture of solvent-type diluent with monomers to seed) would cause the swollen particles which were soft and sticky to cream in the early stages of polymerization and coalesce into a big mass.¹¹ Figure 5.4 and Figure 5.5 show scanning electron micrographs of the linear poly(4-methylstyrene) seed particles and porous particles obtained by this method, respectively. As can be seen from the micrographs, the particles are highly porous. They contained a large number of macropores which were in the order of 1 to $2 \times 10^3 \text{ \AA}$.

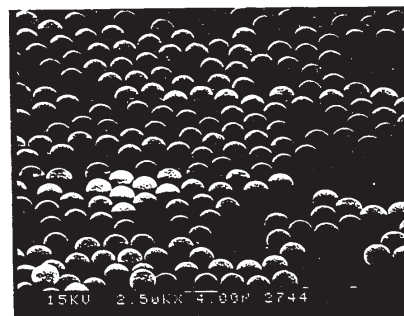


Figure 5.4 SEM micrograph of poly(4-methylstyrene) seed particles. (run 24(4)).

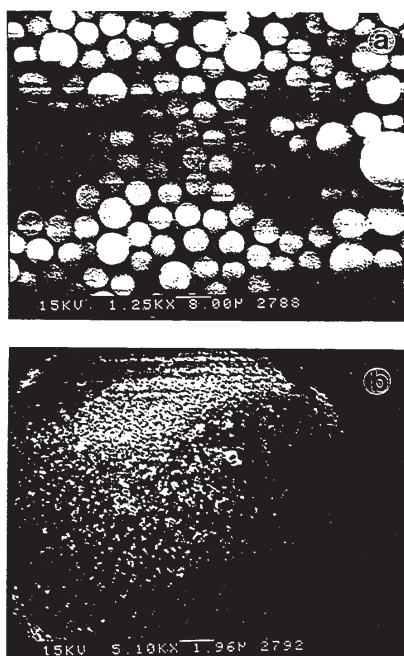


Figure 5.5 SEM micrographs of macroporous particles made by seeded polymerization utilizing linear poly(4-methylstyrene) and n-hexane as porogens. b) is higher magnification of a). (run PPP-2).

Monodisperse porous particle were not obtained in the present system as indicated in Figure 5.5 (a). Most of the particles were in the range of $6 \mu\text{m}$. Some larger particles are seen with diameters between 8 to $14 \mu\text{m}$.

The porous particles obtained were spherical. Few aggregated particles were observed. This indicates that PVP alone is sufficient to stabilize the swollen particles during the swelling and the following polymerization process. Figure 5.5 (b) clearly shows that the pores of these macroporous polymer particles were due to interstices formed between microspheres which were produced during the phase separation process. The formation of porous structure in this type of porous particles has been thoroughly discussed by Cheng *et al.*¹² and Fréchet *et al.*,¹⁴ respectively. Briefly, the swollen seed particles contain monomers, initiator, porogens (linear polymer and nonsolvent) after swelling. Upon heating, small crosslinked nuclei of polymer molecules are produced. Further polymerization results in phase separation between the forming polymer and linear polymer (poly(4-methylstyrene) in this case) and nonsolvent. Voids between microspheres and agglomerates are fixed as the polymerization continues. When the inert diluents are removed, porous polymer particles are obtained.

In order to introduce porosity into polyDVB55 particles, PPDVB55 particles were used as seed by using the same procedure. Table 5.3 shows the recipes used for this experiment. The result, however, showed aggregation of particles with formation of submicron particles during the polymerization. Because of the crosslinked structure in PPDVB55, the diffusion of monomer during swelling process were limited only on the particle surface instead of homogeneously throughout the whole particles like the case of linear polymer seed. The lower absorption of monomer into the particles increased the free monomer phase after swelling, and caused nucleation of a new crop of particles. All these factors contributed to the aggregation and formation of submicron particles. It was

observed that, after polymerization, the large particles had almost the same diameter as the seed, which indicated that swelling of the seed did not occur. The introduction of porosity via seeded polymerization using highly crosslinked seed particles was therefore unsuccessful.

5.4.3 Porous Particles by Dynamic Monomer Swelling

Quite recently Okubo *et al.*¹³ reported that it was possible to obtain an increased swelling of polymer particles with monomer by a so-called "dynamic swelling method" (DSM). We adopted this method to synthesize monodisperse porous particles. Monodisperse poly(4-methylstyrene) microspheres (3.4 μm , run 24(4)) were used as seed particles. Polymerization was conducted according to the procedure described in experimental part. Before seed particles were added, the mixture containing DVB55 monomer, PVP stabilizer and BPO initiator was clear because these substances were miscible in the solution of ethanol and water. Optical microscopy was used to monitor the change of seed particle size during the course of swelling. It was observed that the sizes of these swollen particles increased quite uniformly. No monomer droplet was observed. At the end of swelling process, there was no monomer layer on the top of solution once the stirring was stopped, which would have been the case if the water had been added too fast so that the excluded monomer would not have had a chance to be absorbed by the seed particles. A run with PVA as stabilizer gave coagulated products, whereas, in a run with PVP as stabilizer, large particles with good dispersity were produced. The shape of the particles was preserved even after treatment with THF. However, it was observed that these particles were sensitive to crushing. They were prone to collapse upon touching with a spatula under the optical microscope. SEM micrograph reveals that the particles had egg-shell structure. As seen from figure 5.6, the particles contain polydivinylbenzene

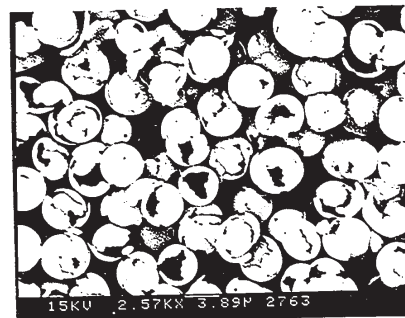


Figure 5.6 SEM of crashed hollow-particles obtained in dynamic swelling method. (sample PPP-3(2)).

shells and empty cores. This was probably caused by the incomplete diffusion of DVB55 from the liquid toward the center. Regardless of particle morphology, these cracked particles had about the same diameters, which indicated that the diffusion of monomer into individual seed was homogeneous.

We may speculate a little bit in terms of the result of this experiment. Apart from the original purpose of this technique, i.e. synthesis of larger particles via seeded polymerization, this result had several meanings. By controlling the diffusion of monomer, it would be possible to synthesize hollow-spheres with different wall thickness. If one repeats to use this procedure to swell seed particles by using different type of monomers in each circle, particles contain several layers which built up by different materials might be synthesized. Finally, if crosslinked particles (such as PPDVB55) are used as seed, a layer containing macroporous structure may be introduced on to the seed particles. From practical application point of view, this type of particles will be very useful not only for use as our template polymer support, but also for many other chromatographic purposes. This, actually, is our ultimate goal in this study. Efforts are continuing on it.

REFERENCES

- 1 I.C. Moore, *J. Polym. Sci. A*, **2**, 835 (1969).
- 2 J. Seidl, J. Malinsky, K. Dusek, and W. Heitz, *Adv. Polym. Sci.*, **5**, 113 (1967).
- 3 D. Horak, F. Svec, M. Ilavsky, M. Bleha, and J. Kalal, *Angew. Makromol. Chem.*, **95**, 117 (1981).
- 4 W. Rolls, F. Svec, and J.M.J. Fréchet, *Polymer*, **31**, 165 (1991).
- 5 T. Ellingsen, O.Aune, J. Ugelstad, and S. Hagen, *J. Chromatogr.*, **535**, 147 (1990).
- 6 L.I. Kulin, P. Flodin, T. Ellingsen, and J. Ugelstad, *J. Chromatogr.*, **514**, 1 (1990).
- 7 J. Ugelstad, K.H. Kaggerud, F.K. Hansen, and A. Berger, *Makromol. Chem.*, **180**, 737 (1979).
- 8 J. Ugelstad, A. Berge, T. Ellingsen, R. Schmid, T.-N. Nilsen, P.C. Mork, P. Stenstad, E. Hornes, and O. Olsvik, *Prog. Polym. Sci.*, **17**, 87 (1992).
- 9 K. Hosoya, and J.M.J. Fréchet, *J. Liq. Chromatogr.*, **16**, 353 (1993).
- 10 K. Hosoya, and J.M.J. Fréchet, *J. Polym. Sci. Polym. Chem.*, **31**, 2129 (1993).
- 11 C.M. Cheng, F.J. Micalé, J.W. Vanderhoff, and M.S. El-Aasser, *J. Polym. Sci. Polym. Chem.*, **30**, 235 (1992).
- 12 C.M. Cheng, J.W. Vanderhoff, and M.S. El-Aasser, *J. Polym. Sci. Polym. Chem.*, **30**, 245 (1992).
- 13 M. Okubo, M. Shiozaki, M. Tsujihira, and Y. Tsukuda, *Colloid Polym. Sci.*, **269**, 22 (1991).
- 14 V. Smigol, F. Svec, K. Hosoya, Q. Wang, J.M.J. Fréchet, *Angew. Makromol. Chem.*, **195**, 151 (1992).
- 15 L.H. Jansson, M.C. Wellons, and G.W. Poehlein, *J. Polym. Sci. Polym. Lett. Ed.*, **21**, 937 (1983).
- 16 F. Lenzmann, Senior Thesis, McMaster University, 1993.

CHAPTER 6

FUNCTIONAL POLYMER MICROSPHERES

6.1 AIM OF THE RESEARCH

The synthesis of monodisperse crosslinked polymer microspheres via precipitation polymerization described in Chapter 4 is a new process. The formation of polydivinylbenzene microspheres in the absence of any type of stabilizer or surfactant leads to clean particle surfaces. In addition, the highly crosslinked structure bestows unique properties such as heat and solvent resistance on these microspheres. Obviously, the potential applications of PPDVB55 microspheres are substantial. Some of their applications will be affected by the polarity of their surfaces. For example, in our template polymer system, hydrophobic surfaces would reduce the accessibility of the specific binding sites toward the template molecules. This would lead to lower efficiency of molecular recognition. Biotechnological uses of PPDVB55 particles also depend on surface chemistry. A key example is the use of these particles as protein antigen carriers, an application currently actively pursued.

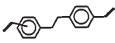
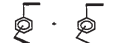
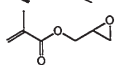
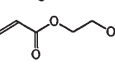
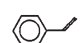
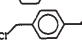
In this chapter, the introduction of different polar functional groups into (or on to) PPDVB55 microspheres as well as linear polymer microspheres obtained by dispersion polymerization are described. Both copolymerization and surface modification techniques were utilized. The purpose of this study was to illustrate the possibility of functionalization of these microspheres.

219

6.2 MATERIALS USED IN THIS STUDY

Monomers used in this study are listed in Table 6.1. Liquid monomers were purified by passing them through short alumina column, and solid monomers were used as received. AIBN initiator (Kodak), acetonitrile (BDH, HPLC grade) and ethanol (Aldrich, HPLC grade) were used without purifications.

Table 6.1 Structures and Sources of Monomers

Monomer	Abbr.	Structure	Source
Acrylamide	AAM	$\text{H}_2\text{C}=\text{CHCONH}_2$	Aldrich
Acrylic acid	AA	$\text{H}_2\text{C}=\text{CO}_2\text{H}$	Aldrich
1,2-Bis(vinylphenyl) ethane	BVE		This work
Commercial Divinylbenzene	DVB80		Fluka
Glycidyl methacrylate	GMA		Aldrich
2-Hydroxyethyl acrylate	HEA		Aldrich
Styrene	St		Aldrich
Vinylbenzyl chloride	VBC		Aldrich Kodak
4-vinylbenzene sulfonic acid sodium salt		$\text{C}_8\text{H}_7\text{SO}_3\text{Na}$	Aldrich

221

6.3 FUNCTIONAL MICRON-SIZE POLYMER MICROSPHERES BY DISPERSION POLYMERIZATION

The preparation of polymer microspheres has received much attention in recent years. Applications of these microspheres including instrument calibration standards, polymer catalysts,^{1,2,3} coating agents,^{4,5} diagnostics,⁶ chromatographic packing materials,⁷ microlithography,⁸ and so on, have been demonstrated. Various latexes bearing reactive residues such as amine,^{9,10} carboxylic acid,¹¹ sulfonic acid,^{12,13} etc. have been synthesized. Most of these reactive or functional latexes were synthesized by emulsion or emulsifier-free emulsion polymerization, and therefore have sizes in the submicron range.

Dispersion polymerization has now become a mature technique for the single step synthesis of monodisperse polymer microspheres in the diameter range of 0.1 to 15 μm .^{14,15,16} Up to date, polystyrene microspheres have been studied overwhelmingly. However, the use of polystyrene microspheres remains limited for some applications such as enzyme immobilization, largely because these microspheres lack hydrophilic functional groups on the surfaces. A few examples of reactive microspheres synthesized by dispersion polymerization were given in a review by Arshady.¹⁷

To introduce functional groups into polymer chains, in general, two approaches can be used: a) polymerization and copolymerization of monomers already containing the desired functional groups, b) chemical modification of a presynthesized polymer. For most practical purposes, relatively low concentrations of functional groups on the particles are required. For this reason, functional monomers are often copolymerized with suitable structural monomers.

222

Very few reports in the literature dealt with particles prepared by copolymerization. Comonomer systems are more complicated if the comonomers polymerize at different rates or partition differently in the system once nucleation has taken place. There is only one report on the synthesis of copolymer microspheres via dispersion polymerization thus far, where poly(styrene-co-n-butyl methacrylate) monodisperse microspheres was synthesized in water/ethanol medium.¹⁸ In the following, we will describe the syntheses of copolymer microspheres, mainly poly(styrene-co-acrylamide) microspheres, by dispersion polymerization. The purpose was to demonstrate that mono or narrow disperse polar copolymer microspheres could be synthesized under certain conditions by means of dispersion polymerization.

6.3.1 Experimental

The reactors used and setup conditions were the same as those used in dispersion polymerization of 4-methylstyrene (see chapter 5). Styrene and functional comonomers were mixed with AIBN initiator (1 wt.%), PVP stabilizer (16 g/L) in absolute ethanol. Total monomer concentration was held constant at 10 vol.%. Before polymerization, the solution was purged with nitrogen for at least 5 min. Polymerizations were carried out at 70°C for 24 h. Particles obtained were washed with methanol, methanol/water (50/50, v/v) successively three times. Yields of microspheres were calculated according to the following equation:

$$\text{Yield (\%)} = 100 \cdot W_p / W_m \quad (6.1)$$

Where W_m is the weight of initial monomers (total) and W_p is the weight of recovered microspheres.

Copolymer microspheres were characterized by ISI DC-130 or JEOL scanning electron microscopy (SEM). SEM specimens were prepared by the technique previously described in Chapter 2. The functional comonomers introduced were characterized by BIO-RAD FT-IR spectrophotometer. FT-IR specimens were made by casting a solution of polymer particles in THF onto a KBr window to form a thin polymer film.

6.3.2 Results and Discussion

Copolymerizations of styrene with acrylamide were performed in ethanol solution. The content of acrylamide was increased from 0 to ca. 30 wt.% (based on total

Table 6.2 Dispersion polymerization of styrene and acrylamide.

Run	comonomer ratio	dn	CV	Yield	particles
FM4	St./AAm (w/w)	(μm)	(%)	(%)	
1	styrene	2.46	4.0	73	spherical
2	20/1	3.60	3.5	61	spherical
3	10/1	5.72 *	6.0 *	47	spherical
4	5/1	—	—	—	coagulated
5	2.5/1	—	—	—	no particles

* data calculated from 4 μm to 6.5 μm .

monomers). The results of the dispersion polymerization are listed in Table 6.2. It was observed that the size of the microspheres was very sensitive to the acrylamide fraction. In the absence of acrylamide, monodisperse polystyrene microspheres of 2.46 μm were produced. Upon addition of ca. 5 and 10 wt.% of acrylamide, the microsphere size increased to 3.6 μm and 5.7 μm , respectively. Further increase of the acrylamide content (ca. 17 wt.%) led to coagulation of the particles. For sample FM4-5 which had ca. 29 wt.% of acrylamide, the solution was clear at the end of the polymerization at 70°C. This solution turned turbid when the temperature was dropped to about 30°C. Figure 6.1 shows the particle size distribution patterns obtained by different monomer ratios. The small peak at 3 μm was due to polystyrene particles which were "touching" each other when they passed through the sensing zone of Coulter Multisizer aperture.¹⁹ The yield of the microspheres was reduced quickly when the content of acrylamide increased. As

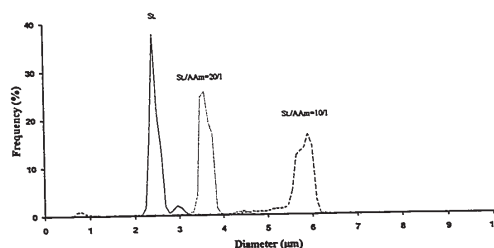


Figure 6.1 Histogram of the size-distribution of poly(St.-co-AAm) microspheres obtained with different monomer ratios as indicated on the top of each peak.

indicated in Table 6.2, a 73% yield was obtained for polymerization of styrene alone. however, only 47% for the copolymerization of styrene and acrylamide with a monomer ratio of 10 to 1.

Acrylamide monomer and its homopolymer are water soluble. The polarity of the copolymer of styrene with acrylamide will increase with increasing amounts of acrylamide. In other words, with more acrylamide, the critical chain length for the nucleation during dispersion polymerization will be longer, which leads to bigger primary particles and bigger final particles as well. In addition, the increasing polarity of the polymer makes the particles more swellable by the solvent (or medium), which favors the diffusion of monomer (mostly styrene) into the particles to polymerize inside the particles. This will also contribute to large final particle diameters.

On the other hand, the increasing polarity of the polymer caused by higher concentrations of acrylamide also enhances the amount of soluble polymer in the solvent. As mentioned above, solid particles were not observed with using 29 wt.% of acrylamide. Obviously, the decreasing yield of poly(St.-co-AAm) microspheres with increasing acrylamide, to a large extent, was due to losing soluble polymers in the medium.

The introduction of amide functional groups was confirmed by FT-IR. Figure 6.2 shows an FT-IR spectrum of poly(St.-co-AAm) polymer microspheres obtained with different monomer ratios. The strong absorption at 1678 cm^{-1} was assigned to amide carbonyl stretching, and two absorptions around 3370 cm^{-1} were assigned to N-H stretching. It is clearly shown in Figure 6.2 that these absorptions appeared when acrylamide was present in the polymerization system, and the intensities of absorptions increased with increasing amounts of acrylamide.

It is well known that homopolymerization of acrylamide is a very fast process in aqueous medium. However, the situation is different if the copolymerization of styrene

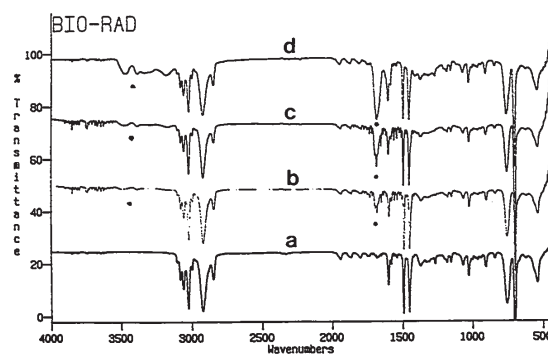


Figure 6.2 FT-IR spectrum of poly(styrene-co-acrylamide) particles. Composition: a) styrene; ratio of styrene/acrylamide (w/w): b) 20/1; c) 10/1; d) 5/1.

with acrylamide is performed in organic solvents. The monomer reactivity ratio for acrylamide and styrene in some organic media has been determined by Saini *et al.*²⁰ As indicated in Table 6.3, in ethanol styrene is much more reactive than acrylamide. This means that, in the present system, styrene monomer will react preferentially with more styrene due to its higher reactivity. The amide units in the particle are expected to be localized mainly on or close to the surface layer. Actually, a low content of acrylamide in the monomer feed is sufficient to introduce desired functional groups on to the surface of particles.

Table 6.3 Monomer Reactivity Ratio for AAm (m₁)-co-St (m₂).²⁰

monomer reactivity ratio	solvent	
	Dioxane	Ethanol
r ₁	1.38	0.30
r ₂	1.27	1.44

The amide functional groups could be converted into other functional groups by means of chemical modification such as hydrolysis, Mannich and Hofmann reactions *etc.*, which have been comprehensively reviewed by Pelton.²¹

Copolymerization of styrene with another water soluble monomer, 2-hydroxyethyl acrylate, was also briefly examined. Basically, observations were similar to those of poly(St-co-AAm). Table 6.4 shows the results of this polymerization. As can be seen, with increasing amount of HEA in monomer feed, diameter of microspheres increased, yield of solid particles decreased, and no particles were formed at the ratio of St/HEA=5/1. Figure 6.3 also shows the monodisperse size-distribution pattern of this copolymer microspheres at low active comonomer concentrations.

Table 6.4 Dispersion Polymerization of Styrene and 2-Hydroxyethyl Acrylate.

Run	comonomer ratio	dn	CV	Yield	particles
FM6	St/HEA (w/w)	(μm)	(%)	(%)	
1	50/1	2.71	3.5	72	spherical
2	20/1	4.0	2.9	54	spherical
3	10/1	—	—	35	spherical*
4	7/1	—	—	—	coagulated
5	5/1	—	—	—	no particles

* sample FM6-3 could not be measured by Coulter Multisizer due to coagulation.

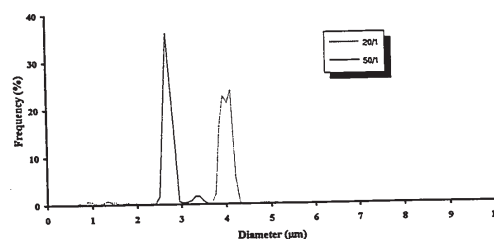


Figure 6.3 Histogram of the size-distribution of poly(St-co-HEA) microspheres obtained with different monomer ratios.

In summary, this study demonstrated that monodisperse functional microspheres can be synthesized via dispersion polymerization. However, the level of reactive monomer must be kept low.

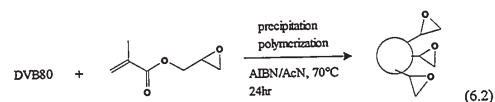
6.4 CROSSLINKED FUNCTIONAL COPOLYMER MICROSPHERES BY PRECIPITATION POLYMERIZATION

One of the advantages of PPDVB55 microspheres is that the surfaces of these microspheres are clean and stabilizer-free. For some applications of polymer microspheres such as uses in biomedical field, clean surfaces are critical. We have been able to synthesize several reactive functional crosslinked microspheres by using the precipitation polymerization process described in Chapter 4. In this section, the syntheses of these functional microspheres are described.

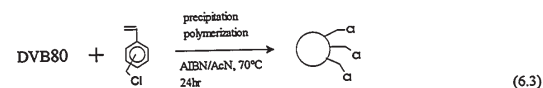
6.4.1 Experimental

The equipment, material purification and polymerization conditions were the same as in the precipitation polymerization of commercial divinylbenzene (Chapter 4). Acetonitrile and AIBN were used as solvent and initiator, respectively. DVB80 and BVE (1,2-bis(vinylphenyl) ethane) were employed as crosslinking reagents. The functional comonomers used were vinylbenzyl chloride (VBC) and glycidyl methacrylate (GMA). Total monomer concentration was held at 2 vol % and typical AIBN concentration was 2 wt %. The reaction equations are shown below.

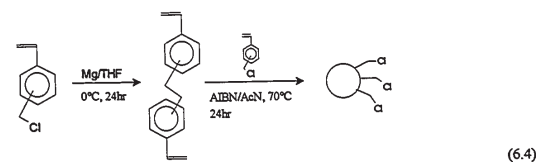
Poly(DVB80-co-GMA) microspheres



Poly(DVB80-co-VBC) microspheres



Poly(BVE-co-VBC) microspheres



6.4.2 Results and Discussion

6.4.2.1 Poly(DVB80-co-Glycidyl Methacrylate) Microspheres

In the precipitation polymerization of DVB55 (or DVB80), the formation of microspheres was governed by the level of crosslinker (Chapter 4). The effect of crosslinker concentration of the poly(DVB80-co-GMA) particles was studied by varying the fraction of glycidyl methacrylate. Table 6.5 shows the results of the precipitation copolymerization of DVB80 and GMA. The diameters of the copolymer microspheres increased with decreasing effective crosslinker concentration. Monodispersity was preserved until the effective crosslinker concentration was below 50%. In contrast to

Table 6.5 Precipitation Polymerization of DVB80 and GMA

sample	Effective DVB	dn	CV	Yield	Particles
FM10a	(wt %)	(μm)	(%)	(%)	
2	75	3.48	4.0	44	spherical
3	70	3.60	3.7	42	spherical
4	65	3.79	4.2	45	spherical
5	60	4.4	3.9	45	spherical
6	55	4.65	4.8	43	spherical
7	50	4.94	7.1	43	spherical
8	45	4.98	7.7	42	spherical, bimodal
9	40	4.04	9.5	42	spherical, bimodal
		5.10	4.4		
10	35	3.18	21.8	43	spherical, bimodal
		4.69	6.31		

PPDVB55, no coagulation was observed when the effective crosslinker was reduced down to 30%, although the size distribution was broad or even bimodal. Like in all precipitation polymerizations mentioned before, the overall conversion was low. All runs had conversion of total monomers between 42 and 45%.

In order to regulate size and yield of the microspheres, the effect of initiator amount on the polymerization was examined. The recipe for run FM10a-5, i.e. 60% effective crosslinker and 25% of GMA comonomer, was used in this study. The results were similar to that in either PPDVB55 or PPDVB80. As seen from Table 6.6, with increasing initial amount of AIBN, both particle size and conversion increased simultaneously. This trend continued until 20 wt % of AIBN was used. Bimodal distribution patterns of microspheres, that is mixtures of large particles with extremely small particles, were seen for AIBN concentrations from 20 wt % to 30 wt % (relative to monomers). The lower yields for these runs were due to the loss of these tiny particles during workup.

The surface morphology of poly(DVB80-co-GMA) microspheres shows their nonporous structure (Figure 6.4).

6.4.2.2 Poly(DVB80-co-Vinylbenzyl Chloride) Microspheres

The results from the syntheses of poly(DVB80-co-VBC) were surprising. As indicated in Figure 6.5, monodisperse polymer microspheres were obtained in the range of effective crosslinker concentration from 55% to 25%. Particles were still formed when the effective crosslinker concentration was as low as 10%. Below 5%, no solid particles were observed.

Table 6.6 Effect of AIBN Loading on Poly(DVB80-co-GMA) Microspheres

Sample	AIBN	dn	CV	Yield	Particles
FM10b	(wt %)	(μm)	(%)	(%)	
1	1	3.63	3.7	31	spherical
2	2	4.88	3.5	43	spherical
3	4	6.23	3.1	54	spherical
4	5	7.47	2.6	59	spherical
5	8	7.35	3.4	64	spherical
6	10	7.83	3.0	66	spherical
7	15	8.86	2.9	68	spherical
8	20	9.91	3.1	68	spherical
		<1			bimodal
9	25	9.89	3.1	64	spherical
		<1			bimodal
10	30	9.03	4.2	52	spherical
		<1			bimodal

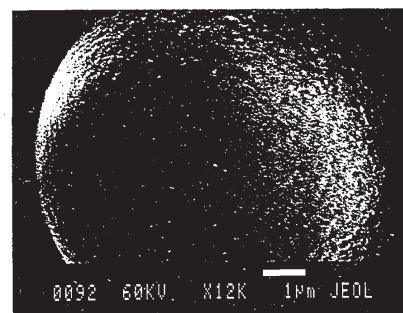


Figure 6.4 Surface morphology of poly(DVB80-co-GMA) microspheres.

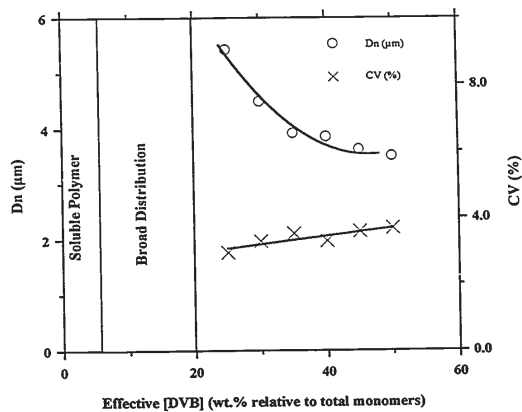


Figure 6.5 Effects of crosslinker concentration on poly(DVB80-co-VBC) copolymer particles.

Figure 6.6a is a SEM micrograph of poly(DVB80-co-VBC) microspheres. The surfaces of these microspheres were rather smooth and nonporous as indicated in Figure 6.6b.

Using reverse phase HPLC (on Separon column with methanol/water (70/30, v/v) as eluent), we found that the polymerization rate of vinylbenzyl chloride was lower than that of either *p*- or *m*-divinylbenzene, however, higher than those of *m*- and *p*-ethylstyrene in the present system. Figure 6.7 shows the conversion-time curve for each individual monomer in this system measured by reverse-phase HPLC. As discussed earlier (Chapter 4), the differences in reaction rate of each monomer led to particles containing cores rich in *p*- and *m*-DVB and shells (or surfaces) rich in *m*- and *p*-EVB and in VBC. The slight enrichment of VBC in the outer layer of the particles may, in some way, stabilize the forming poly(DVB80-co-VBC) microspheres. In the case of polymerization of vinyl chloride, the existence of charged particles has been demonstrated.²² These charges stemmed from chloride ions resulting from the presence of some HCl formed during polymerization. This electrostatic stabilization has been used to account for the stabilities of PVC particles by Törnell²³ and by Kiparissides and Hamielec *et al.*²⁴ Perhaps, a similar event may exist in the present system, stabilizing poly(DVB80-co-VBC) particles even at low levels of crosslinker. Further investigations into this system are necessary.

The introduction of chloro methyl groups into the microspheres was confirmed by surface analysis using X-ray microanalysis (Figure 6.8).

6.4.2.3 Copolymerization of DVB80/4-Vinylbenzenesulfonic Acid Sodium Salt

Attempts were made to synthesize microspheres containing sulfonic groups on the surface. Copolymerization of DVB80 with VBS led only to coagulated products under various conditions.

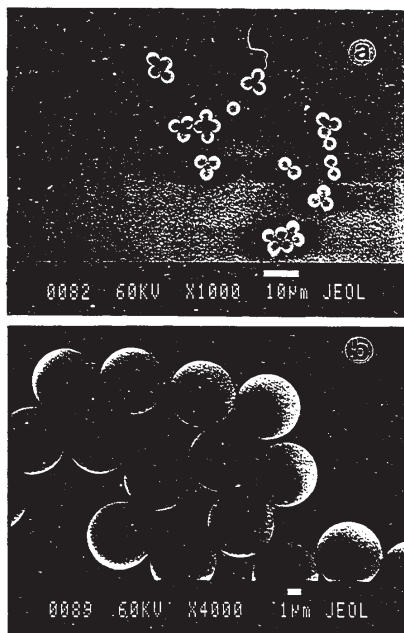


Figure 6.6 SEM micrographs of poly(DVB80-co-vinylbenzyl chloride) microspheres (a) (sample FM8e⁻³) and surface structure (b) (sample FM8e⁻⁷).

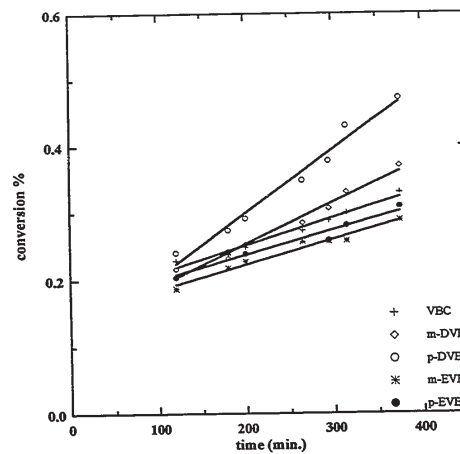


Figure 6.7 Conversion-time plot of polymerization of DVB80 and vinylbenzyl chloride.

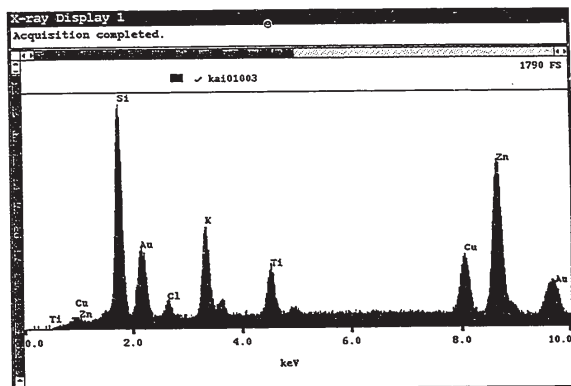


Figure 6.8 Spectrum of X-ray microanalysis for poly(DVB80-co-VBC) microspheres.

6.4.2.4 Poly(Bis(Vinylphenyl) Ethane-co-Vinylbenzyl Chloride)

The stability of PPDVB55 or PPDVB80 microspheres is due to the highly crosslinked structure as we have discussed in Chapter 4. In principal, this will be applicable not only for divinylbenzene crosslinker, but also other types of styryl crosslinker. To test this hypothesis, polymer particles containing chloro methyl groups were synthesized by copolymerization of bis(vinylphenyl) ethane (BVE) and vinylbenzyl chloride (see equation 6.4). The synthesis of BVE crosslinker has been described in Chapter 1. Copolymerization was carried out under our standard precipitation polymerization (2 wt % total monomer loading in acetonitrile, 2 wt % AIBN, at 70°C for 24 h). Nearly monodisperse poly(BVE-co-VBC) microspheres were obtained as shown in Figure 6.9. This result indicated that the synthesis of monodisperse polymer microspheres by precipitation polymerization may be a general process for other styryl type crosslinkers as well.

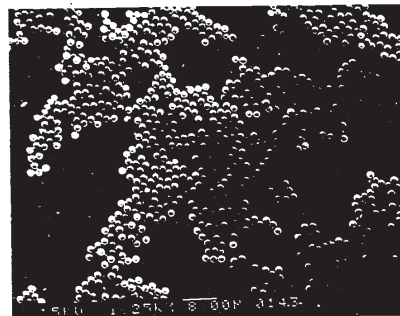


Figure 6.9 SEM micrograph of poly(bis(vinylphenyl) ethane-co-vinylbenzyl chloride) microspheres. Conditions: BVE/VBC = 50/50 (w/w); acetonitrile, 2 wt % AIBN; 70°C; 24 h.

6.4.3 Surface Modification of Preformed Polymer Microspheres

We have discussed above the introduction of functional groups into polymer microspheres either by dispersion copolymerization or by precipitation copolymerization. Here, we discuss chemical modification of preformed polymer to synthesize reactive polymer microspheres. No reports on chemical modification of preformed polymer microspheres obtained by dispersion polymerization have yet appeared, although Margel *et al.*²⁵ synthesized polychloromethylstyrene microspheres and discussed several possible ways to modify these microspheres in order to introduce hydrophilic functional groups. From a practical point of view, synthesis of reactive microspheres by chemical modification is advantageous because the active functional groups will mainly be located on the surface of the microspheres, and the bulk properties of the microspheres will be unchanged.

Recently, Stöver *et al.*²⁶ described the homogeneous cobalt catalyzed oxidation of poly(4-methylstyrene) homopolymer in organic medium to prepare functional polymers. The 4-methyl groups on the polymer were selectively converted to aldehyde and carboxylic acid functional groups. This opens a way to synthesize functional microspheres by cobalt catalyzed oxidation of polymer microspheres bearing methyl groups on the surface.

In this section, surface modification of poly(4-methylstyrene) (PMSt) and PPDVB55 microspheres by using cobalt catalyst is described.

6.4.3.1 Surface modification of poly(4-methylstyrene) microspheres

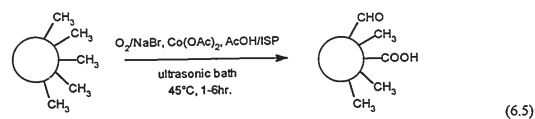
Experimental: The oxidation of PMSt microspheres setup is shown in Figure 6.10. The glass bottle reactors were placed in an ultrasonic water bath. The temperature of the ultrasonic bath was controlled by circulating water from a thermostat water bath. The ultrasonic bath supplied the necessary agitation to prevent the sedimentation and/or coagulation of the microspheres during the oxidation reaction.

The reaction was carried out after the technique presented by Stöver *et al.*²⁷. To a 100 ml reactor, 1.0 g cobalt(II) acetate tetrahydrate ($\text{Co}(\text{OAc})_2 \cdot 4\text{H}_2\text{O}$), 0.5 g sodium bromide (NaBr) and 50 ml of a mixture of iso-propanol and glacial acetic acid in different ratios were added. For each run, 0.2 g of PMSt microspheres were added to the mixture. O_2 was bubbled through the solution at a flow rate of 60 ml/min. Oxidation proceeded at 45°C for 1 to 6 h. At the end of the reaction, oxidized polymer was separated from the medium and washed with methanol and a mixture of methanol/water alternately for three times; then, dried at ambient temperature followed by further drying in a vacuum oven at 70°C for two days.

Oxidation of PMSt microspheres: In linear homopolymer of poly(4-methylstyrene), the methyl groups can be selectively oxidized to 4-vinylbenzaldehyde and/or 4-vinylbenzoic acid units in mixtures of acetic acid with different organic cosolvents. In order to preserve the shape of the microspheres, a non-solvent system, that would dissolve the catalysts but not the polymer spheres, had to be adopted. Earlier work on PMSt membranes had shown acetic acid/iso-propanol to be a suitable non-solvent system.²⁸ The reaction proceeded as shown by eq. 6.5.



Figure 6.10 Reaction setup for oxidation of PMSt microspheres.



Oxidation of PMSt microspheres

It was found that the degree of functionalization and the morphology of the PMSt microspheres depended on several parameters including the reaction temperature, ratio glacial acetic acid (AcOH) to *iso*-propanol, and the reaction time.

Effect of AcOH ratio: The oxidation of PMSt microspheres in pure glacial acetic acid (AcOH) led to rapid deformation of the microspheres even at room temperature. This is because PMSt was plastized by AcOH, which resulted in a lowering of the T_g of the polymer. Accordingly, the combination of *iso*-propanol with AcOH was used.²⁸

When the concentration of AcOH changed from 10 vol% to 50 vol%, changes of particle morphology were observed. For the first hour reaction, size and size distribution of PMSt microspheres did not change when [AcOH] < 30%. The diameter slightly increased for concentrations of acetic acid of 40 and 50 vol%, respectively (Figure 6.11).

The second hour of oxidation led to broad size distributions (multimodal distribution). Both the population of the larger particles and their distribution increased substantially depending upon the concentration of AcOH;

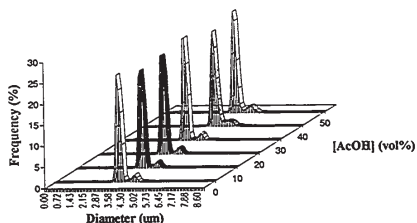


Figure 6.11 Influence of [AcOH] on particle size and size distribution of oxidized PMSt microspheres at 45°C for one-hour oxidation.

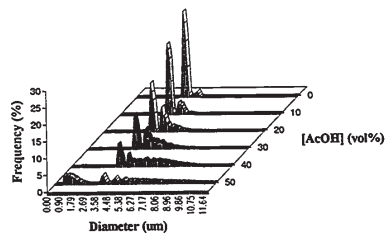


Figure 6.12 Influence of [AcOH] on particle size and size distribution of oxidized PMSt microspheres at 45°C for two-hour oxidation.

and oxidation with 50% AcOH gave not only large particles, but also smaller ones (Figure 6.12).

Apparently, the increasing size and distribution of particles were due to coagulation caused by the solvent's plastizing effect. The higher the concentration of acetic acid is, the lower the softening point of the polymer will be; and this makes the surface of the microspheres more sticky. Diffusion of polymer across boundaries (interfaces) among those microspheres will happen, leading to larger, irregular shaped particles with broad distribution. As well, the rate of oxidation of PMSt was faster at high concentration of AcOH. The selectivity of the oxidation for methyl groups over tertiary methine groups at the backbone of poly(4-methylstyrene) was estimated to be 25:1 in solution. Some bond cleavage will be inevitable.

Figure 6.13 shows SEM micrographs of PMSt microspheres oxidized with different amounts of acetic acid. As indicated in Figure 6.13b, a few twin particles with relative clear boundary can be seen. As the concentration of AcOH increases, the diffusion happens and microspheres merge with each other, more pear-like particles and aggregation of several microspheres appeared (Figure 6.13c & d). SEM photograph of the polymer oxidized with 50% AcOH (Figure 6.13e) shows a relative large portion of fine powder like materials, which is probably the fragmentation of the polymer microspheres due to the bond cleavage.

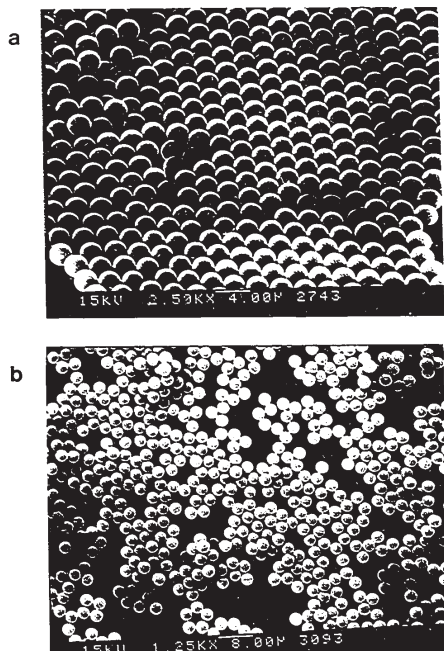


Figure 6.13 (cont. on the next page).

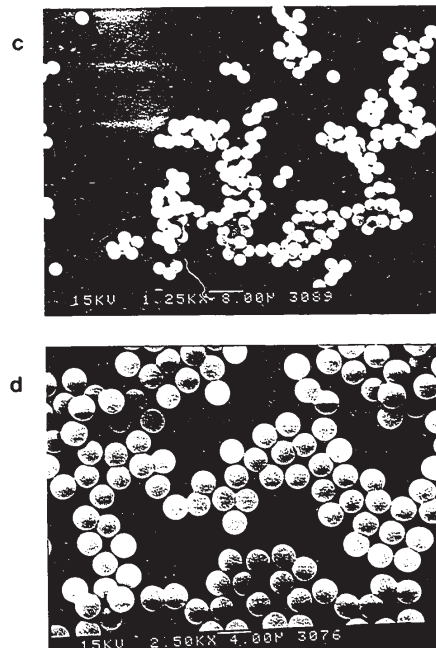


Figure 6.13 (cont. on the next page).

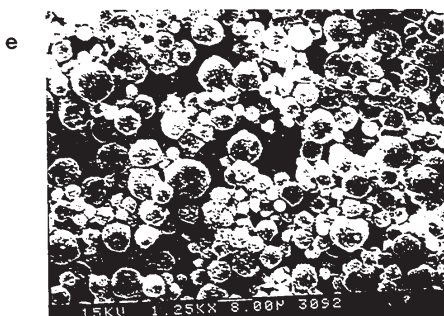


Figure 6.13 SEM of PMSt microspheres oxidized at 45°C for one-hour. Concentration of acetic acid (vol%): (b) 20; (c) 30; (d) 40; (e) 50. (a) is a SEM of the PMSt microspheres prior to oxidation

Figure 6.14 is the FT-IR spectrum of poly(4-methylstyrene) microspheres before and after oxidation with 50% AcOH for two-hours. Two absorptions centered at 1700 cm^{-1} correspond to the carbonyl stretching of the carboxylic acid functional groups and the carbonyl stretching of the aldehyde group, respectively. The FT-IR spectra of other samples oxidized with lower concentration of AcOH, somehow, did not give clearly distinguishable absorptions around this region. Presumably, this is because the extremely low concentration of carbonyl functionalities compared with the bulk polymer.

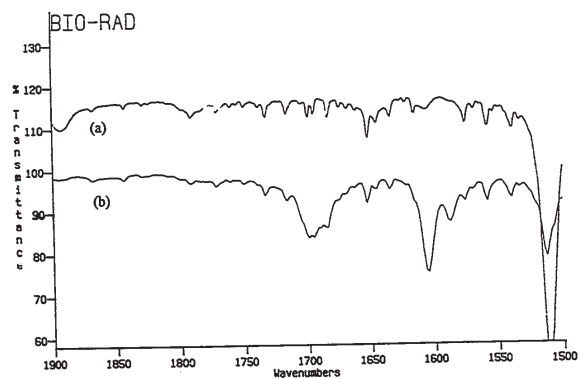


Figure 6.14 FT-IR of PMSt microspheres before oxidation (a) and the microspheres oxidized with 50 vol% AcOH for two-hours (b). (specimens were prepared with casting solution of polymer particles in THF on NaBr disc).

Effect of reaction time: To increase the degree of functionalization, a more concentrated AcOH solution would be desirable. However, the deformation of microspheres combined with bond cleavage will happen, as we have seen above. An alternate way would be to prolong the reaction time. In homogeneous oxidation of poly(4-methylstyrene) in dimethoxyethane, it was found that the degree of oxidation depended on the reaction time, and the conversion of methyl group to functional groups (aldehyde and/or carboxylic acid groups) could be changed from 6% to more than 60% when the reaction time increased from 1.5 h to 24 h.²⁹

For the present oxidation reaction, the time effect is shown in Figure 6.15. Its trend is similar to the effect of concentration of acetic acid, i.e., the longer reaction time, the larger both size and size distribution of PMSt microspheres become.

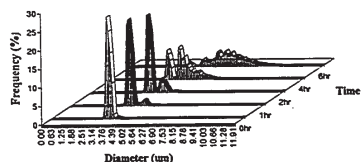


Figure 6.15 Particle-size distribution of PMSt microspheres oxidized. Reaction conditions: 10 vol% of AcOH; 45°C.

Figure 6.16 shows the SEMs of these microspheres and particles. For the first two-hour oxidation, PMSt microspheres virtually keep their shapes unchanged (Figure 6.16a and b). Figure 6.16c shows that four-hour oxidation led to larger size of particles with broad size distribution (bimodal) as well as some fine particle fragments. It is interesting to see that even the large particles formed have spherical shapes. The coagulation of the microspheres did happen after six-hours of reaction (Figure 6.16d).

For the reactions with 20 vol% and 30 vol% AcOH, the size and morphology of PMSt microspheres were similar. However, the degree of oxidation increased with increasing AcOH concentration as examined by FT-IR. No particles bigger than 0.2 μm were found after a four-hour reaction with 40 vol% AcOH. Figure 6.17 indicates how the molecular weight and molecular weight distribution pattern changed with oxidation time. Clearly, the bimodal distribution pattern was due to the bond cleavage. The lower molecular weight fraction was from the oligomers cleaved off surface during the reaction, and further degraded to small chain fragments. The higher molecular weight fraction corresponds to the bulk particles. This fraction shows a small molecular weight decrease due to some cleavages within the particles.

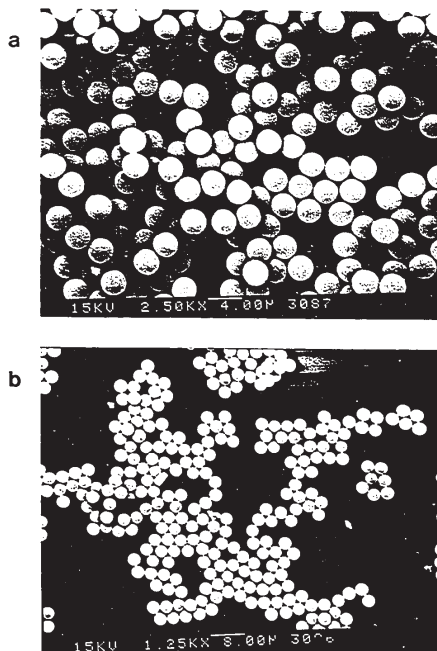


Figure 6.16 (cont. on the next page).

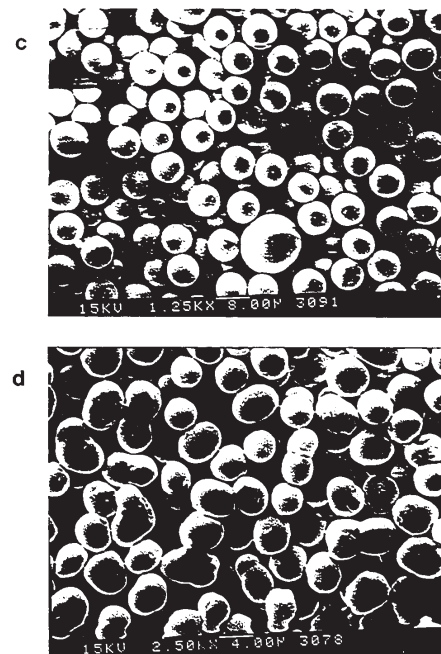


Figure 6.16 SEM of PMSt microspheres oxidized at different time: (a) 1hr.; (b) 2hr.; (c) 4hr.; (d) 6hr.; Reaction conditions: 10 vol% of AcOH; 45°C.

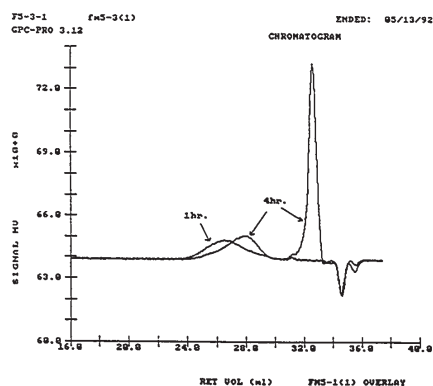


Figure 6.17 GPC profile of PMSt. microspheres oxidized in 50 vol% AcOH solution at different time: (a) 1 hr.; (b) 4 hr.

With 50 vol% AcOH, four-hour oxidation led to highly oxidized product. The solution was clear with green color because all polymer microspheres had been degraded into small molecular weight oligomers which were soluble in the reaction medium.

Effect of reaction temperature: The T_g of the polymer microspheres was lowered due to the plasticizer effect. The oxidation reaction at low temperature, therefore, is conducted. It was observed that for the oxidation of PMSt microspheres with 30 vol% and 50 vol% AcOH at 20°C the size and monodispersity of PMSt microspheres were kept. Even for 50 vol% acetic acid, after twenty-six hour reaction, the size and size distribution of PMSt. microspheres were unchanged. However, the rate of oxidation was slow because all these samples did not give detectable carbonyl groups measured by FT-IR.

In summary, the functionalization of PMSt microspheres in cobalt catalyst system was examined. It has been found that the degree of functionalization is dependent upon several factors, including temperature, concentration of acetic acid and reaction time. Strong deformation of PMSt microspheres and bond cleavage of the polymer were observed, which inhibits the higher degree functionalization. To overcome these problems, monodisperse microspheres with methyl (or ethyl) groups on the surface having crosslinked structure would be necessary. This will be described in the next section.

6.4.3.2 Surface modification of PPDVB55 microspheres

Because commercial divinylbenzene consists of ca. 42% of ethylstyrene, the surface of PPDVB55 microspheres is expected to have a large number of ethyl groups. Like methyl groups, these ethyl groups will be oxidized to ketone and carboxylic acid under the conditions mentioned above, although the rate of oxidation may be slower. In addition, PPDVB55 microspheres also contain a certain amount of pendent double bonds due to the incomplete crosslinking reaction. These pendent double bonds are prone to be oxidized under these conditions as well. Considering the highly crosslinked structure of PPDVB55 microspheres, the problem of polymer bond cleavage encountered in the poly(4-methylstyrene) microspheres will be minimized. Surface modifications of PPDVB55 microspheres by means of cobalt catalyzed oxidation have been examined and are described below.

Experimental: NaBr (0.64 g) and $\text{CoAc}_2 \cdot 4\text{H}_2\text{O}$ (1.56 g) were dissolved in 100 ml of HOAc. To this solution, 100 ml of heptane was added. 30 ml of this mixture was combined with 0.11 g PPDVB55 microspheres (sample 38-3) in a reactor. Oxidation reaction was performed at 80°C. The workup procedure for oxidized PPDVB55 microspheres was the same as for the PMSt microspheres.

Considering their rigid structure, PPDVB55 microspheres were not oxidized in the reactor used for oxidation of PMSt microspheres, because ultrasonic vibration may cause the degradation of particles. Instead, the reaction was conducted in a column type reactor as shown in Figure 6.18. O_2 was passed through the column from the bottom to the top at a rate of 60 ml/min. The bubbles generated inside the column caused a mild agitation to prevent the sedimentation of microspheres. The reaction temperature was controlled by circulating thermostatted water through the jacketed glass tube.

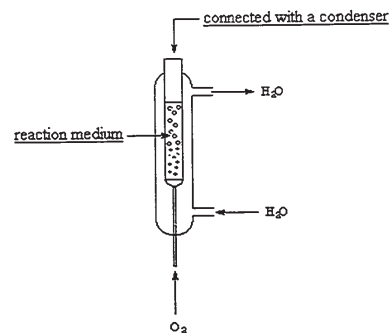


Figure 6.18 A reactor for oxidation reaction of PPDVB55 microspheres with cobalt catalyst.

Oxidation of PPDVB55 microspheres: As expected, no deformation or coagulation of microspheres was observed in the present oxidation system. The reaction mixture was monitored by optical microscopy. With increasing reaction time, some very small particles were seen due to the fractures from the minor surface degradation of microspheres. However, the microspheres were still spherical and their sizes were preserved. Table 6.7 shows the size and size distribution of PPDVB55 microspheres vs. oxidation time with Coulter Multisizer. Obviously, the size and size distribution of microspheres were kept constant even after 18 h oxidation at 80°C.

Table 6.7 Cobalt Catalyzed Oxidation of PPDVB55 Microspheres

sample	1	2	3	4	5	6	7	8	9
FM9a									
RT* (h.)	0.5	1	1.5	2	2.5	3	3.5	4.5	18
d_n (μm)#	3.61	3.62	3.65	3.63	3.61	3.63	3.63	3.59	3.62
CV (%)	3.2	3.2	3.3	3.2	3.3	3.2	3.2	3.3	3.4

* RT = reaction time; # main peak calculation.

Oxidized PPDVB55 microspheres were evaluated by FT-IR (KBr pellets) by monitoring the following absorptions: ca. 1700 cm^{-1} (carbonyl stretching), 1630 cm^{-1} (C=C stretching vibration), and 990 cm^{-1} (out of plane deformation $\gamma_{\text{C-H}}$).³⁰ Figure 6.19a is the spectrum of PPDVB55 (sample 38-3) microspheres. It was observed that, with increasing oxidation time, band at 1700 cm^{-1} appeared and its intensity increased as well. In contrast, the intensities of vinyl absorptions (1630 cm^{-1} , (1410 cm^{-1}) and 990 cm^{-1}) decreased. Figure 6.19b shows the comparison of samples before oxidation and after 18 hour oxidation. The strong absorption centered at 1700 cm^{-1} indicated that the existence of carboxylic and aldehyde groups. However, substantial amount of vinyl groups still existed. This was because only these vinyl groups which were on the surface or in other accessible places could be oxidized. In fact, the reaction of these surface vinyl pendant groups was complete within 0.5 hour. As indicated in Figure 6.20, the band at 1630 cm^{-1} was reduced to a certain extent after 0.5 h reaction, which then kept unchanged for prolonged reaction time. Similar observations have been obtained with bromination of

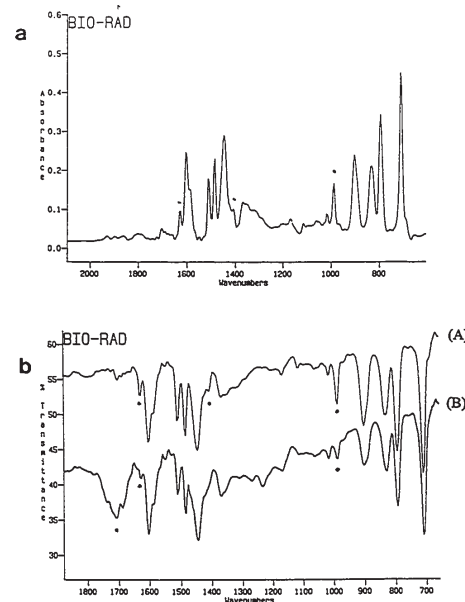


Figure 6.19 (a) FT-IR spectrum of PPDVB55 microspheres
(b) FT-IR spectra of PPDVB55 microspheres after 0 h (A) and 18 h (B) oxidation.

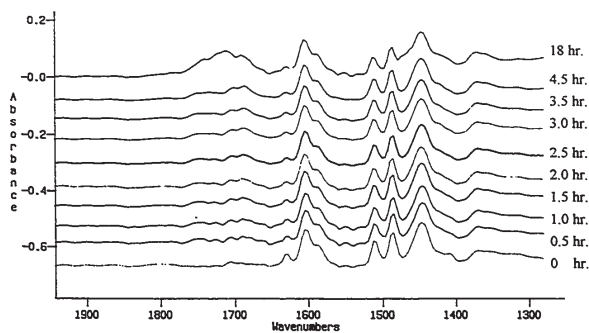


Figure 6.20 FT-IR spectra of oxidized PPDVB55 microspheres at different reaction times.

PPDVB55 microspheres. The increasing absorption around 1700 cm^{-1} was largely due to the oxidation of ethyl groups on the surface of PPDVB55 microspheres.

In summary, because of their highly crosslinked structure, PPDVB55 particles could be easily oxidized in their surfaces without causing particle coagulation or break down. The resulting carbonyl and acid groups may permit binding of proteins and other amines.

REFERENCES

- M. Hassanein, W.T. Ford, *J. Org. Chem.*, **54**, 3106 (1989);
- R.S. Chandran, W.T. Ford, *J. Chem. Soc., Chem. Commun.*, 104 (1988).
- J.H. Kim, M.S. El-Aasser, A. Klein, J.W. Vanderhoff, *J. Appl. Polym. Sci.*, **35**, 2117 (1988).
- E.G. Bobalek, E.R. Moore, S.S. Levy, and C.C. Lee, *J. Appl. Polym. Sci.*, **8**, 625 (1964)
- K. Makuuchi, A. Katakai, and N. Nakayama, *J. Coat. Tech.*, **55**, 29 (1983)
- J.L. Robbins, G.A. Hill, B.N. Carle, J.H. Carlquist, S. Marcus, *Proc. Soc. Exp. Biol. Med.*, **109**, 321 (1962).
- S. Margel and M. Offarim, *Anal. Biochem.*, **128**, 342 (1982)
- F. Lenzmann, K. Li, A.H. Kitai, and H.D.H. Stöver, *Chem. of Mater.*, **6**, 156 (1994).
- K. Sakota, T. Okaya, *J. Appl. Polym. Sci.*, **20**, 1725 (1976).
- M. Choubal, W.T. Ford, *J. Polym. Sci., Polym. Chem.*, **27**, 1873 (1989).
- H. Kitano, Z.H. Sun, N. Ise, *Macromolecules*, **16**, 1306 (1983).
- M.S.D. Juan, I.M. Krieger, *J. Polym. Sci. Polym. Chem.*, **14**, 2089 (1976).
- J.H. Kim, M. Chainey, M.S. El-Aasser, J.W. Vanderhoff, *J. Polym. Sci. Polym. Chem.*, **27**, 3187 (1989).
- C.K. Ober, K.P. Lok and M.L. Hair, *J. Polym. Sci. Polym. Lett. Ed.*, **23**, 103 (1985).
- M.D. Croucher and M.A. Winnik, in *Future Directions In Polymer Colloids* (M.S. El-Aasser and R.M. Fitch, Eds.), NATO ASI Series, E138, p209, 1987.
- C.M. Tseng, Y.Y. Lu, M.S. El-Aasser and J.W. Vanderhoff, *J. Polym. Sci., Polym. Chem. Ed.*, **24**, 2995 (1986).
- R. Arshady, *Biomaterials*, **14**, 5 (1993).
- C.K. Ober, and K.P. Lok, *Macromolecules*, **20**, 268 (1987).
- C.M.L. Atkinson, and R. Wilson, *Powder Technol.*, **34**, 275 (1983).
- G. Saini, A. Leoni, and S. Franco, *Makromol. Chem.*, **144**, 235 (1971).
- R. Pelton, "Chemical Reactions at the latex-solution interface", in *Scientific Methods for the Study of Polymer Colloids and Their Applications*, NATO ASI Series, p493, 1990.
- J.A. Davidson and D.E. Witenhafer, *J. Polym. Sci. Polym. Phys.*, **18**, 51 (1980).

-
- 23 B.F. Törnell, J.M. Uustalu, and B. Jonsson, *Colloid Polymer Sci.*, **264**, 439 (1986).
 - 24 C. Kiparissides, I. Moustakis, and A. Hamielec, *J. Appl. Polym. Sci.*, **49**, 445 (1993).
 - 25 S. Margel, E. Nov, and I. Fisher, *J. Polym. Sci. Polym. Chem.*, **29**, 347 (1991).
 - 26 L.P. Ferrari, H.D.H. Stöver, *Macromolecules*, **24**, 6340 (1991).
 - 27 R.T. Shaver, H.D.H. Stöver, *Macromolecules*, submitted for publication.
 - 28 R.T. Shaver, "Functional Polymer Films and Membranes", *Senior Research Thesis*, McMaster University, 1992.
 - 29 L.P. Ferrari, "Cobalt Catalyzed Oxidation of Poly(4-methylstyrene)", *Senior Research Thesis*, McMaster University, 1991.
 - 30 D.-Y.D. Chung, M. Bartholin, and A. Guyot, *Angew. Makromol. Chem.*, **103**, 109 (1982).